

# **Hydrologic Implications of 20<sup>th</sup> Century Warming and Climate Variability in the Western U.S.**

Alan F. Hamlet

A dissertation submitted in partial fulfillment of the requirements for the degree of

Doctor of Philosophy

University of Washington

2006

Program Authorized to Offer Degree:

Department of Civil and Environmental Engineering

University of Washington  
Graduate School

This is to certify that I have examined this copy of a doctoral dissertation by

Alan F. Hamlet

and have found that it is complete and satisfactory in all respects, and that any and all  
revisions by the final examining committee have been made.

Chair of the Supervisory Committee:

---

Dennis P. Lettenmaier

Reading Committee:

---

Dennis P. Lettenmaier

---

Stephen J. Burges

---

Richard N. Palmer

Date: \_\_\_\_\_

In presenting this dissertation in partial fulfillment of the requirements for the doctoral degree at the University of Washington, I agree that the Library shall make its copies freely available for inspection. I further agree that extensive copying of the dissertation is allowable only for scholarly purposes, consistent with "fair use" as prescribed in the U.S. Copyright Law. Requests for copying or reproduction of this dissertation may be referred to ProQuest Information and Learning, 300 N. Zeeb Rd, Ann Arbor, MI 48106-1346, 1-800-521-0600, to whom the author has granted "the right to reproduce and sell a) copies of the manuscript in microform and/or b) printed copies of the manuscript made from microform".

Signature: \_\_\_\_\_

Date: \_\_\_\_\_

University of Washington

**Abstract**

**Hydrologic Implications of 20<sup>th</sup> Century Warming and Climate Variability in the Western U.S.**

Alan F. Hamlet

Chair of the Supervisory Committee:  
Professor Dennis P. Lettenmaier  
Department of Civil and Environmental Engineering

Variations in 20th century climate across the western U.S. from 1915-2003 are characterized by regionally-specific, decadal-scale shifts in precipitation regimes, combined with systematic increases in temperature across essentially the entire West. In a series of integrated studies we use both observations and hydrologic models to examine the hydrologic implications of these climatic changes. In many areas of the West that have substantial snow accumulation in winter, warming has resulted in reductions in spring snowpack, earlier snowmelt, increased runoff in winter and less runoff in summer, earlier peak runoff and soil moisture recharge, and changes in natural flooding regimes. Evaporation, while apparently increasing somewhat in many areas, has so far had relatively minor effects in comparison with interannual variations in precipitation. Flood risks are affected by decadal and interannual variations in precipitation, by changes in precipitation variability apparent after the mid-1970s, and by warming via changes in antecedent snowpack and contributing basin area during storms.

These hydrologic changes, although broadly characteristic of the West as a whole, vary spatially as a function of mid-winter temperature regimes. Downward trends in spring snowpack, and related timing shifts in streamflow, soil moisture recharge, and evaporation, for example, are strongest in areas along the coast with mid winter temperatures close to the freezing point, and are largely due to temperature related effects. Colder areas are also affected by warming to some degree, but variations in precipitation remain the dominant driver. Simulated changes in natural flood risks that

accompany large scale warming are also a complex function of mid-winter temperature regimes. In strongly snowmelt dominant river basins, simulated flood risks are shown in most cases to decline with 20th century warming, because of reductions in spring snowpack. For river basins near the freezing level in mid-winter the effects of warming on flood risks vary widely and increases or decreases in flood risks can occur in response to warming depending on the relative importance of changes in contributing basin area and antecedent snow conditions that are coincident with storms. Flood risks in rain dominant basins are largely stationary in response to warming.

# Table of Contents

	Page
List of Figures .....	iii
List of Tables .....	v
1. Introduction.....	1
2. Overview of Hydroclimatic Foundation Research .....	5
2.1. Climatic Variations in the Western U.S. Associated with ENSO and PDO.....	5
2.2. Climate Variability in the Context of Regional Warming.....	7
3. Long-Term Precipitation and Temperature Data Sets .....	9
3.1. Introduction and Background .....	9
3.2. Data Processing Methods.....	11
Sources of Data.....	11
Preprocessing, Quality Control, and Gridding.....	12
Temporal Adjustments.....	12
Topographic Adjustments.....	15
Wind Data.....	16
3.3. Results.....	16
Macro Scale Evaluation of Results Using Naturalized Streamflow Data.....	16
Macro Scale Evaluation of Results Using Observed Snow Water Equivalent.....	19
Data Availability and Archiving.....	19
3.4. Summary and Conclusions .....	20
4. Effects of 20 <sup>th</sup> Century Warming and Climate Variability on Snowpack Trends .....	21
4.1. Introduction and Background .....	21
4.2. Hydrologic Model and Meteorological Driving Data.....	24
VIC Hydrologic Model.....	24
Meteorological Driving Data .....	25
Role of Temperature and Precipitation Driving Data in the Snow Simulations.....	27
Evaluation of Simulated SWE trends .....	27
4.3. Methods and Experimental Design.....	29
4.4. Results and Discussion .....	33
Notes on Presentation of Results and Interpretation of Figures .....	33
SWE Trends for March 1, April 1, and May 1 for 1916-2003 (“A”).....	33
Results for 1916-2003(“A”).....	34
Results for 1924-1976 (“B”).....	35
Results for 1947-2003 (“C”).....	36
Results for 1924-1946 concatenated with 1977-1995 (“D”).....	38
Effects of Climatic Regimes .....	39
Trends in the Timing of Snow Accumulation and Melt .....	41
4.5. Summary and Conclusions .....	44
5. Effects of 20 <sup>th</sup> Century Warming and Climatic Variability on Trends in Runoff, Evaporation, and Soil Moisture .....	47
5.1. Introduction and Background .....	47
5.2. Hydrologic Simulation Model and Driving Data .....	51

5.3. Evaluation of the Hydrologic Model .....	51
Snowpack .....	51
Snowmelt .....	52
Streamflow .....	53
Soil Moisture and Evapotranspiration .....	55
5.4. Analytical Methods .....	56
5.5. Results and Discussion .....	59
Notes on Figure Presentation .....	59
Trends in Precipitation and Temperature .....	59
Long-Term Water Balance Simulations .....	61
Overall Trends in the Timing of Runoff, SM, and ET .....	63
Trends in Evapotranspiration and Runoff Ratio .....	65
Trends in Runoff Timing .....	68
Trends in Soil Moisture .....	72
5.6. Summary and Conclusions .....	74
6. Sensitivity of Flood Risk to 20 <sup>th</sup> Century Warming and Climate Variability .....	77
6.1. Introduction .....	77
6.2. 20 <sup>th</sup> Century Climate Variations in the Western U.S. ....	80
6.3. Physical Mechanisms Associated with Western U.S. Flooding .....	83
6.4. Methods and Experimental Design .....	86
Climatic Data .....	87
Flood Frequency Estimation .....	89
Model Evaluation .....	90
Test Basins .....	94
6.5. Results and Discussion .....	95
Effects of Century-Scale Warming .....	96
Effects of Climate Variability on Flooding Risks .....	100
6.6. Summary and Conclusions .....	105
7. Final Overview and Conclusions .....	108
References .....	112

# List of Figures

Figure Number	Page
Figure 3.1: Example of temporal corrections for January precipitation at a single grid location .....	15
Figure 3.2: Comparison of adjusted and unadjusted VIC simulations and naturalized observations for the S.F. Flathead River at Hungry Horse Dam, MT.....	18
Figure 3.3: Root mean square error for simulated April-September average streamflow from 1931 to 1950.....	19
Figure 4.1 Topographic and climatic characteristics of the 1/8 <sup>th</sup> degree VIC hydrologic model simulation domain .....	30
Figure 4.2 Relative trends (% per year) in simulated SWE for three calendar dates for the period from 1916-2003.....	34
Figure 4.3 Relative trends (% per year) in simulated April 1 SWE for 1916-2003.....	35
Figure 4.4 Relative trends (% per year) in simulated April 1 SWE for 1925-1976.....	36
Figure 4.5 Relative trends (% per year) in simulated April 1 SWE for 1947-2003.....	37
Figure 4.6 Relative trends (% per year) in simulated April 1 SWE for 1925-1946 combined with 1977-2003 .....	39
Figure 4.7 Location of winter climatic regimes associated with strong downward SWE trends .....	40
Figure 4.8 Cumulative changes (trend * number of years) in calendar date of: a) 10% SWE accumulation, b) maximum SWE accumulation, and c) 90% melt for 1916-2003 .....	42
Figure 5.1: Map and climatological characteristics of the simulation domain .....	47
Figure 5.2: Simulated and observed total monthly snowmelt.....	53
Figure 5.3: Comparison of naturalized streamflow observations and simulated natural streamflows.....	54
Figure 5.4: Trends in Oct-Mar precipitation (relative trend) and temperature (absolute trend) .....	59
Figure 5.5: Trends in Apr-Sept. precipitation (relative trend) and temperature (absolute trend) .....	60
Figure 5.6: Long-term water balance for four large river basins .....	62
Figure 5.7: 50-year cumulative trends (absolute trend*50) in runoff, SM, and ET from 1919-2003.....	63
Figure 5.8: Same as figure 5.7 except for the period from 1947-2003 .....	64
Figure 5.9: Trends in April-June ET for VIC cells with more than 50mm of average snow water equivalent .....	66
Figure 5.10: Same as for Figure 5.9 except for July-Sept ET.....	67
Figure 5.11: Trends in the annual runoff ratio for 1947-2003 .....	69



Figure 5.12: Same as Figure 5.9, except showing relative trends in the fraction of annual flow occurring in March .....	70
Figure 5.13: Same as Figure 5.9, except showing relative trends in the fraction of annual flow occurring in June.....	71
Figure 5.14: Same as Figure 5.9, except showing relative trends in April 1 soil moisture.....	73
Figure 5.15: Same as Figure 5.9, except showing relative trends in July 1 soil moisture.....	74
Figure 6.1 Study domain and a long-term, spatially-averaged time series of cool season (Oct-March) standardized anomalies of precipitation (PCP), maximum daily temperature (TMAX), and minimum daily temperature (TMIN).....	79
Figure 6.2 Standardized anomalies for cool season precipitation, maximum temperature, and minimum temperature shown in Figure 6.1, smoothed with a 12-year running mean .....	82
Figure 6.3. Flood statistics from the VIC simulations compared with observations from the HCDN network from 1953-2003 .....	92
Figure 6.4 Evaluation of model climate sensitivity .....	93
Figure 6.5. Ratio of estimated 20-year flood quantiles (2003 temperature regime/ 1915 temperature regime).....	96
Figure 6.6. Same as Figure 6.5, but showing results for three different basin sizes.....	97
Figure 6.7. Same as Figure 6.6, but showing the estimated 100-year quantiles.....	98
Figure 6.8 Spatial and scatter plots for the smallest basin size (as in Figure 6.5) showing the ratio of the estimated 100-year flood for warm, neutral, and cool PDO as compared to the unconditional case.....	101
Figure 6.9. Same as Figure 6.8 but showing warm,neutral, and cool ENSO. ....	102
Figure 6.10. Same as Figure 6.8 except showing only warm-PDO/warm-ENSO and cool-PDO/cool-ENSO composites.....	103
Figure 6.11. Same as for Figure 6.8 except showing composites based on all years from 1973-2003 for the 20-year, 50-year, 100-year return intervals.....	104

# List of Tables

Table Number	Page
Table 4.1 Areal averages of the relative trends for each grid cell calculated for each portion of the domain .....	43
Table 4.2 Relative trend in the areal average snow water equivalent for each portion of the domain.....	43
Table 6.1 Retrospective definitions of warm, neutral, and cool ENSO and PDO.....	88
Table 6.2 Size definitions for simulated test basins used in the west-wide sensitivity study .....	95

## Acknowledgements

The author wishes to acknowledge and thank Dennis Lettenmaier and the rest of the supervisory committee: Steve Burges, Rick Palmer, and Nate Mantua at the University of Washington, and Dan Cayan at the University of California, San Diego for their support and constructive suggestions during the course of this work. Thanks also to Ed Miles and Adrienne Karpov at the CSES Climate Impacts Group for both moral and financial support during the process of juggling work and school obligations over the last five years. Philip Mote at the CSES Climate Impacts Group and Martyn Clark at the Western Water Assessment contributed greatly to the ideas and experimental design of these studies, and provided both observed data and various related analyses for the snow water equivalent and runoff studies. Thanks to Andy Wood, Kostas Andreadis, and Ted Bohn from the Hydro lab for providing data and code from their research, and to Jenny Adam for an early review of the flood study. Lastly, my heartfelt thanks to my wife, Carys, and children Rhys and Anya for their enthusiastic support and graceful sacrifice over the long haul.

This research was funded by the Joint Institute for the Study of the Atmosphere and Ocean (JISAO) under NOAA Cooperative Agreement No. NA17RJ

## 1. Introduction

Although in the past climate has frequently been assumed to be stationary in time, it is now widely recognized as an important variable affecting hydrologic processes at a number of different time scales (Cayan et al. 1998; Dettinger et al. 1998; Hamlet and Lettenmaier 1999a; Mote et al. 2003; Piechota et al. 1997; Redmond and Koch 1991; Sheppard et al. 2002). This improved understanding of the role of climate has resulted in major research initiatives to improve the understanding of climate dynamics and the impacts of climate variability and climate change on various scientific, engineering, and management problems. Understanding past hydroclimatic variability is a central component of this research. Historic observations are the basis for relating climatic variability to hydrologic processes, and provide the foundation for constructing and evaluating hydrologic models based on these physical relationships. Using models, it is possible to more fully analyze the impacts of climate in the observed record, and also to project the impacts of climate forwards in time with lead times ranging from a few months up to a century or more (Hamlet and Lettenmaier 2000).

Given suitable hydrologic simulation models and meteorological driving data sets, another important use of the observed climate record is to produce simulated hydrologic data as surrogates for long-term observations. Such an approach can improve the temporal and spatial resolution of observed hydroclimatic data, provide surrogates for unmeasured variables, and provide a means for more fully evaluating observed changes in climate and hydrologic variability at the regional and river basin scale. The use of models, for example, can facilitate clearly-defined diagnoses and sensitivity analyses that are not possible using observations alone. Models also facilitate the examination of relatively large areas in a consistent manner, avoiding problems with inconsistencies between observing systems, missing data, or other issues frequently encountered in the analysis of observed data. Furthermore, given that neither model simulations nor

observations are perfect realizations of the past, corroborating data from both sources greatly strengthens conclusions derived from analysis of the historic record.

Global warming and its complex expression at the regional scale has presented many new challenges to the scientific and resource management communities associated with understanding the nature and implications of a rapidly evolving climate system.

Although no attempt will be made here to rigorously attribute observed changes in regional scale climate to anthropogenic changes in the global climate system, there is a growing body of evidence that future hydrologic variability in the West may be systematically different from that of the past, particularly with regard to temperature related effects (e.g. Gleick 2000). Many climate models, for example, suggest that the western U.S. should be getting warmer and wetter in winter due to greenhouse warming and a resulting enhancement of the global hydrologic cycle (Dettinger et al. 2004; Gleick and Chalecki 1999; Mote et al. 2003; Stewart et al. 2004). Because these effects are gradually evolving over time, and at least for temperature are expected to continue for centuries, there is a need to understand the current extent of regional warming, its coincidence with global changes, how far it has progressed in relation to the expected trajectory in the 21st century, what areas are most sensitive to warming, and so forth. These issues, in general, cannot be adequately addressed using observed data alone due to limitations in the kinds of observations that are available and to their spatial and/or temporal resolution and coverage. In addition, retrospective investigations using models create a way for researchers to examine the extent to which the models used in forecasting future changes in hydroclimatic variability are successfully capturing the observed behavior in the historic record, an important issue associated with the design and implementation of global warming scenarios needed for long-term planning.

Another underlying goal of this research has been to place the projected future impacts of regional warming in the context of changes that have occurred in the historic record and are actively taking place in the present tense. Understanding what has happened (and is

currently happening) to the regional water cycle is arguably more effective than forecasting future impacts with lead times of several decades to a century, a time scale of prediction which has probably done more to foster indifference towards the impacts of warming on the part of many managers and planners than it has to promote an interest in adaptation (Gamble et al. 2003).

In the following chapters we will develop long-term temperature and precipitation data sets and employ macro-scale hydrologic simulation tools to examine some key features of hydroclimatic variability in the western U.S. This research is intended to improve the understanding of observed hydroclimatic variability in the western U.S. in the 20th Century and to examine linkages to climate variability at interannual and decadal timescales in the context of an evolving climate system. The research is motivated in part by the following scientific questions:

- How have variations in temperature and precipitation from the early 20th Century on (1916-2003) affected trends in hydrologic variables such as snowpack, volume and timing of runoff and baseflow, seasonal evaporation and soil moisture, and flood risk in the western U.S.?
- Is the warming that has occurred over the western U.S. consistent with global warming signals, and is it possible to make a clear distinction between “natural” variations and the effects associated with the regional expression of large scale warming? Are temperature and precipitation different in this regard?
- What role do regional climatic regimes and topographic variations play in defining the role of temperature and precipitation variability on hydrologic variations? What areas of the western U.S. are most sensitive to changes in temperature or precipitation changes and why?

- Do the hydroclimatic variations observed in the western U.S. over the 20th century corroborate simulations of climatic changes produced by global climate model scenarios? For instance, is a hypothesis of wetter conditions in the western U.S. due to an intensified global hydrologic cycle born out in the observations? If so, how have these changes affected hydrologic variability?
- How do flood risks vary in response to changing climate and how can these risks be characterized and predicted in the context of interannual and interdecadal climate variability and longer-term variations associated with the regional expression of global warming?

## **2. Overview of Hydroclimatic Foundation Research**

This chapter provides a brief overview of some hydroclimatic foundation research relevant to the investigations in subsequent chapters.

### **2.1. Climatic Variations in the Western U.S. Associated with ENSO and PDO**

The El Niño Southern Oscillation (ENSO) is a cyclical climate phenomenon which expresses itself as variability of sea surface temperature (SST), wind, and rainfall in the tropical Pacific Ocean. These patterns include changes in the location of tropical convection, which results in pronounced perturbations in the global climate system on seasonal to inter-annual time scales, particularly in the northern hemisphere winter. The ENSO has been the subject of intense research, and an extensive tropical Pacific Ocean monitoring system (the Tropical Atmosphere Ocean (TAO) observing system) has been put in place which, in conjunction with physical and statistical models, has resulted in substantial long-range forecasting skill for ENSO (Barnston et al. 1994; Battisti and Sarachik 1995; Latif et al. 1998; Trenberth et al. 1998 ). ENSO affects hydroclimatic variability in the western U.S. via changes in storm track behavior and winter temperatures (Dettinger et al. 1998; Piechota et al. 1997). In the Pacific Northwest (PNW), for example, warm ENSO events are typically associated with warmer and dryer winter conditions while cool ENSO years are typically associated with cooler and wetter winters (Hamlet and Lettenmaier 1999a; Mote et al. 2003).

The Pacific Decadal Oscillation (PDO) (Mantua et al. 1997; Zhang et al. 1997) is a low frequency ENSO-like phenomenon that is associated with decadal scale variations in winter climate in the western U.S. (Hamlet and Lettenmaier 1999a; Hidalgo and Dracup 2003; Sheppard et al. 2002) . In the PNW, for example, warm PDO epochs are associated with warmer and dryer winter conditions, whereas cool phase epochs are



typically cooler and wetter (Mote et al. 2003). There are also apparent interactions between the teleconnections associated with the PDO and the ENSO (Dettinger et al. 1998; Gershunov et al. 1998). Based upon observed data from the 20th century, for example, the two phenomena have their greatest effects in the PNW when they are “in phase” with each other. Warm PDO, warm ENSO years, for example, are frequently associated with below average winter precipitation and droughts in the PNW, whereas cool PDO, cool ENSO years are frequently associated with above average winter precipitation and river flow (Mote et al. 2003).

The physical processes that cause the decadal scale climate variations associated with the PDO are the subject of intense debate in the atmospheric science community. Some researchers argue that the PDO is not a true oscillatory climate phenomenon like the ENSO, but is rather the low frequency response of the global climate system to a particular sequence of ENSO forcing events (see e.g. Newman et al. 2003). Others argue that the PDO, while affected by ENSO, is also partially independent from ENSO and is coupled to the global climate system in other ways (perhaps with feedbacks influencing ENSO itself) that account for its observed persistence and the clear association with decadal climate variability (see e.g. Latif and Barnett 1994). A rigorous understanding of the predictability of the PDO and the physical causes of the observed abrupt transitions between predominantly warm or cool phase PDO epochs in the 20th century (sometimes called “regime shifts”) has not yet been established.

The use of an interannual PDO index value (as opposed to predominantly warm or cool PDO epochs) in the analysis of retrospective data yields comparable linkages to hydroclimatic variability in the PNW. This suggests that the PDO, while associated with a longer time scale of variation than ENSO, is also robustly linked to hydroclimatic variability at shorter time scales (Hamlet and Lettenmaier 1999a; Hamlet and Lettenmaier 2000). Furthermore, the time series of the PDO index (Mantua et al. 1997) is highly autocorrelated in time and is also strongly correlated on an interannual time

scale with ENSO. Consequently simple regression techniques based on the previous year's PDO index value and a forecast of an ENSO index (e.g. Nino 3.4) can be used to predict the coming mid-winter PDO index with considerable skill (Newman et al. 2003). Thus, in practical terms, it would appear to be possible to use forecasts of the interannual PDO index value in various climate applications with comparable lead times to those associated with ENSO forecasts.

Relationships between PDO and ENSO and hydroclimatic variability have been used in developing experimental streamflow forecasting applications using both resampling approaches and integrated climatic and hydrologic modeling systems (Clark and Hay 2004; Clark et al. 2004; Hamlet and Lettenmaier 1999a; Wood et al. 2002, 2005). In retrospective studies, like those presented in chapters 4, 5, and 6, the ENSO and PDO indices are useful as diagnostic indicator variables, which can be used to segregate the historic climate record into climatically similar periods in a consistent manner (e.g. Miles et al. 2000; Mote et al. 2003).

## **2.2. Climate Variability in the Context of Regional Warming**

Global change research has raised many important questions about the stationarity of climate and the relative roles of interannual and interdecadal climate variations (which are themselves potentially non-stationary in time) in comparison with more systematic long-term changes in the climate system due to global warming and its expression at the regional scale (IPCC 2001). Many recent studies have identified the potential loss of snowpack and resulting streamflow timing shifts in the western U.S. as a significant impact pathway associated with warming (Gleick 2000; Hamlet and Lettenmaier 1999b; Knowles and Cayan 2002; Lettenmaier et al. 1999; Mote et al. 2003). These effects are also apparent in observed records of western U.S. snowpack and streamflow over the last 50 years or so (Dettinger and Cayan, 1995; Mote et al. 2005; Stewart et al. 2005). Because of the relatively short observed record it has been somewhat uncertain to what

extent these observed changes are due to natural climate variability as opposed to more systematic changes occurring at longer time scales (such as the regional expression of global warming). These issues inform this dissertation's focus on quantifying the hydrologic changes that have taken place in the 20<sup>th</sup> century in the western U.S. and on improving the understanding of the underlying linkages to 20<sup>th</sup> century climatic variations.

### **3. Long-Term Precipitation and Temperature Data Sets**

This chapter summarizes and excerpts research published as:

Hamlet, A.F., Lettenmaier, D.P., 2005: Production of temporally consistent gridded precipitation and temperature fields for the continental U.S., *J. of Hydrometeorology*, 6 (3): 330-336

#### **3.1. Introduction and Background**

Digitized records of daily maximum and minimum temperature (TMAX and TMIN) and daily total precipitation (PCP) have been available for some time in electronic form from the National Climatic Data Service's Cooperative Observer (Co-op) network for the period from 1948 to a few months prior to the present time. These data have been gridded to produce long-term daily time step forcings for hydrologic models (e.g. Maurer et al. 2002) that in turn have been used in land surface water and energy balance studies (e.g. Maurer et al. 2001; Roads et al. 2003). These data have recently been extended in electronic form to the beginning of the archival record [National Climatic Data Center (NCDC) DSI-3206 product], resulting in the potential to produce relatively high resolution gridded data sets for most of the last century. Unfortunately, use of gridding methods like those described by Maurer et al (2002), or variations used by Cosgrove et al. (2003) are not generally appropriate for long-term trend analysis because of changes in stations and station locations over time. In the western U.S., for instance, changes in station locations imply changes in the representation of topographic effects on precipitation and temperature, and can result in spurious trends in precipitation and temperature, and any variables derived from them.

The motivation for this study came from problems initially encountered in attempting to use the data processing methods developed by Maurer et al. (2002) to produce longer precipitation and temperature records. Despite good results for recent decades, our first

attempts to create longer data sets back to 1915 using the DSI-3206 data sets revealed serious problems with temporal inhomogeneities. Simulated streamflows prior to 1950, for example, produced by essentially the same hydrologic models used by Maurer et al. (2002) were often strongly biased in comparison with those after 1950 (See e.g. Figure 3.2), and it was clear that long-term trends in simulated hydrologic variables would be strongly influenced (if not dominated) by the temporal inhomogeneities in the driving data.

Several issues must be considered in producing gridded meteorological data sets for hydrologic modeling studies. These issues include:

- quality control of the raw station data (including filling of voids, flagging of implausible values, corrections for measurement error, or adjustments for temporal inconsistencies in the data),
- criteria for accepting or rejecting a particular set of station records for use as input to the gridding process,
- choice of gridding techniques,
- techniques for adjusting precipitation and temperature for topographic variations not present in the raw data,
- and verification and evaluation of the final gridded data sets

We address some of these specific issues in this paper, however for the most part we take as our starting point the data processing techniques developed by Maurer et al. (2002). These specific techniques, although not necessarily optimal in every regard, have been found to produce high quality macro-scale hydrologic simulations from 1950-2000 over the continental U.S. (Maurer et al. 2002). On the basis of these consistently good results, we argue that these specific data processing methods are an appropriate and well-tested foundation for the research described here. There is no loss of generality in this choice, however, because the methods for making temporal adjustments to gridded data sets that

we develop here can be applied equally well to other gridded data sets produced by other procedures.

This chapter describes data processing methods to produce temporally and topographically adjusted meteorological driving data for hydrologic models that can be used to produce derived variables (e.g. soil moisture, snow water equivalent, runoff, and streamflow, among others) that are amenable to long-term trend analysis. The methods we have developed are efficient in the sense that they do not require detailed station metadata (which are frequently unavailable) or labor-intensive, station-by-station corrections. The temporal adjustment procedures are intended to maintain as much spatial information from the relatively high-density Co-op station network as possible, while adjusting the time series characteristics of the gridded data so that they have long-term trends consistent with gridded data sets derived from a smaller number of carefully quality-controlled stations from the U.S. Historical Climatology Network (HCN) (Karl et al. 1990) and the Historical Canadian Climate Database (HCCD) (Mekis and Hogg 1999; Vincent and Gullett 1999). The HCN and HCCD data archives are composed of long, continuous station records that have been corrected for changes in station location, instrumentation, time of observation, land use, etc.

## **3.2. Data Processing Methods**

### *Sources of Data*

Three primary sources of meteorological data are used in the data processing sequence. The first is the daily time step NCDC Co-op data, supplemented by station data from Environment Canada (ECAN) for southern British Columbia in the Pacific Northwest (PNW). The second is monthly time step HCN and HCCD data which are used as a “standard” in making temporal adjustments to the gridded Co-op data. The third is the monthly precipitation maps produced by the Precipitation Regression on Independent Slopes Method (PRISM) method of Daly et al. (1994) which are used for topographic adjustments to the precipitation data.

### ***Preprocessing, Quality Control, and Gridding***

Raw Co-op station data for TMAX, TMIN and PCP from 1915-2003 were first extracted from NCDC archives. For quality control purposes, upper limits were set on daily precipitation based on approximate climatological limits (from regional observations). Values less than zero or above the upper limit were removed and replaced with a missing data flag (-99). The same was done for TMAX and TMIN for values less than -50 C or greater than 55 C. These simple quality control checks were primarily intended to screen out implausible values due to, for instance, data entry errors or misinterpretation of data fields in written records. Stations that did not have at least 365 days of data with no gaps, or did not have at least 1825 total days (about five years) of data were also removed. This procedure typically retains more stations in the gridding process than were used by Maurer et al. (2002), who limited the stations to those with more than 20 years of data from 1950-2000.

The data were then gridded to 1/8-degree latitude longitude resolution using the Symap algorithm (Shepard 1984 as applied by Maurer et al. 2002) using four nearest neighbors. The target grid points were the center of each 1/8 degree grid cell. During the gridding process TMAX and TMIN were both lapsed by the pseudo adiabatic lapse rate (6.1 C per km) to account for differences between the target grid point and the elevations of the nearest stations used in the interpolation. These steps are identical to those described by Maurer et al. (2002). Exactly the same gridding process was applied to the monthly time step HCN and HCCD data except the number of nearest neighbors for PCP gridding was increased to 15 in the Symap algorithm to prevent sharp discontinuities in the gridded data as a result of the relatively low station density.

### ***Temporal Adjustments***

The next step was to perform temporal adjustments to the Co-op data set. First, the gridded daily time step Co-op data were aggregated to monthly time step and both the monthly Co-op and HCN/HCCD data were indexed by calendar month. Then, for each

calendar month, both the Co-op and HCN/HCCD time series were temporally smoothed using a Butterworth filter (Hamming 1989). The time series was filtered forwards and backwards to remove the phase shift, using the long term mean of the time series as initial starting values for the filter. The parameters used in the filtering process result in a temporal smoothing roughly equivalent to a three month running mean (Figure 3.1). The choice of filtering parameters was based primarily on the criterion (five years of available data) for including a Co-op station in the gridding process. In other instances a different filtering choice might be more appropriate. In general decreasing the low pass cutoff frequency in the filter (i.e. more temporal smoothing) allows more spatial information from the Co-op data to remain in the final product, but also decreases the response time to sudden changes in the Co-op data time series. Occasionally, filtering of monthly precipitation data produced small negative values. These values were reset to zero. For each month in the gridded time series, the smoothed values were compared between the two data sets, and a new monthly value was obtained for the gridded Co-Op data as follows:

For TMAX and TMIN:

$$\text{Co-opADJ}(t) = \text{Co-opRAW}(t) + [\text{HCNHCCDFILT}(t) - \text{Co-op FILT}(t)]$$

For PCP:

$$\text{Case 1: } [\text{HCNHCCDFILT}(t) - \text{Co-op FILT}(t)] \geq 0$$

$$\text{Co-opADJ}(t) = \text{Co-opRAW}(t) + [\text{HCNHCCDFILT}(t) - \text{Co-op FILT}(t)]$$

$$\text{Case 2: } [\text{HCNHCCDFILT}(t) - \text{Co-op FILT}(t)] < 0$$

$$\text{Co-opADJ}(t) = \text{Co-opRAW}(t) * [\text{HCNHCCDFILT}(t) / \text{Co-op FILT}(t)]$$

Where  $\text{Co-opADJ}(t)$  is the adjusted monthly value for the Co-op data at time  $t$ ,  $\text{Co-opRAW}(t)$  is the unadjusted monthly value for the Co-op data at time  $t$ ,  $\text{HCNHCCDFILT}(t)$  is the value of the smoothed HCNHCCD time series at time  $t$ , and  $\text{Co-op FILT}(t)$  is the value of the smoothed raw Co-op time series at time  $t$ . The two



cases for rescaling the precipitation values were introduced to avoid unreasonably large multiplicative corrections that can occur in case 1, and potential negative precipitation values in case 2.

Once the monthly Co-op values were adjusted in this manner, all the values for each calendar month were reassembled into a single gridded time series. The final adjustment step was to force the daily time step Co-op data to reproduce the adjusted monthly values by rescaling the daily values within each month. That is:

For PCP:

$$\text{Daily\_Co-opRESCALED}(t) = \text{Daily\_Co-opRAW}(t) * [\text{Co-opADJ}(T) / \text{Co-opRAW}(T)]$$

For TMAX and TMIN:

$$\text{Daily\_Co-opRESCALED}(t) = \text{Daily\_Co-opRAW}(t) + [\text{Co-opADJ}(T) - \text{CoopRAW}(T) ]$$

Where  $t$  is the day in the daily time series, and  $T$  is the month in the monthly time series in which the day  $t$  occurs. Note that PCP values are daily and monthly totals, and TMAX and TMIN values are daily values and monthly averages.

It should be noted that the objective of the procedures described above is to remove gross temporal inconsistencies in the daily Co-op data at the time scale of the temporally filtered data. Spatial information at the daily time step is retained from the Co-op data, and even the monthly Co-op data are not required to exactly match the equivalent HCN/HCCD monthly values. Rather only the two smoothed time series are forced to match each other. In this way trends in the final data closely match those in the more temporally homogeneous HCN and HCCD data, without forcing a perfect match between the gridded HCN HCCD data and the gridded Co-op data that would effectively remove the increased spatial information from the Co-op data (Figure 3.1).

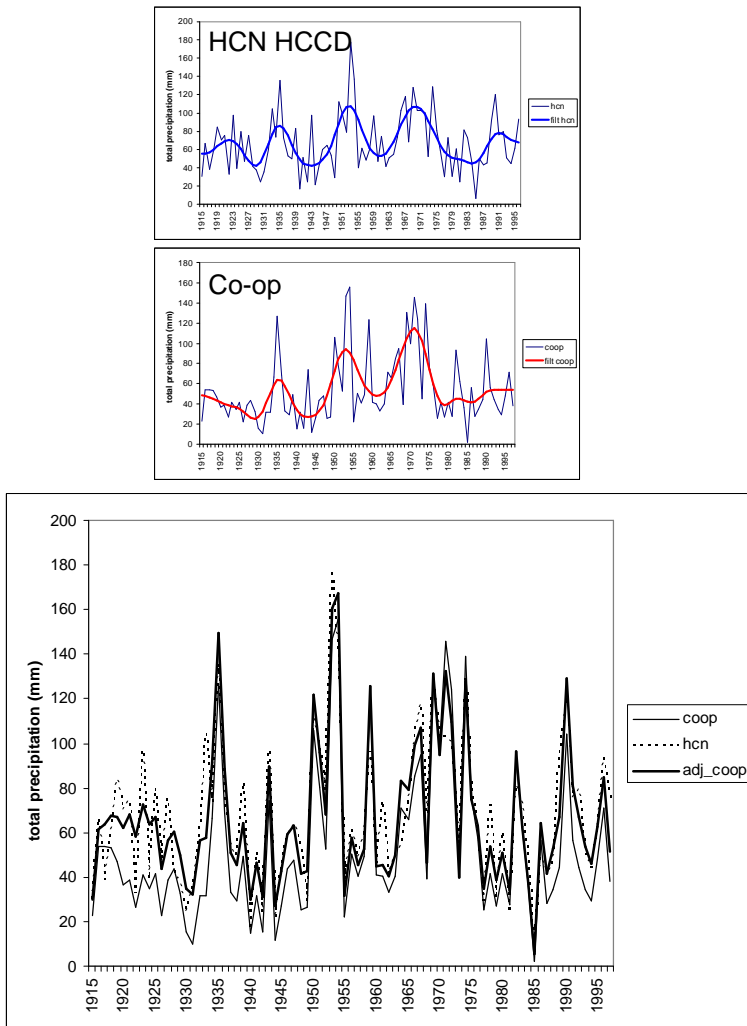


Figure 3.1: Example of temporal corrections for January precipitation at a single grid location. Upper panels show temporally smoothed monthly time step Co-op and HCN HCCD data. Lower panel shows HCN HCCD data, unadjusted monthly Co-op data, and the adjusted monthly Co-op data.

### *Topographic Adjustments*

Once the temporal adjustments were applied to the daily time series, the topographic adjustments to precipitation described in Maurer et al. (2002) were carried out. These adjustments, which were indexed to the period 1961-1990, forced the long term mean of the temporally adjusted Co-op data for each grid cell to match those in the PRISM precipitation maps (Daly et al. 1994). Although here we followed the simple procedure outlined by Maurer et al. (2002) for adjusting temperature data for topography (discussed

above), similar methods to those used for topographic adjustment of precipitation could also be used to adjust temperature data.

### *Wind Data*

In addition to precipitation and temperature and other variables derived from these data (e.g. downward solar and longwave radiation, and specific humidity) hydrologic models (and in particular the Variable Infiltration Capacity model described below) also use estimates of daily 10m wind speed, which Maurer et al (2002) took from the NCEP-NCAR Reanalysis (Kalnay et al. 1996). The reanalysis products are available from 1949 on; prior to 1949, a daily wind climatology derived from the post 1949 period was used.

## **3.3. Results**

### *Macro Scale Evaluation of Results Using Naturalized Streamflow Data*

We simulated daily time step streamflow (subsequently aggregated to monthly) using the Variable Infiltration Capacity (VIC) model (Liang et al. 1994; Cherkauer and Lettenmaier 2003) driven by the adjusted gridded forcing data. The VIC model was implemented at 1/8th degree spatial resolution over the western U.S., and was run in daily water balance mode with a one hour snow model time step (see Hamlet et al. 2004 for additional VIC implementation details). The models had been calibrated using data from 1950-2000, and the model was not recalibrated for the period prior to 1950.

To evaluate the effect of the adjustments to the driving data described above we compared VIC simulations for “adjusted” and “unadjusted” driving data sets for the Pacific Northwest. Both driving data sets were derived from exactly the same station records and were processed in an identical manner, except the “unadjusted” data set did not include the temporal corrections. Simulated streamflow records from VIC were compared with naturalized streamflow observations (water management effects removed) for sixteen locations in the Columbia River Basin. All of these sites are snowmelt dominant and most of the annual runoff occurs from April-September. After about 1950,

characteristic differences between simulated streamflows derived from the adjusted and unadjusted data sets are relatively small in comparison with the pre-1950 period. As an example, Figure 3.2 (upper panel) shows a time series of April-September average streamflows for the South Fork Flathead River at Hungry Horse Dam from 1931-1989 for unadjusted VIC simulations, adjusted VIC simulations, and naturalized observations. Figure 3.2 (lower panel) shows a time series of the absolute errors for the two VIC simulations relative to the observed data. Prior to about 1950, the simulations based on the unadjusted met data are very strongly biased in comparison with the post-1950 period, and the time series of absolute errors (Figure 3.2b) displays an obvious downward trend with time due to spurious trends in precipitation in the unadjusted gridded data set. By contrast the simulations associated with the adjusted met data show relatively stationary error characteristics over time. Note that this particular basin is fairly small (~4280 km<sup>2</sup>), and the loss of spatial information associated with the temporal adjustments appears to reduce the accuracy of the simulations in a few years in the post-1950 period. In larger basins, loss of spatial information is less important and the simulations derived from adjusted and unadjusted data sets are typically in very close agreement after about 1950.

Figure 3.3 shows a scatter plot of the root mean square error (RMSE) for the time series of April-September average streamflow derived from the “adjusted” (x axis) and “unadjusted” (y axis) VIC simulations from 1931-1950 for sixteen sites in the Columbia Basin. Note that the adjustment procedure tends to produce robust improvements prior to 1950: either reducing the RMSE or leaving it essentially unchanged. Although a long unadjusted driving data set for testing was only produced for the Pacific Northwest, VIC streamflow simulations in the Colorado and Sacramento/San Joaquin basins were also compared with naturalized observations and were found to have stationary error characteristics throughout the time series using the temporally adjusted met data.

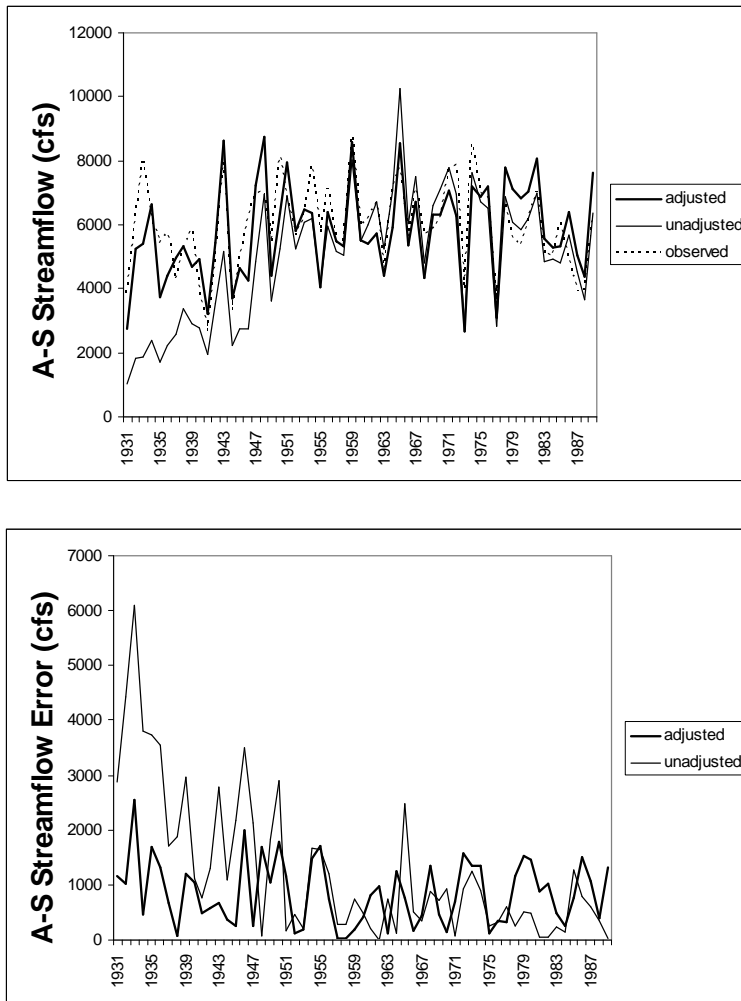


Figure 3.2: Comparison of “adjusted” and “unadjusted” VIC simulations and naturalized observations for the S.F. Flathead River at Hungry Horse Dam, MT. Upper panel shows a time series of April-September average streamflow from 1931-1989. Lower panel shows a time series of absolute error for the adjusted and unadjusted streamflow simulations from 1931-1989.

In larger sub basins, the agreement with observations over the entire time series was quite good for the most part. These evaluations demonstrate that the temporal corrections to the driving data sets result in temporally homogeneous monthly water balance simulations for a wide range of topographic and climatic conditions throughout the West without any recalibration of the hydrologic model for the earlier parts of the record.

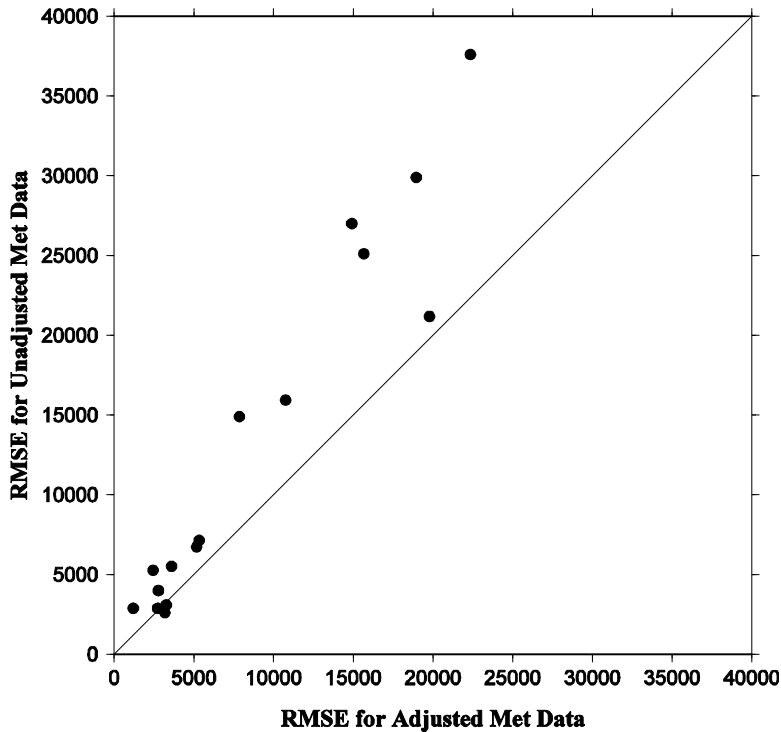


Figure 3.3: Root mean square error for simulated April-September average streamflow from 1931 to 1950 relative to naturalized flow observations for sixteen locations in the Columbia River basin shown as a scatter plot with the RMSE associated with “adjusted” data on the x-axis and RMSE associated with “unadjusted” data on the y axis.

### ***Macro Scale Evaluation of Results Using Observed Snow Water Equivalent***

Comparison with relative trends in April 1 snow water equivalent (SWE) from snow course observations also show excellent broad-scale agreement between the VIC simulations and observations over the West for the last 50 years (see Mote et al. 2005 and Hamlet et al. 2005 for details). For the model to be able to reproduce these spatial and temporal features of snow accumulation and melt, the meteorological forcing data must accurately represent both the time history and topographic characteristics of both temperature and precipitation over a wide range of conditions.

### ***Data Availability and Archiving***

At the time of this writing the forcing data sets and associated hydrologic testing were complete for river basins west of the continental divide, and are available at the web site [www.hydro.washington.edu/Lettenmaier/gridded\\_data/index.html](http://www.hydro.washington.edu/Lettenmaier/gridded_data/index.html). The forcing data set

for the continental US will be completed over the next six months to a year and will be made publicly available at the same URL. Archival details have not yet been decided, but the data will be available in a comparable format to the previous forcing data sets described by Maurer et al. (2002).

### **3.4. Summary and Conclusions**

Without temporal adjustments, long-term gridded meteorological data sets frequently contain significant temporal inhomogeneities that prevent meaningful trend analysis of simulated hydrologic variables. The data processing procedures described in this paper are shown to produce meteorological driving data sets that are temporally consistent over long periods of record. Based on VIC hydrologic simulations from 1916-2003 and comparison to observations of streamflow and snow water equivalent, we conclude that the meteorological forcing data produced by these methods (and the associated hydrologic simulations) are broadly suitable for trend analysis of simulated hydrologic variables at the macro scale.

Although these data processing methods were implemented to produce meteorological forcing data sets in the continental U.S. and southern British Columbia, they are equally suitable for other areas of the globe for which there are long, temporally consistent station records and appropriate data upon which to base topographic adjustments to precipitation. Use of the data from the Global Historical Climatology Network, for example, would permit the temporal corrections described here to be applied to many developed areas outside the U.S. (e.g. in Europe and Asia).

## **4. Effects of 20<sup>th</sup> Century Warming and Climate Variability on Snowpack Trends**

This chapter summarizes and excerpts research published as:

Hamlet, A.F., Mote, P.W., Clark, M.P., Lettenmaier, D.P., 2005: Effects of temperature and precipitation variability on snowpack trends in the western U.S., *J. of Climate*, 18 (21): 4545-4561

### **4.1. Introduction and Background**

Snowpack is crucial to the water resources of the western U.S. (Serrese et al. 1999). A dominant fraction (by some accounts more than 70 %) of streamflow in the western U.S. originates as melting montane snowpack. Over most of the western U.S., precipitation in the mountains is strongly winter-dominant and snow accumulation (along with storage in the soil and groundwater) are the primary physical mechanisms by which winter precipitation is stored and transferred to the relatively dry summers. For river basins with substantial snow accumulation, scenarios of increasing winter and spring temperatures in climate change assessments typically result in increased winter runoff, reduced peak water equivalent stored as snow, earlier peak streamflows, and reduced summer streamflow volumes (e.g. Cayan 1996; Dettinger et al. 2004; Gleick and Chalecki 1999; Gleick 2000; Hamlet and Lettenmaier 1999b; Lettenmaier and Gan 1990; Leung et al. 2004; Knowles and Cayan 2002; Lettenmaier et al. 1999; McCabe and Wolock 1999; Mote et al. 2003; Service 2004).

Observational studies have also shown increasing trends in both temperature and precipitation over the western U.S. in the 20<sup>th</sup> century (McCabe and Wolock 2002; Mote et al. 2003, Mote 2003a; Shepard et al. 2002) and wide-spread trends towards earlier runoff timing in the western U.S. associated with earlier spring snowmelt (Dettinger and



Cayan 1995; Stewart et al. 2005; Reganda et al. 2004). Mote (2003b) examined trends in April 1 SWE for the U.S. Pacific Northwest (PNW) and Mote et al. (2005) have extended the earlier study to examine snow course records over the entire western U.S. and southern British Columbia (BC). These studies both show strong downward trends in April 1 SWE over most of the domain from about 1950 onwards. Mote et al. (2005) also corroborated observed SWE trends by comparing simulated and observed SWE trends from 1950 to 1997 and used correlations between April 1 SWE and winter temperatures to show that temperature trends were a major driver of these observed trends, particularly at moderate elevations with relatively warm winter temperatures. The role of temperature and precipitation in determining snowpack variations was also examined by Serrese et al. 1999.

Observed data provide direct empirical evidence of trends in SWE over the western U.S., but model simulations are needed to corroborate and extend these observations in order to avoid problems with limited spatial coverage, coarse temporal resolution, and longevity of observed data sources (see also Mote et al. 2005). Observations from snow course measurements (i.e. direct measurements of average SWE over a small transect), for example, have had a reasonably consistent level of coverage over the western U.S. for the period from about 1950-present, but the number of observations declines rapidly prior to 1950, and coverage is very uneven before about 1940 (Mote et al. 2005). These changes in station density prevent a consistent analysis for a period of record longer than about a half century. This is important because the period of record 1950-present has been shown to contain substantial (and regionally specific) trends in precipitation and temperature that are strongly influenced by climatic variability associated with the El Niño Southern Oscillation (ENSO) and the Pacific Decadal Oscillation (PDO) (Dettinger et al. 1998, Gershunov and Barnett 1998; Hamlet and Lettenmaier 1999a; Hidalgo and Dracup 2003; Mantua et al. 1997; Mote et al. 2003; Shepard et al. 2002). In particular, the precipitation trends that accompany the well-known shift in the PDO from cool phase to warm phase in 1976-1977 (Mantua et al. 1997) are a confounding element in the

attempt to attribute observed losses of SWE from 1950-present to long-term changes in climate.

Another important issue is that observations of SWE are representative of only a small subset of the spatial domain, and relatively few observations are available at very high elevations or in the transient snow zone where winter snowpacks are ephemeral. These areas that are not well observed are a dominant fraction of the land area and of the SWE contributing to streamflow in the mountainous western U.S. and, in the case of the transient snow zone, they represent one of the most sensitive areas to warming. Thus a comprehensive understanding of long-term changes in western U.S. snowpacks and associated water resources impacts requires attention to not only a period of record longer than the last 50 years, but to parts of the domain not covered by the snow course observations, the locations of which were dictated by short-term water supply forecasting needs, rather than detection of the impacts of climate variations.

In addition, snow course observations lack temporal resolution (they are typically reported only on the first of the month), and are unavailable before mid-winter at most stations. Automated observations of SWE via the Natural Resources Conservation Service Snowpack Telemetry (SNOTEL) network are available at daily time step throughout the snow season, but the longest records available for these observations go back only slightly more than 20 years in all but a few isolated cases. Thus observations alone cannot provide useful information about long-term trends in patterns of snow accumulation and melt (such as date of peak accumulation, date of 90% melt, etc.).

While the use of model simulations introduces uncertainties into the analysis that are not present in observational studies, these uncertainties can be minimized if the model forcing data are carefully quality controlled, and the use of model simulations avoids a number of important limitations in the observed data sets discussed above. Here we examine simulations of spring SWE on March 1, April 1, and May 1, with particular

attention to the critical April 1 date, which corresponds roughly to the date of maximum snow accumulation over much of the mountainous western U.S.. By isolating the effects of temperature and precipitation trends in the model's forcing data set in separate model runs, we also use the model to examine explicitly the effects of temperature and precipitation variability on SWE trends. The role of decadal-scale variability on SWE trends is also examined by selecting periods of record for analysis that reflect known shifts in decadal variability associated with the PDO (Mantua et al. 1997).

It is worth noting here that the trends in precipitation in the PNW appear to be consistently related to the PDO time series (i.e. dry to wet from 1925 to 1976 associated with warm to cool PDO; and wet to dry from 1947 to 2003 associated with cool to warm PDO) (Hamlet and Lettenmaier, 1999a; Mote et al. 2003; Mote 2003a), whereas a consistent relationship between precipitation trends and the PDO over time is not necessarily apparent in other parts of the domain, perhaps most notably in the Colorado River basin (Hidalgo and Dracup 2003).

The questions that motivate this paper are: 1) To what extent are observed trends in western U.S. snowpack attributable to precipitation and temperature trends, and how do these effects vary with region, topography, climate and the time period examined? 2) What areas of the western U.S. show the greatest trends in simulated snowpack, and what are the specific climatic regimes associated with these areas? 3) What is the role of decadal climate variability in determining the observed snowpack trends? 4) What changes in the timing of snow accumulation and melt are apparent and how do they vary with region, topography, and climate?

## **4.2. Hydrologic Model and Meteorological Driving Data**

### *VIC Hydrologic Model*

We use the Variable Infiltration Capacity (VIC) hydrologic simulation model (Liang et al. 1994; Cherkauer and Lettenmaier 2003) implemented at 1/8 degree

(latitude/longitude) spatial resolution over the western US and southern BC. The 1/8 degree grid cells are roughly 12km by 10km, varying in size to some degree with latitude over the domain. Daily SWE for each grid cell (which represents the areal average SWE for the mosaic of elevation bands and vegetation types within the cell) is the primary output used in this study. SWE simulations from each elevation band were also used for comparison with point data from the snow course records, although these results are only briefly discussed here. We do not examine other variables from the simulations in this study, but the model also simulates a detailed water balance in each cell. Simulated daily runoff from the model produced by the runs in this study will be used in subsequent studies to examine changes in the water balance associated with changes in snow accumulation and melt. The VIC model has been used in numerous climate studies of large river basins around the world (e.g. Nijssen et al. 2001), and has been well validated with streamflow observations, particularly in the mountainous western U.S. (Christensen et al. 2004; Hamlet et al. 2006 (Chapter 6); Hamlet and Lettenmaier 1999b; Maurer et al. 2002; VanRheenen et al. 2004). The model has also been used extensively for streamflow forecasting applications (Hamlet and Lettenmaier 1999a; Hamlet et al. 2002; Wood et al. 2002) and for climate change assessments (Christensen et al. 2004; Hamlet and Lettenmaier 1999b; Payne et al. 2004; Snover et al. 2003, VanRheenen et al. 2004; Lettenmaier et al. 1999). For this study we primarily make use of the detailed energy balance snow model incorporated in the VIC model (Cherkauer and Lettenmaier 2003). The snow model is well suited for simulating mountain snowpack and includes the effects of forest canopy on snow interception and the attenuation of wind and solar radiation, which are fundamental drivers of snow accumulation, sublimation, and melt processes (Storck 2000; Storck et al. 2002).

### ***Meteorological Driving Data***

For this study, a new climate data set was developed following methods outlined by Hamlet and Lettenmaier (2005)(Chapter 3). This data set was intended specifically for application to problems where careful quality control to avoid spurious trends in long

records of daily temperature and precipitation is necessary. Daily values of maximum temperature, minimum temperature, and total precipitation were obtained for 1915-2003 at the 1/8 degree latitude-longitude spatial resolution by interpolating daily values from National Weather Service Cooperative Observer stations using the Symap algorithm (Shepard 1984) following methods described in Maurer et al (2002). Temperatures were lapsed by  $6.1^{\circ}$  C per km (i.e. the theoretical moist adiabatic lapse rate) during the interpolation process, and precipitation was scaled for topographic effects using monthly precipitation maps produced by the PRISM algorithm (Daly et al., 1994). Maurer et al. (2002) describe these data processing steps in more detail. Temporal inhomogeneities (e.g. inconsistencies in time due to changing station groups, station moves, changes in instrumentation, urban heat island effects, etc.) in the regridded time series were adjusted for each calendar month using regridded and temporally smoothed data from the US Historical Climatology Network and the monthly Historical Canadian Climate Database. Additional technical details are available in Hamlet and Lettenmaier (2005)(Chapter 3).

Despite the fact that the model forcing data are carefully quality controlled, there are inevitably some limitations associated with the approach. One is that the gridded (precipitation and temperature) forcing data are derived primarily from low or moderate elevation stations. Because the trends in the temperature and precipitation data are ultimately derived from the time series of these low elevation stations, there is no explicit information contained in the driving data set regarding potentially different trends at very high elevations. In some parts of the domain, the primary driving data are also quite sparse, which may result in gridded data that may artificially suppress spatial variability, especially at short (e.g. daily) time steps. Topographic adjustments to the precipitation and temperature data (discussed above) likewise tend to suppress spatial variability in the gridded product. These limitations in the forcing data, while important for high resolution modeling applications, are generally of secondary importance here. One major reason is that snow accumulation and ablation in mountainous regions is dominated by the characteristics of accumulated precipitation in snowpacks, and issues associated with

suppression of spatial variability tend to be filtered out. In any event, the model is able to reproduce observed trends in spring snowpack quite well at a macro scale over the western U.S. (as discussed below), hence it meets the requirements for a study such as ours that focuses on macroscale aspects of the snow accumulation and ablation process.

### ***Role of Temperature and Precipitation Driving Data in the Snow Simulations***

The relationship between hourly snowfall and precipitation estimates in the model forcing data is fairly straight-forward. The phase of the precipitation is determined by a simple partitioning scheme based on estimated hourly time step temperatures (derived from  $T_{max}$  and  $T_{min}$ ) during the simulation. Temperatures below  $-0.5\text{ }^{\circ}\text{C}$  are assumed to result in precipitation that is 100% snow, those above  $0.5\text{ }^{\circ}\text{C}$  are assumed to result in 100% rain, and a linear relationship is assumed between these two extremes.

Temperature driving data play a much more complex role in the simulations. Aside from the direct effects of temperature on convective heat transfer from the air to the snowpack (e.g. Storck 2000), temperature also affects snow accumulation and melt in the model due to meteorological variables that are derived from the temperature data. The difference between  $T_{max}$  and  $T_{min}$  determines the attenuation of solar radiation and variations in long-wave radiation due to cloudiness, for example, and  $T_{min}$  is used in calculating the dew point and vapor pressure deficit which influence snow sublimation (Thornton and Running 1999). Thus trends in temperature are also indirectly related to trends in long and short wave radiation, humidity, and vapor pressure contributing to sublimation and snowmelt and in the model. When we refer to “temperature related trends” in later sections of the paper, we are referring to trends associated with these indirect effects as well.

### ***Evaluation of Simulated SWE trends***

In corroborating trends in observations with the model results from this study, Mote et al. (2005) show remarkable broad-based agreement over the western U.S. between observed trends in April 1 SWE from 1950-1997 and trends derived from VIC simulations of SWE

for the same period. Although some differences in the absolute value of relative trends are apparent, it is clear that the model successfully captures the large-scale characteristics of the spatio-temporal trends of snow accumulation and melt over the western U.S.. It is largely on the basis of this comparison and the longer streamflow comparisons discussed by Hamlet and Lettenmaier (2005)(Chapter 3) that we argue that the model results provide a reasonable surrogate for observations from 1916 to 2003 and are suitable for a trend analysis at these spatial scales.

It should be noted however that on a point by point basis, there are often substantial differences between the SWE observations analyzed by Mote et al. 2005 and the VIC simulations, both in absolute value and in relative trends. These differences between simulations and observations are primarily due to the fundamental differences in spatial scale between observations and simulations, and to frequent discrepancies between the actual precipitation and temperature at snow course sites (a point within the VIC cell) and the gridded meteorological driving data used in the VIC simulations. Snow courses are also generally located in open areas, which is inconsistent with the VIC simulations in parts of the domain with substantial forest canopy.

The issues associated with the model forcing data are to be distinguished from validation of the VIC snow model itself. When the model is driven by accurate temperature, precipitation and vegetation characteristics (i.e. in locations where there is a nearby meteorological station and detailed information about the vegetation), the model very closely reproduces daily snow accumulation measurements recorded at these same locations (see e.g. Storck 2000). Furthermore, additional analysis (not shown) found good general agreement between monthly VIC snow accumulation and melt statistics (e.g. date of peak snow accumulation, volume of accumulation and melt in each month, etc.) and those extracted from daily time step observations from SNOTEL stations. These comparisons with the SNOTEL observations helps to confirm that the VIC model

captures the primary physical mechanisms associated with winter climate and topography that ultimately determine trends in mountain snowpack.

Mote et al. (2005) also examined the model's ability to capture the relationship between winter temperature regimes and trends in April 1 SWE in the observations from 1950 to 2003. The model successfully reproduces this relationship over most of the western U.S., however in some specific parts of the domain the model does display some bias. There are, for example, some apparent systematic errors in the trends in high elevation precipitation in the Sierra Nevada Mountains in the model forcing data that result in a general bias towards smaller simulated upward trends in the high elevation areas in the southern part of the domain, and there are larger downward trends in simulated SWE at moderate elevations in California from 1950 to 1997 than are apparent in the observations. In the case of the lower elevation sites in CA, this problem might be partly attributable to sampling bias in the observations, or to inaccurate temperature lapse rates in spring when the weather is clear (i.e. the model forcing temperatures are probably biased towards warmer temperatures on clear days at high elevations because of the assumption of a fixed pseudo-adiabatic lapse rate--see Hamlet and Lettenmaier 2005 (Chapter 3)).

### **4.3. Methods and Experimental Design**

The VIC model (version 4.0.5) was run from 1915 to 2003 at 1/8-degree resolution over the 16526 grid cells that comprise the continental U.S. west of the Continental Divide, plus the portion of the Columbia River Basin that lies in southern British Columbia (see Figure 4.1). In the following we will refer to the Pacific Northwest (PNW), California (CA), Colorado River Basin (CRB), and Great Basin (GB) as sub-regions of this domain. The snow model time step was one hour, which was required to capture the effects of the diurnal cycle of temperature and solar radiation on snow accumulation and melt. In the absence of shorter time step observations, daily total precipitation was equally distributed throughout the 24 hours of the day. To represent subgrid topographic variability, the



model uses up to five equal-area elevation bands with a vertical interval of approximately 500 m. Simulated SWE values are reported as the area weighted average SWE over all the elevation bands in each cell, each of which includes a vegetation mosaic comprised of up to 10 vegetation types. The vegetation characteristics of each cell were assumed to be stationary with time in the simulations. Note that the SWE values reported from the model represent the average snow water content over the entire grid cell which can be quite different from the value that would be simulated for any particular point location within the cell. Elevation bands in each grid cell with July mean temperatures below 10° C were assumed to be above the tree line (Körner 1998) and vegetation classes with an overstory (if any) were removed from these bands during the simulation. The first nine months of the simulation (Jan 1, 1915-Sept 30, 1915) were used as model spin up and were discarded. This spin up is adequate for snow simulations, for which there is essentially no year to year carryover effect. Figure 4.1 shows the 1/8<sup>th</sup>-degree digital elevation model for the simulation domain, average DJF temperatures for each grid cell, and average Nov-March precipitation summarizing the model forcing data.

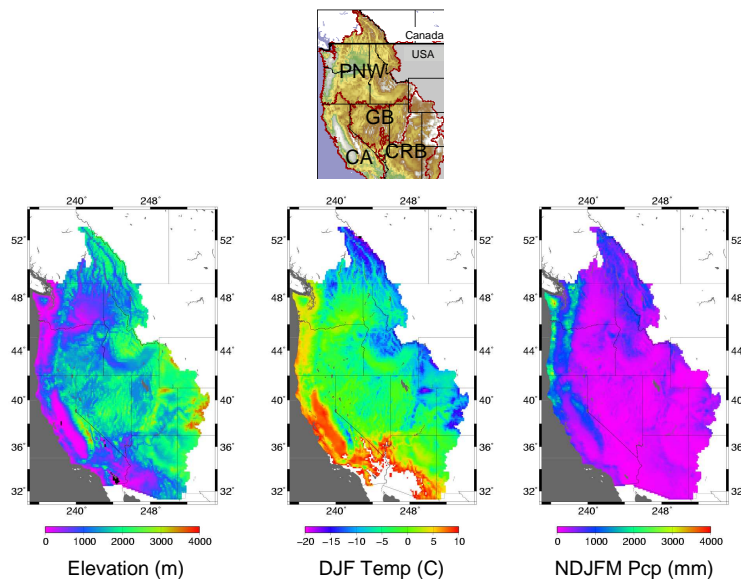


Figure 4.1 Topographic and climatic characteristics of the 1/8<sup>th</sup> degree VIC hydrologic model simulation domain

Three different model runs were made:

- 1) Base Run: Unperturbed precipitation and temperature data from the meteorological input files (daily total precipitation and minimum and maximum temperature and wind speed) were used to drive the model. Trends in SWE are the result of both temperature and precipitation variations.
- 2) Fixed Precipitation (fixed P) Run: The precipitation forcing data were fixed (for each calendar month) at the climatological value for each grid cell, but daily temperature was allowed to vary as in the original time series. Trends in SWE are the result of trends in temperature and other temperature-related meteorological variables alone.
- 3) Fixed Temperature (fixed T) Run: The temperature forcing data were fixed (for each calendar month) at the climatological value for each grid cell, but daily precipitation varied as in the original time series. Trends in SWE are the result of precipitation trends alone.

For the fixed P and fixed T runs, the forcing data were perturbed as follows: For each grid cell, a monthly climatological value for either precipitation or temperature was calculated for each calendar month (i.e. a separate climatology for January, February, etc.). Then the daily time series of the variable to be held constant was forced to reproduce this climatological value in each month of the simulation – that is, the daily values were allowed to vary within the month as in the original time series, but the monthly totals (precipitation) or averages (maximum and minimum temperature) in each calendar month are identical in each year of the simulation. This method preserves the daily covariance between temperature, precipitation, solar radiation, etc., while removing the trends and monthly variation in the fixed variable from the simulation. Note that an average seasonal cycle remains in the fixed variable after this adjustment. Wind data

were allowed to vary as in the original time series in each case. If precipitation and minimum and maximum temperature were all held fixed as described above, the mean of the resulting simulated SWE would be comparable (but not equal) to the long-term mean for each calendar date in the base simulation and any trends in the simulated SWE would be small. It should be noted that the *timing* of precipitation within the month is unaffected by these adjustments. This has some important implications when evaluating the fixed P trends in the calendar date of 10% snow accumulation discussed in later sections, for example.

March 1, April 1, and May 1 SWE values were extracted from the model output files for four time periods based on warm and cool PDO epochs defined by Mantua et al. (1997) as follows:

- A) 1916-2003 (full period)
- B) 1925-1976 (warm PDO to cool PDO)
- C) 1947-2003 (cool PDO to warm PDO)
- D) 1925-1946 concatenated with 1977-2003 (warm PDO to warm PDO)

Linear trends were calculated for the time series for each grid cell, and were normalized by the long term mean of the simulated April 1 SWE for each cell over the time period of analysis (i.e. the trends for scenario “C” were normalized by the mean SWE calculated from the 1947-2003 data). Cells included in the plots were required, on average, to have at least 50 mm of SWE on April 1 in order to avoid including spurious trends in the analysis.

For each grid cell, a time series of the date of peak SWE [day 1 = Sept 1, day 365 (or 366 in leap years) = Aug 31] was extracted from the daily time series of simulated SWE, as well as the day associated with 10% of peak accumulation and 90% melt. Linear

trends were calculated for each of these variables from 1916 to 2003 for the Base, fixed P and fixed T simulations.

#### **4.4. Results and Discussion**

##### *Notes on Presentation of Results and Interpretation of Figures*

The results in this section will be summarized primarily using spatial plots of the trends in SWE in each grid cell and scatter plots showing the relationship between average mid-winter (DJF) temperatures in each cell and the trends in SWE. The dots in the scatter plots are color coded so that the different regions in the domain can be distinguished. By comparing the patterns in these figures for the base, fixed P and fixed T runs, qualitative conclusions about the effect of temperature and precipitation trends on the overall trends can be drawn. DJF average temperatures for each grid cell used in the scatter plots of trend vs. winter temperature were calculated from the VIC driving data from 1916 to 2003 and are independent of the period of analysis used.

##### *SWE Trends for March 1, April 1, and May 1 for 1916-2003 (“A”)*

To begin with, we show overall trends in simulated SWE for March 1, April 1, and May 1 for the base run from 1916 to 2003 (Figure 4.2). As noted above, only grid cells with average SWE greater than 50 mm on April 1 are shown. The results show downward trends over many grid cells in the domain, and a relationship between mid-winter temperatures and the relative trends in SWE characterized by an inverted “J” shape in the scatterplots. As we shall see in subsequent sections this relationship is characteristic of downward trends in snowpack associated with warming. Downward trends in SWE on April 1 and May 1 are more widespread than for March 1. A substantial part of the domain shows upward trends in SWE, particularly over much of the Columbia River basin. As we shall see in subsequent sections, these upward trends in SWE are primarily due to upward trends in precipitation. The increased scatter for May 1 that is evident in Figure 4.2 is probably due to the fact that many grid cells have relatively small amounts of snow remaining on May 1.

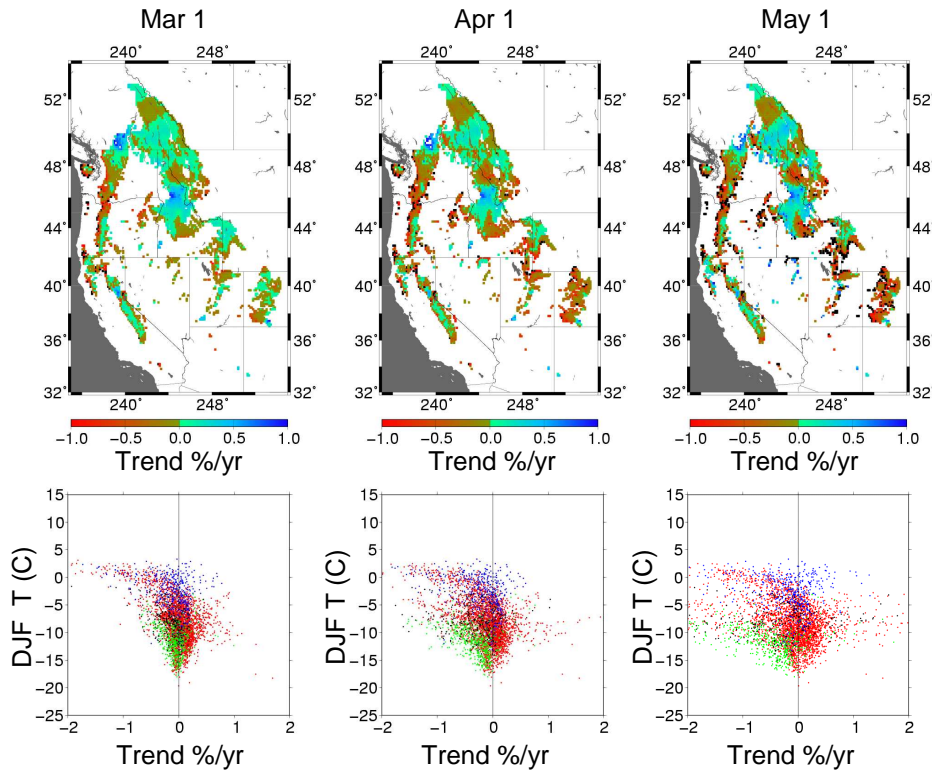


Figure 4.2 Relative trends (% per year) in simulated SWE for three calendar dates for the period from 1916-2003 [Black pixels in the spatial plots are off scale on the low side. Scatter plots are color coded: PNW = red, CA = blue, CRB = green, GB = black

### ***Results for 1916-2003("A")***

This period is characterized by widespread, modestly upward trends in precipitation that result in upward trends in SWE in the fixed T simulations (Figure 4.3c) and strong downward trends in SWE due to upward temperature trends over essentially the entire domain in the fixed P simulations (Figure 4.3b). Thus the majority of the downward trends in SWE from 1916 to 2003 are attributable to large scale warming which overwhelms the effects of wide-spread increases in winter precipitation. Note, for example, the predominantly upward trends in grid cells in CA associated with precipitation (Figure 4.3c), but predominantly downward trends for CA in warmer areas with DJF temperatures above about  $-2.5^{\circ}\text{C}$  (Figure 4.3a). Several distinct climatic regimes are also apparent in these results, which will be discussed separately below.

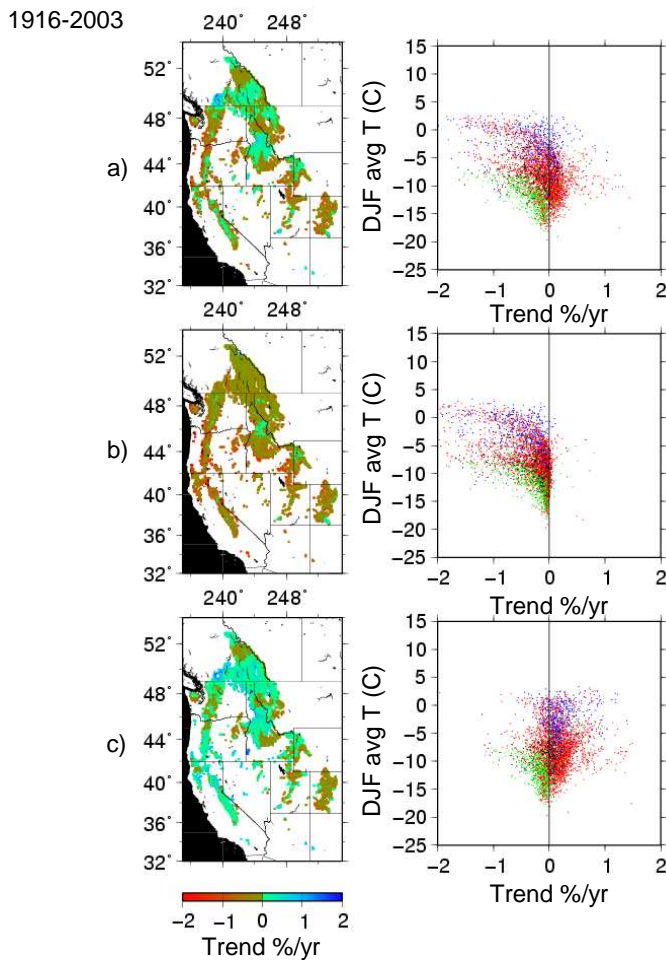


Figure 4.3 Relative trends (% per year) in simulated April 1 SWE for 1916-2003: a) combined effects of temperature and precipitation trends, b) effects of temperature trends alone, c) effects of precipitation trends alone. [scatter plots are color coded: PNW = red, CA = blue, CRB = green, GB = black]

### ***Results for 1924-1976 (“B”)***

Strong upward trends in precipitation throughout the region dominate the SWE trends in this period (Figure 4.4c), and upward trends in SWE follow these precipitation trends over most of the domain (Figure 4.4a). The overall trends in precipitation appear to reflect a shift from wide-spread drought from 1925-1946 to wetter conditions overall in the second half of the period. The fixed P analysis (Figure 4.4b) shows that there is not a consistent trend in SWE due to temperature alone, and this is the only period examined

for which there were substantial upward trends in SWE associated with downward trends in temperature (and solar radiation) alone.

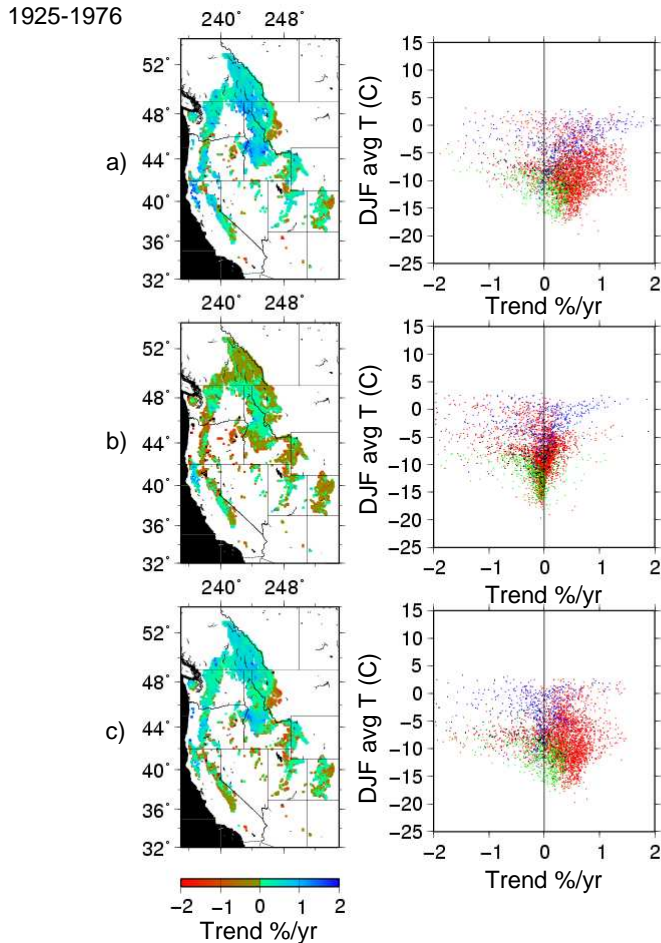


Figure 4.4 Relative trends (% per year) in simulated April 1 SWE for 1925-1976: a) combined effects of temperature and precipitation trends, b) effects of temperature trends alone, c) effects of precipitation trends alone. [scatter plots are color coded: PNW = red, CA = blue, CRB = green, GB = black]

### ***Results for 1947-2003 (“C”)***

The 1947 to 2003 period of analysis corresponds most closely with the period of record covered by the snow course and streamflow observations that were discussed in the introduction. This period is characterized by different precipitation trends in different regions (Figure 4.5c) and by strong downward trends in SWE associated with temperature trends (Figure 4.5b). The trends in precipitation in each region are broadly

consistent with patterns of observed climate variability associated with the PDO since 1947 that were discussed in the introduction. The fixed P analysis for this period (Figure 4.5b) shows that without precipitation trends, essentially the entire domain would have experienced strong downward trends in April 1 SWE.

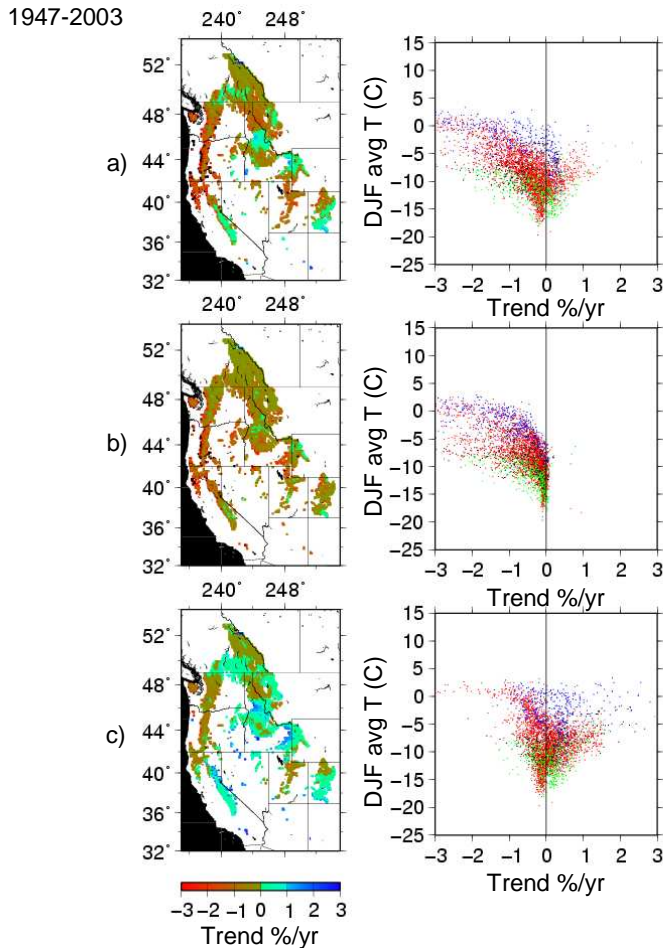


Figure 4.5 Relative trends (% per year) in simulated April 1 SWE for 1947-2003: a) combined effects of temperature and precipitation trends, b) effects of temperature trends alone, c) effects of precipitation trends alone. [scatter plots are color coded: PNW = red, CA = blue, CRB = green, GB = black]

Because the temperature-related trends are almost always downward for this period, areas with downward precipitation trends (e.g. most of the PNW cells with DJF temperatures above -5 C) exhibit very strong downward trends in SWE. Some areas with upward precipitation trends (e.g. about half the cells in CA) show downward SWE trends due to temperature effects despite increases in precipitation. This effect is less evident in the



colder areas of the domain (e.g. the CRB), but can still be seen in the base run (Figure 4.5a) as a shift towards stronger downward trends in SWE when the effects of temperature trends are combined with the effects of precipitation trends. Trends in the base run analysis (Figure 4.5a) are less than  $-0.25\%$  per year (strong downward trends) over about 70% of the cells shown in the figures. This is a considerably larger fraction of the total area with downward SWE trends than for the base run for 1916-2003, in part because of wide-spread downward precipitation trends in the colder areas of the PNW from 1947 to 2003.

***Results for 1924-1946 concatenated with 1977-1995 (“D”)***

The intent here is to minimize the effects of decadal variability associated with the PDO by combining two climatologically similar epochs. The fixed P analysis for this period (Figure 4.6b) shows somewhat more scatter than the fixed P analysis for 1947-2003, but again the trends associated with temperature alone are overwhelmingly downwards. The fixed T analysis (Figure 4.6c) shows little consistent trend in SWE associated with precipitation trends in comparison with the 1916-2003 or 1925-1976 periods. As in the 1916-2003 and 1947-2003 periods, a major driver of the SWE trends in this period is a large scale warming which affects most of the domain, and the analysis suggests that this warming cannot be readily explained by decadal scale variability associated with the PDO. In particular the earlier warm phase PDO epoch was clearly much cooler overall than the most recent warm phase epoch. Further evidence that decadal variability is a poor explanation for the temperature related trends can be seen by comparing Figure 4.3b, 4.5b, 4.6b. It is apparent that any period paired with the 1977-2003 period shows dramatic downward trends in SWE due to temperature trends alone.

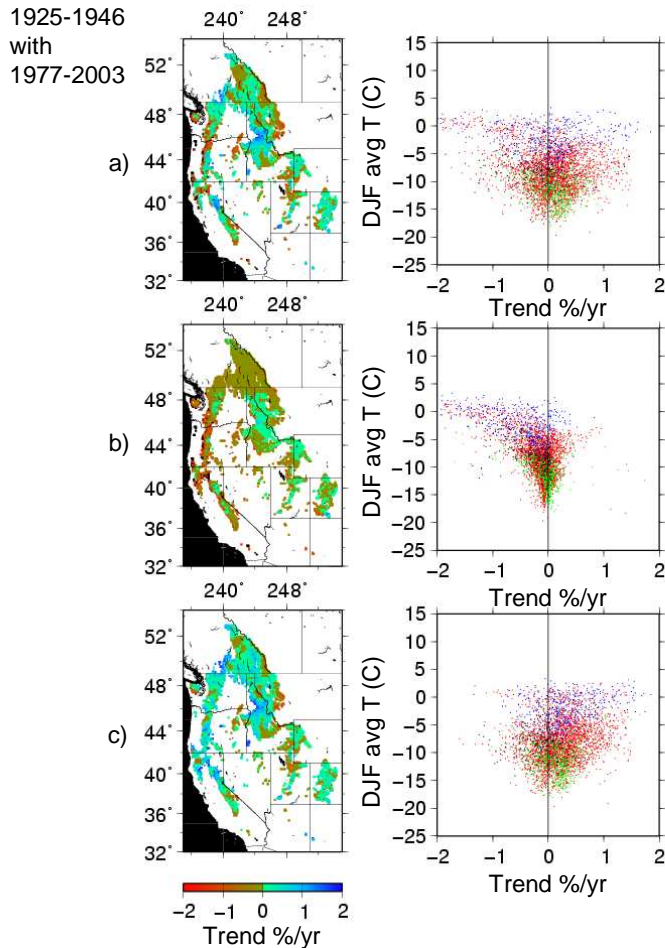


Figure 4.6 Relative trends (% per year) in simulated April 1 SWE for 1925-1946 combined with 1977-2003: a) combined effects of temperature and precipitation trends, b) effects of temperature trends alone, c) effects of precipitation trends alone. [scatter plots are color coded: PNW = red, CA = blue, CRB = green, GB = black]

### *Effects of Climatic Regimes*

Three distinct climatic regimes are apparent in the areas that experienced downward trends in April 1 SWE from 1916 to 2003 (Figure 4.7). Areas with large downward trends in April 1 SWE and DJF temperatures between  $-1.0$  and  $+2.5$  C are shown to be coastal areas in the PNW and northern CA (Figure 4.7 upper right panel). Areas with large downward trends in April 1 SWE and DJF temperatures between  $-10.0$  and  $-1.0$  C are shown to be inland areas with a more continental climate (Figure 4.7 middle and lower right panels). These differences have to do with specific interactions between

precipitation and temperature regimes that determine the time scales of snow accumulation and melt. Coastal mountain ranges are warmer, but are able to produce very large snowpacks in mid winter that can persist until April 1 because of high mean precipitation and cool, cloudy spring conditions.

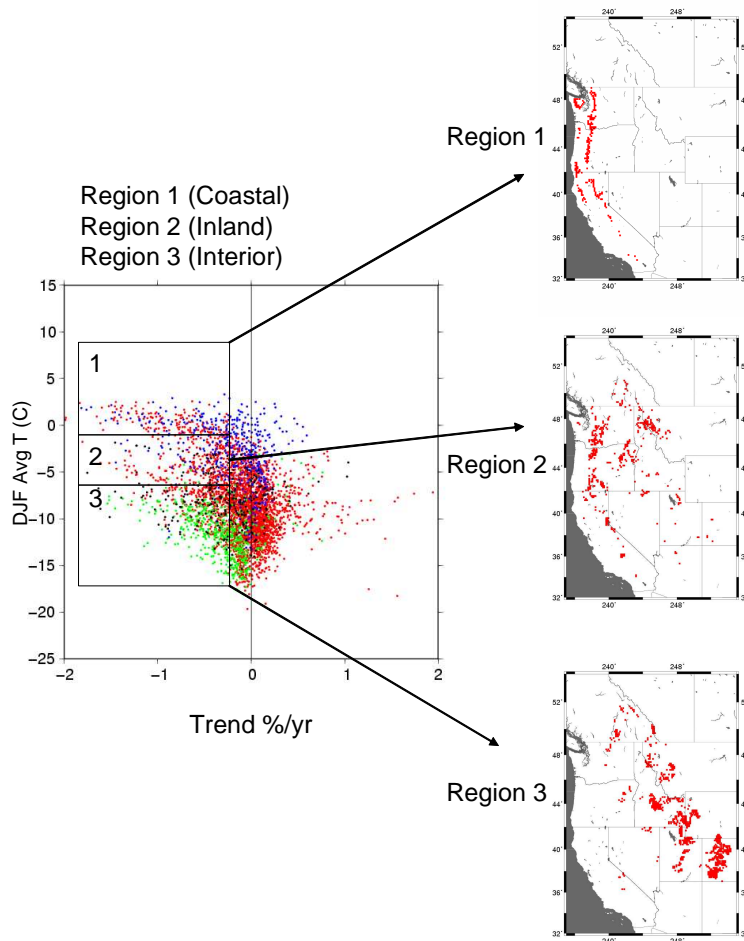


Figure 4.7 Location of winter climatic regimes associated with strong downward SWE trends ( $< 0.25$  %/yr) from 1916-2003. Mid-winter (DJF) temperatures in region 1 are above  $-1$  °C, in region 2 between  $-1$  °C and  $-7$  °C, and in region 3 below  $-7$  °C.

These areas are affected by temperature increases from mid winter through spring (which also explains why they are most sensitive to warming). Continental areas, by contrast, are typically dryer and colder, and snow accumulation that ultimately persists until April 1 takes place over a number of months from late fall to early spring. Analysis of winter

precipitation and the seasonal cycle of snow accumulation in these areas (not shown) showed that precipitation trends over the entire winter and warmer temperatures during the late spring were the predominant drivers of the overall trends in SWE. For areas with cold mid winter temperatures (Figure 4.7 lower right panel), the temperature sensitivity becomes relatively small and the large downward trends in SWE are associated primarily with strong downward trends in winter precipitation (compare Figure 4.7 with Figure 4.3c). These climatic regimes are consistent with climatic characteristics observed by Serreze et al. (1999) in SNOTEL observations.

### ***Trends in the Timing of Snow Accumulation and Melt***

Figure 4.8 shows the trends in the date of simulated peak snow accumulation and the date of 90% melt, and that these trends are strongly related to DJF average temperatures. Almost all the cells with winter temperatures warmer than -5 C, for example, show earlier dates of peak accumulation and 90% melt. In sensitive areas (such as the coastal areas in the PNW and CA shown in Figure 4.7, peak accumulation occurs between 15 and 45 days earlier, and 90% melt occurs 15 to 40 days earlier. Comparison of the base run scatter plots with those from the fixed P and fixed T runs (Figure 4.8) shows that the changes in the timing of peak snow accumulation and 90% melt are a complex function of precipitation and temperature changes, but that the dominant effect is due to temperature trends. A similar examination of the scatter plots shows that trends in the date of 10% accumulation, are predominantly due to upward trends in precipitation in the beginning of the snow accumulation season. These changes in snow accumulation and melt are consistent with observed changes in streamflow timing discussed in the introduction. Interestingly, the time between 10% accumulation and 90% melt has not changed very much overall. This somewhat counter intuitive result occurs because the 10% accumulation date are most affected by precipitation trends (compare base and fixed T runs in Figure 4.8), whereas the peak SWE and 90% melt dates are most affected by temperature trends (compare base and fixed P runs in Figure 4.8). Despite different mechanisms at different times of the year, the overall trends in the date of snow

accumulation and melt are characterized by shifts in the entire snow accumulation season earlier in time, but with a smaller amount of peak SWE.

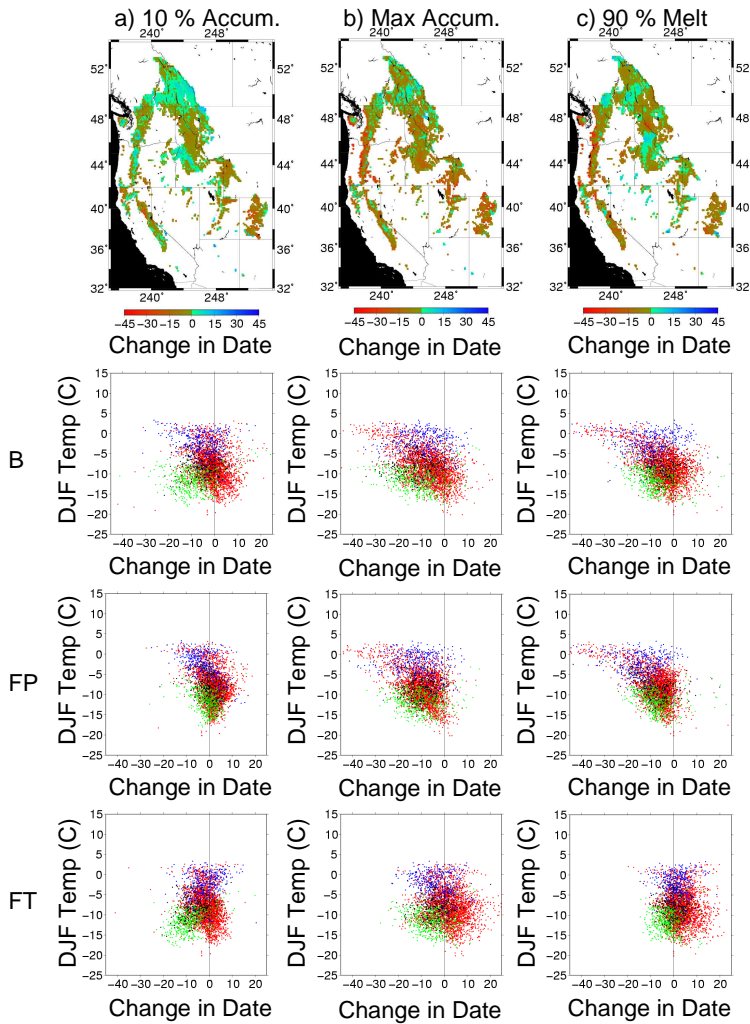


Figure 4.8 Cumulative changes (trend \* number of years) in calendar date of: a) 10% SWE accumulation, b) maximum SWE accumulation, and c) 90% melt for 1916-2003 for three model runs. Top panel shows a spatial plot for the Base run. Panels below show scatter plots for the Base (B), Fixed P (FP), and fixed t (FT) runs respectively.

The results for the four time periods are summarized for different portions of the domain and the different model runs in Table 4.1 and Table 4.2. Table 4.1 shows the areal average of the relative trends calculated for each cell (i.e. the spatial average of the trends shown in Figure 4.3-4.6). Table 4.2 shows the trend in the areal average SWE (i.e. a time

series of SWE averaged over each domain is extracted first, and the trend in this aggregate time series is reported).

Table 4.1 Areal averages of the relative trends for each grid cell calculated for each portion of the domain (percent per year)

	<b>PNW</b>	<b>CA</b>	<b>GB</b>	<b>CRB</b>
<b>1916-2003</b>				
Base	-0.14	-0.21	-0.40	-0.69
Fixed P	-0.60	-0.91	-0.95	-0.71
Fixed T	0.40	0.44	0.40	-0.22
<b>1925-1976</b>				
Base	1.52	1.05	1.47	0.74
Fixed P	0.73	0.29	1.33	0.68
Fixed T	0.67	-0.05	0.37	0.36
<b>1947-2003</b>				
Base	-0.39	-0.84	0.46	0.39
Fixed P	-0.94	-1.61	-0.72	-0.35
Fixed T	0.45	0.42	0.63	0.26
<b>1925-1946_1977-2003</b>				
Base	0.53	-0.35	0.09	-0.22
Fixed P	-0.36	-1.75	-0.62	-0.80
Fixed T	0.98	0.54	0.75	0.43

Table 4.2 Relative trend in the areal average snow water equivalent for each portion of the domain (percent per year)

	<b>PNW</b>	<b>CA</b>	<b>GB</b>	<b>CRB</b>
<b>1916-2003</b>				
Base	-0.06	-0.13	-0.25	-0.26
Fixed P	-0.18	-0.39	-0.40	-0.22
Fixed T	0.10	0.14	0.04	-0.14
<b>1925-1976</b>				
Base	0.48	0.40	0.12	0.12
Fixed P	-0.06	-0.04	-0.13	-0.12
Fixed T	0.38	-0.03	-0.14	0.03
<b>1947-2003</b>				
Base	-0.40	-0.51	-0.51	-0.19
Fixed P	-0.34	-0.73	-0.60	-0.30
Fixed T	-0.03	0.21	0.34	0.13
<b>1925-1946_1977-2003</b>				
Base	0.07	-0.04	-0.28	-0.29
Fixed P	-0.26	-0.57	-0.55	-0.36
Fixed T	0.27	0.24	0.03	-0.10

The results for 1925-1976 shown in Table 4.2 are somewhat confusing and require some additional explanation. For CA, for example, the fixed P and fixed T runs for this period

show small downward trends in areal average SWE, yet the trend in the base run has a strong upward trend. These counter intuitive effects are associated with the spatial distribution of the upward and downward trends associated with temperature and precipitation trends. For example, if specific areas in the domain that are getting wetter are also getting colder, then the overall trend may be strongly upward (as for CA for this period), whereas if areas that are getting wetter are also getting warmer there may be little overall trend. These complex effects are not seen in the other time periods because the temperature related trends (and in many cases the precipitation related trends as well) are much more spatially homogeneous.

#### **4.5. Summary and Conclusions**

Widespread warming has occurred in the western U.S. from 1916 to 2003, resulting in downward trends in April 1 SWE over large areas of the domain. High elevation areas with upward precipitation trends, however, are shown to produce upward trends in SWE over the same time period. The results show that almost all the upward trends in SWE from 1916 to 2003 are due to modest upward precipitation trends and that many of the downward trends in SWE are caused by wide-spread warming. In areas with relatively warm winter temperatures, such as coastal areas of the PNW and CA, the effects of warming frequently overwhelms the effects of increasing precipitation. Colder areas are predominantly driven by precipitation changes, and temperature effects on SWE trends, while apparent in the combined trends, are relatively small.

The period from 1925 to 1976 was characterized by widespread increases in precipitation, which dominated temperature trends to produce widespread upward trends in SWE. The period from 1925 to 1976 was also the only period in which widespread upward trends in SWE are observed due to temperature trends alone. From 1947 to 2003 regionally-specific precipitation trends associated with decadal variability combine with strong downward trends in SWE due to widespread warming. The effects of warming are

frequently large enough to overwhelm upward trends in SWE associated with precipitation trends alone in warmer areas of the domain.

The results for the back-to-back warm PDO epochs combined with the 1916-2003 and 1947-2003 analysis described above strongly suggest that widespread regional warming trends are not well explained by decadal scale variability, but that the decadal variability probably does account for the trends in winter precipitation that have been apparent over shorter periods of the record. Although the precipitation trends from 1916 to 2003 are broadly consistent with many global warming scenarios, it is not clear whether the modestly increasing trends in precipitation that have been observed over the western U.S. for this period are primarily an artifact of decadal variability and the time period examined, or due to longer-term effects such as global warming.

Several distinct climatic regimes exist in areas that have experienced downward trends in April 1 SWE in the simulations. Coastal areas are strongly affected by warming throughout the winter and spring, whereas areas with a more continental climate are more sensitive to precipitation trends during the winter and to warming in late spring. Many high elevation areas in the Rockies and southern Sierra are relatively insensitive to temperature trends, and downward trends in SWE are primarily due to downward trends in precipitation.

The dates of peak snow accumulation and 90% (of peak) melt have generally been occurring earlier in the year, and these trends are clearly sensitive to winter temperature regimes, with the greatest changes apparent in areas with warmer winter temperatures (e.g. near-coastal mountains in the PNW and CA). These effects are consistent with the observed trends towards earlier peak snowmelt runoff. The sensitivity analysis shows that the changes in the timing of peak accumulation and 90 % melt are primarily a temperature related effect. The date of 10% (of peak) accumulation has also trended



earlier in the year, but is shown to be related primarily to trends in fall precipitation rather than to trends in temperature.

The results of this study demonstrate that regional warming is one of the major drivers of downward trends in SWE in the western U.S.. Furthermore, we should expect, based on projections of continued warming, that these downward trends will continue. Because precipitation variability seems most strongly related to decadal variability rather than to long-term trends, the use of observed precipitation variability in conjunction with scenarios of warmer temperatures may currently be the best approach for understanding the overall effects of global warming on the hydrologic cycle in the western U.S.. Such an approach implies, as well, that both “warm and wet” and “warm and dry” periods are likely to occur in the future at different times, and that water resources planning should consider both scenarios in testing alternative management plans.

## 5. Effects of 20<sup>th</sup> Century Warming and Climatic Variability on Trends in Runoff, Evaporation, and Soil Moisture

This chapter summarizes and excerpts research submitted to Journal of Climate as:

Hamlet, A.F., Mote, P.W, Clark, M.P., Lettenmaier, D.P., 2006: 20th century trends in runoff, evapotranspiration, and soil moisture in the western U.S., J. of Climate (in review)

### 5.1. Introduction and Background

Figure 5.1 shows a map of the four large river basins that comprise our study domain in the western U.S.: the Pacific Northwest (PNW—which includes the Columbia River basin and coastal drainages), California (CA – mostly the Sacramento and San Joaquin River basins), Great Basin (GB – which consists of numerous rivers that flow to the closed interior of the GB), and Colorado River Basin (CRB).

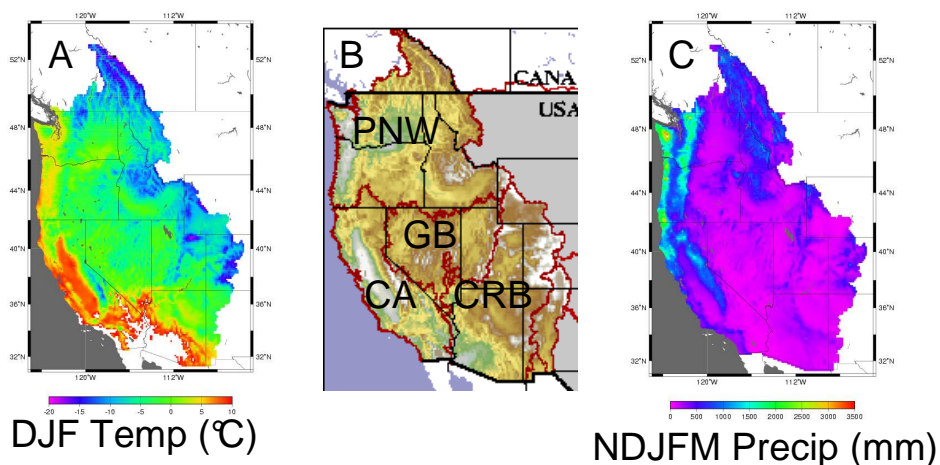


Figure 5.1: Map and climatological characteristics of the simulation domain. a) average Dec-Feb temperature, b) map of the domain, c) average Nov-Mar precipitation

Strong topographic controls on precipitation (P) and temperature (T) are present in the western U.S. Much of the P occurs in the mountainous parts of the region and P is strongly winter dominant, particularly at higher elevations. Near-coastal mountains in Washington, Oregon, and California are relatively warm in winter in comparison with the Rocky Mountains, and also have much greater winter precipitation (Figure 5.1a, c). These different winter temperature regimes largely determine how much of the winter P is typically stored as snow, and also play a strong role in determining the T sensitivity of snow accumulation and melt processes in different areas (Knowles and Cayan, 2004; Mote et al. 2005; Hamlet et al. 2005 (Chapter 4)). Snowpack plays a central role in runoff production in the western U.S. In many mountain watersheds the water stored as snow in spring accounts for a dominant fraction of the summer (April-September) runoff contributing to streamflow.

Over the past several decades a number of hydrologic modeling studies at the river basin scale have demonstrated that estimated increases in winter temperatures associated with rising global greenhouse gas concentrations would alter the hydrologic cycle in mountain watersheds in the western U.S. (e.g. Gleick 2000; Hamlet and Lettenmaier 1999b; Knowles and Cayan 2002; Lettenmaier et al. 1999; Miller et al. 2003; Mote et al. 2003; Stewart et al. 2004). Systematically warmer temperatures in snowmelt-dominant and transient-snow watersheds result in reduced (and earlier) peak snowpack, more runoff in winter, earlier spring peak flows, reduced summer water availability and late summer low flows, increased evapotranspiration (ET) in summer, and (in some studies) an altered seasonal cycle of soil moisture (SM) recharge and depletion (see e.g. Hamlet and Lettenmaier 1999b). These kinds of hydrologic changes have also been shown to have important water resources implications in a number of case studies (Christiansen et al. 2004; Hamlet et al. 1999; Knowles and Cayan 2004; Payne et al. 2004; Van Rheenen et al. 2004). One question that we address in this paper is, given observed precipitation and temperature changes over the last century (Mote et al. 2005; Mote 2006), have accompanying changes in the seasonal water balance occurred?

In previous work we have examined in detail 20<sup>th</sup> century trends in simulated spring snowpack over the West and have compared them to observed trends from snow course data (Hamlet et al. 2005 (Chapter 4); Mote et al. 2005). Some important conclusions from these studies include:

- Hydrologic model simulations reproduce the spatio-temporal variations in observed spring snowpack to a remarkable degree, demonstrating that observed trends in T and P coupled with topographic variations in winter climate are adequate to explain most of the observed trends in spring snowpack over the western U.S.,
- Without observed trends in P, essentially the entire western U.S. would have experienced losses of April 1 snowpack during the 20<sup>th</sup> century due to widespread warming.
- The observed trends in SWE depend strongly on winter temperature regimes. The areas where the greatest SWE changes have occurred are in near-coastal parts of WA, OR and CA where winter temperatures are typically close to freezing in mid winter.
- The date of peak snow accumulation and 90% melt have been moving earlier in the year (up to 45 days earlier in sensitive areas) from 1916-2003, despite modest increases in P over this same time period. These changes are shown to be almost entirely due to T trends.
- While there is clear evidence in snowpack records of wide spread warming across the western U.S. in the 20th century, there is little evidence of any consistent long-term trends in snowpack across the western U.S. associated with P. This

supports the hypothesis that P variability is predominantly controlled by decadal scale climate variability rather than effects associated with warming

Given the importance of snow dynamics to the hydrologic cycle in western watersheds, the observed changes in snowpack strongly suggest that we should also expect systematic changes in runoff, ET, and SM dynamics like those discussed above both in observed records and hydrologic simulations. Several recent studies have shown that temperature-related shifts in runoff timing are indeed evident in observed unregulated streamflow records (Regonda et al. 2005; Stewart et al. 2005).

Observational studies are crucial to the assessment of observed climate change, however modeling studies are also needed to extend records back to the early part of the century (when relatively few observations are available) and to provide spatial and temporal resolution and continuity that are missing from the observed records. Furthermore, model simulations can explicitly show the role of T and P trends in the observed changes, and can be used to analyze components of the hydrologic cycle that are typically unmeasured (e.g. ET and SM).

In this study (following methods first developed in the companion study by Hamlet et al. 2005 (Chapter 4)) we will use a physically-based hydrologic model and a carefully prepared, long-term meteorological driving data set to reconstruct the water balance of four large river basins in the western U.S. from 1916-2003 at 1/8<sup>th</sup> degree spatial resolution. Using the surrogate observations produced by the model, we will quantify trends in ET, runoff, and SM associated with observed trends in T and P for each model grid cell over two retrospective periods (1916-2003 and 1947-2003). Trends in these water balance variables will also be analyzed in the context of various geographic, topographic, and climatic drivers.

## 5.2. Hydrologic Simulation Model and Driving Data

In this study (as in the companion studies on snowpack described above) we use the Variable Infiltration Capacity (VIC) hydrologic model (Liang et al. 1994; Cherkauer and Lettenmaier 2003) implemented over the western U.S. at 1/8<sup>th</sup> degree spatial resolution (Figure 5.1). A temporally-adjusted, gridded daily time step P and T data set from 1915-2003 was used to drive the VIC model. By construction, these adjusted data sets reproduce, at monthly time scales, the trends in T and P from the Historical Climatology Network (HCN) (Karl et al. 1990) and the Historical Canadian Climate Database (HCCD) (Mekis and Hogg 1999; Vincent and Gullett 1999). The methods used to produce the driving data, and evaluation of the resulting hydrologic simulations using observed streamflow records, are reported in more detail in Hamlet and Lettenmaier (2005) (Chapter 3). Daily time step water balance simulations were carried out using a one-hour snow model time step. The first nine months of the simulations (1/1/1915 – 9/30/1915) were used for model spin-up and have been excluded from the subsequent analysis resulting in a time series of 88 water years (Oct-Sep) from 1916-2003. Model spin-up requirements are somewhat different for SM than for ET and runoff. In relatively wet areas (like the cells that accumulate significant snowpack in winter that we examine here) a few years of model spin up has been shown to be adequate for SM studies (e.g. Cosgrove et al. 2003). To ensure that the initial conditions do not unduly influence the long-term trends in the early parts of the record, however, we examine SM trends from 1920 onwards, allowing for a 5-year model spin-up. Additional details on the hydrologic model and its implementation are reported by Hamlet et al. (2005) (Chapter 4).

## 5.3. Evaluation of the Hydrologic Model

### *Snowpack*

Simulated trends in April 1 snow water equivalent (SWE) produced using the VIC model over the western U.S. have been previously evaluated in detail by Mote et al. (2005). Good overall agreement was also found between the results produced by the physically

based model (Hamlet et al. 2005 (Chapter 4)) and those produced by alternative statistical approaches (Mote 2006). Over most of the domain the model closely reproduces the macro-scale trends in the observations and displays little bias in comparison with the point observations for different winter temperature regimes. Some systematic error in the model's SWE trends was observed in the Sierra Nevada Mountains in CA, however, where the VIC simulations tended to overestimate the magnitude of observed negative trends in snowpack. These discrepancies are believed to be associated primarily with a spring temperature bias in the VIC meteorological driving data associated with the use of a fixed temperature lapse rate used during the gridding processing (see Hamlet et al. 2005 (Chapter 4) for more details), but could also be related to temperature inversions at high elevations, or other more complicated meteorological features not captured in the driving data sets. Results for CA shown in this study should be interpreted with some caution because of the model bias in this part of the domain.

### *Snowmelt*

Daily time step point observations from the National Resources Conservation Service (NRCS) Snowpack Telemetry (SNOTEL) observing network provide useful information on the timing of snowmelt that can be used to evaluate the spatial/temporal patterns of snowmelt produced by the VIC model. Due to differences in scale (point vs grid cell area weighted average), aspect, vegetation coverage (SNOTEL sites are usually located in open areas, whereas the model simulates canopy effects over a large area) and potential delays in snowmelt in the SNOTEL data due to the thermal inertia of snow pillows, we do not expect excellent fine-scale agreement between the model simulations and the point observations. However Figure 5.2 shows that the relationship between mid-winter temperatures and the seasonal cycle of snowmelt are broadly captured by the model. Overall the model produces more melt in March and less in May than is apparent in the observations, however it is not immediately clear if the model or the observations is more representative of average conditions over the domain. (It should be noted that the sum of

the fractions shown in Figure 5.2 are frequently larger than 1.0 during the snowmelt season, particularly in areas where there is substantial transient snow.)

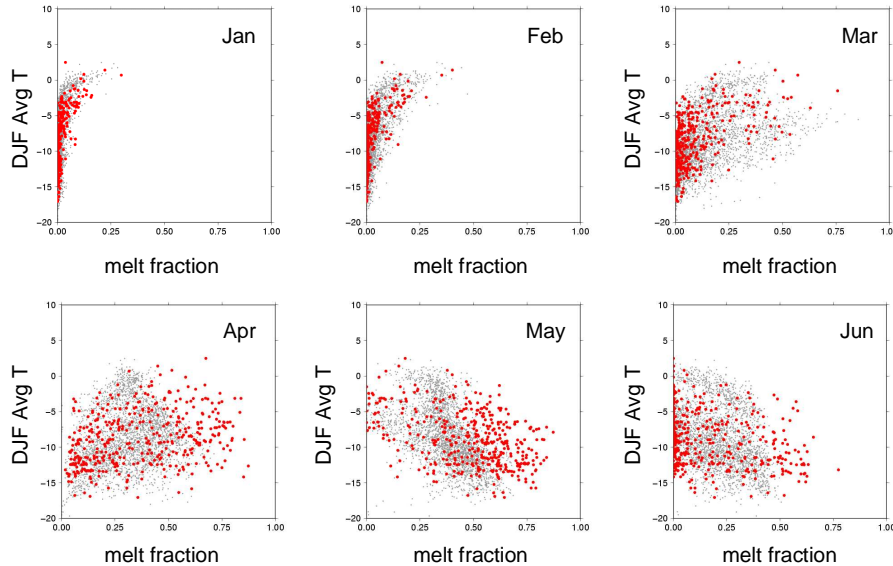


Figure 5.2: Simulated and observed total monthly snowmelt (including transient melt) normalized by the long-term mean of the peak snowpack from 1984-2003 at each location. Grey dots are VIC cells, red dots are SNOTEL stations. Only sites with more than 200 mm of SWE on April 1 are included in the plots to remove low elevation sites from the VIC analysis.

### *Streamflow*

The VIC model, in general, produces high quality monthly streamflow simulations (note that throughout this paper, we refer to simulated naturalized flows, i.e., the streamflows that would occur in the absence of water management, such as regulation by upstream dams, and/or streamflow diversions) in moderate to large river basins across the West (see also Maurer et al. 2002). A complete evaluation of all the simulations that are available is beyond the scope of what can be shown in this paper, however a comparison of naturalized observed and simulated streamflow in the Colorado River at Lee's Ferry, Arizona and in the Sacramento River at Shasta Dam, CA (Figure 5.3) shows typical model performance in moderate to large river basins across the West. The VIC model has been calibrated using data only from the post 1950 period, and the consistent validation of the model simulations in the pre-1950 period attests both to the temporal consistency of the driving data used in this study and the ability of the model to successfully capture



the hydrologic variability associated with different climatic regimes from first principals using P and T data as the primary drivers. Simulated streamflows in smaller river basins are subject to greater random errors due primarily to errors in the spatial distribution of P. Although random errors tend to be larger at smaller spatial scales, Hamlet and Lettenmaier (2005) (Chapter 3) demonstrate that *trends* in the errors are relatively small, again attesting to the temporal consistency of the driving data sets and their appropriateness for the kind of trend analyses we undertake in this study.

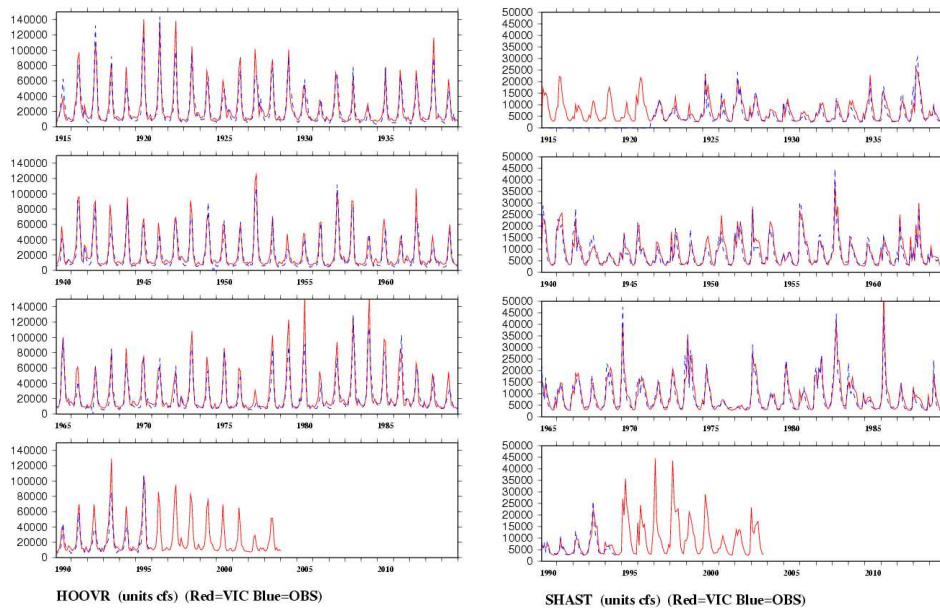


Figure 5.3: Comparison of naturalized streamflow observations and simulated natural streamflows for the a) Colorado River at Lee's Ferry, AZ (inflows to Hoover Dam) and b) the Sacramento River at Shasta Dam near Redding, CA (inflows to Shasta Dam)

The model was also found to be well suited to the task of identifying long-term trends in the seasonality of streamflow at the river basin scale. Trends in the simulated fraction of annual streamflow occurring from May-Sept and June-Sept (not shown) were evaluated for several river sites where suitable naturalized flow observations were available. The model's performance in estimating the long-term trends in seasonal streamflow timing was, in general, quite good, random errors in the year-to-year values notwithstanding.

### ***Soil Moisture and Evapotranspiration***

The VIC model uses a fairly complex and explicit conceptual framework in accounting for variations in ET and SM. ET in the model is based on the Penman Monteith approach (Shuttleworth 2003) and explicitly accounts for interception of precipitation and the attenuation of wind and solar radiation associated with the vegetation canopy (Liang et al. 1994). Model parameterization of vegetation characteristics includes an explicit representation of rooting depth, which determines how the model extracts moisture from the three soil layers during simulation of transpiration. The soil column in VIC (as implemented here) is divided into three layers. The thin upper layer (~10 cm) simulates “fast” runoff processes in near-surface soil layers, and thicker intermediate (~50 cm) and lower layers (~1.0-1.5m) represent “slower” storage and drainage processes contributing to baseflow.

The VIC model’s simulation of the seasonal cycle of SM has been evaluated in detail for a limited number of observing sites at which long term records are available in the U.S. and Eurasia (Maurer et al. 2002; Nijssen et al. 2001). In these comparisons, the model reproduced the seasonal dynamics of SM storage reasonably well. There are few direct observations of ET and SM storage in the western U.S. with which to explicitly evaluate the model simulations over the different climatic regimes and soil characteristics considered in this study, however Robock et al. (2003) found good overall agreement between the spatial variability of simulated SM and SM observations from the Oklahoma Mesonet. Given that the model reproduces the seasonal timing of water inputs from snow melt (Figure 5.2) and the resulting timing of runoff reasonably well, we are also confident that the model’s seasonal water balance is representative at the monthly time scales examined here. We also argue, based on the model’s physically-based representation of the hydroclimatic system, that the model simulations are a reasonable surrogate for observations of SM and ET in that they respond in a well-understood and clearly-defined manner to the climatic variations in the model’s driving data and to the estimated characteristics of the land surface.

Simulated ET in the model is sensitive to the difference between Tmax and Tmin in the meteorological driving data (which ultimately determines the short-wave radiation attenuation due to inferred “cloudiness” in the model) using methods developed by Thornton and Running (1999). These methods parameterize the relationship between the attenuation of solar radiation and the difference between Tmax and Tmin. It is not entirely clear if the empirically derived parameters remain stationary with changing climate, however the model does simulate changes in ET associated with a declining difference between Tmax and Tmin that are consistent with a systematically higher atmospheric moisture content and greater attenuation of incoming solar radiation. The Penman Monteith equation is also sensitive to increasing daily average temperatures (which determine the saturation vapor pressure) and to Tmin, which determines the dew point in the model simulations, and therefore the vapor pressure deficit used in the Penman Monteith equation. The temperature-related effects to ET in the model simulations can therefore be broadly interpreted as the trends in ET due to changing energy availability and saturation vapor pressure associated with trends in both inferred “cloudiness” and absolute temperature, respectively.

Simulated ET is also sensitive to wind speed, although any systematic effects due to wind variations are secondary to those associated with precipitation and temperature trends in the simulations, particularly since a daily wind climatology is used in the early part of the simulation period (1915-1948) (Hamlet and Lettenmaier 2005 (Chapter 3)).

#### **5.4. Analytical Methods**

For each 1/8<sup>th</sup> degree grid cell, the VIC model produces a daily time series of water balance variables. Linear trends in simulated monthly ET, runoff (the sum of surface runoff and baseflow contributing to streamflow in the model), and SM are then calculated for each grid cell. ET and runoff are reported as monthly totals, whereas SM is reported as an instantaneous value on the first day of each month. Runoff is also reported as a

fraction of annual flow occurring in different months in order to evaluate the trends in runoff timing. Note that these quantities are not integrated spatially, and linear trends for each variable are calculated independently for each grid cell.

As in Hamlet et al. (2005) (Chapter 4), three separate model simulations were carried out to help understand the relative role of trends in P and T on the results:

- 1) Base Run (BR): Unperturbed P and T data from the gridded meteorological data (daily total P, T<sub>min</sub> and T<sub>max</sub>, and wind speed) were used to drive the model. Trends in hydrologic variables are the result of both T and P variations.
- 2) Fixed P run (FPR): The P forcing data were fixed (at monthly time scales) at the climatological value for each grid cell, but daily T was allowed to vary as in the original time series [as in 1) above]. Trends in hydrologic variables are predominantly determined by T trends alone.
- 3) Fixed T run (FTR): T<sub>max</sub> and T<sub>min</sub> were fixed (at monthly time scales) at the climatological value for each grid cell, but daily precip varied as in the original time series [as in 1) above]. Trends in hydrologic variables are predominantly determined P trends alone.

For the FPR and FTR, the forcing data were perturbed as follows: For each grid cell, a monthly climatological value for P, T<sub>max</sub>, T<sub>min</sub> was calculated for each calendar month. Then the daily time series of the variable to be held constant was forced to reproduce this climatological value in each month of the simulation – that is, the daily values were allowed to vary within the month as in the original time series, but the monthly totals (P) or averages (T<sub>max</sub> and T<sub>min</sub>) were the same for each month of the simulation. This method preserves the daily covariance between T, P, solar radiation, and other forcing variables, while removing the trends and monthly variation in the fixed variable from the

simulation. If P, Tmax, and Tmin were all held fixed in this manner, the monthly mean of the resulting simulated hydrologic variables would be comparable (although not equal) to the long-term mean for each calendar date in the base simulation and any trends in the simulated hydrologic variables would be small and related to secondary effects such as daily variability within the month.

In the FTR, trends in inferred cloudiness, although not completely eliminated, are strongly reduced. The number of cloud free days in each month remains the same as in the unperturbed driving data, however the sum of (Tmax-Tmin) over all the days in each month (which is related to the estimated total shortwave radiation input in each month in the model) has no trend. Similar time scale issues are present with regard to daily precipitation values in the FPR. The timing of precipitation within the month remains as in the original time series, but the monthly precipitation totals have no trend.

Several different metrics are used to evaluate systematic changes in timing and absolute value of water balance terms. 50-year, cumulative trends (i.e. absolute trend times 50) in the date of occurrence of 50 percent of total cumulative water year runoff and ET, and the date of occurrence of 80 percent of maximum water year SM are used to assess systematic changes in seasonal timing of these variables. For runoff, trends in the fraction of total water year runoff occurring in a particular month is also employed as a timing sensitive metric. Similar metrics have been used in observational studies by Redonda et al. (2005) and Stewart et al. (2005). For ET and SM, relative trends (i.e. absolute trends normalized by the mean value) in particular months or seasons are also used to show systematic changes in these variables, which are not necessarily related to overall timing shifts.

## 5.5. Results and Discussion

### *Notes on Figure Presentation*

With a few exceptions, the figures showing trends in hydrologic variables are all arranged in a similar manner, and show absolute or relative trends for the three experiments (BR, FPR, FTR) and for two time periods 1916-2003, 1947-2003 (see caption for Figure 5.9). For each time period and run, a spatial plot shows a map of the trends for each grid cell, and a scatter plot shows the relationship between average winter temperature regime and the hydrologic trends in each cell. The scatter plots are also color coded so that particular parts of the domain can be identified (see caption for Figure 5.9).

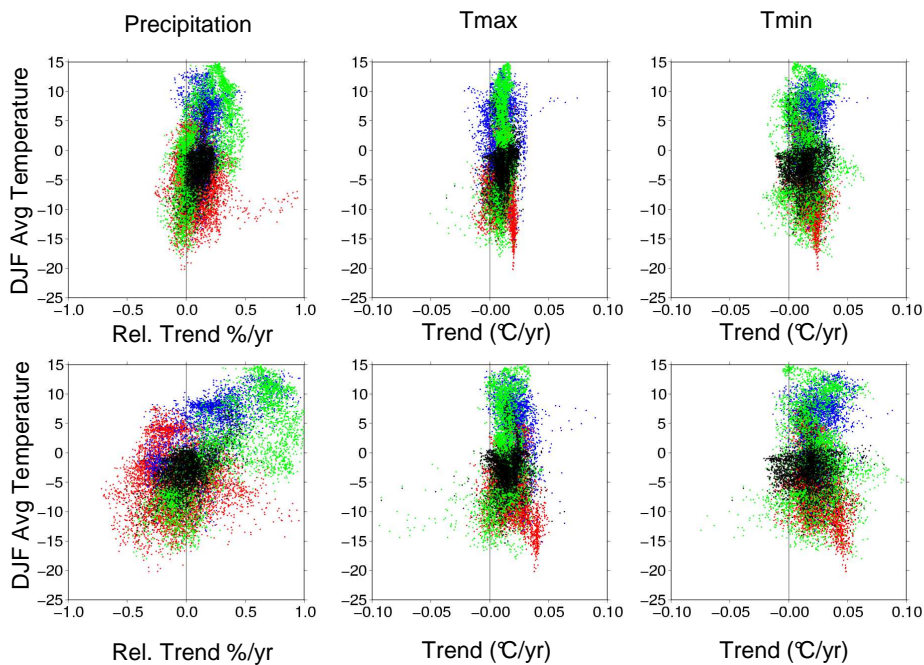


Figure 5.4: Trends in Oct-Mar precipitation (relative trend) and temperature (absolute trend) extracted from the gridded meteorological driving data set. Upper row of panels 1916-2003. Lower row of panels 1947-2003

### *Trends in Precipitation and Temperature*

Figure 5.4 and 5.5 show linear trends in P, Tmax, and Tmin extracted from the model driving data for the snow accumulation season in winter (October-March, Figure 5.4) and

summer (April-September, Figure 5.5) for the period from 1916-2003 (upper panels) and 1947-2003 (lower panels). As reported in Hamlet and Lettenmaier (2005) (Chapter 3) these trends are, by construction, in close agreement with those present in the U.S. Historical Climatology Network (HCN) (Karl et al. 1990) and the Historical Canadian Climate Database (HCCD) (Mekis and Hogg 1999; Vincent and Gullett 1999) (See also Figure 6 in Mote et al. 2005). Temperature trends are larger in winter than in summer, trends in maximum temperature (Tmax) are smaller than for minimum temperature (Tmin), and temperature trends for the latter period from 1947-2003 are larger than for the longer record from 1916-2003 and show a greater difference in the rate of warming between Tmin and Tmax.

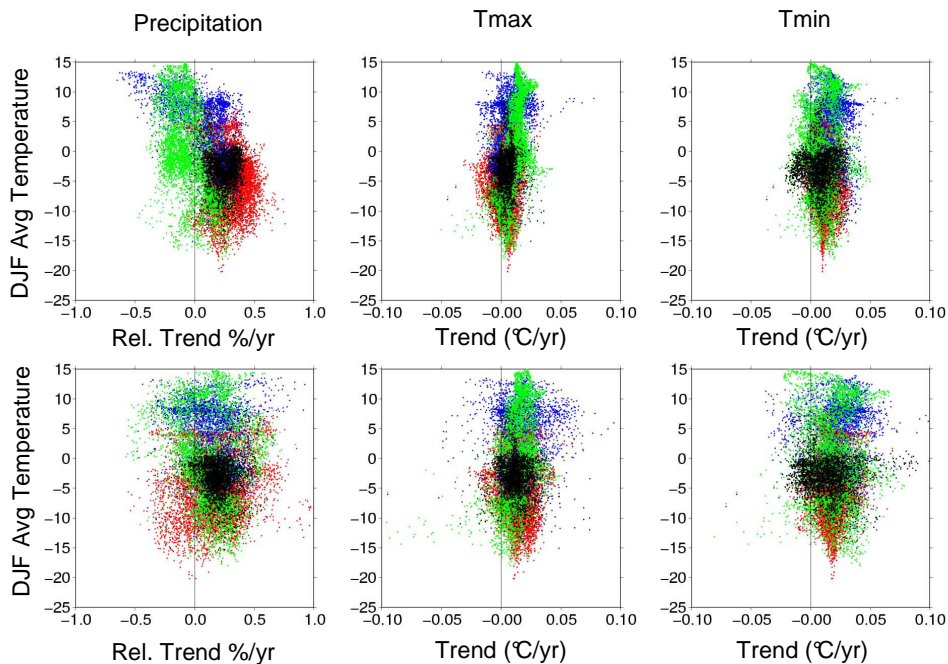


Figure 5.5: Trends in Apr-Sept. precipitation (relative trend) and temperature (absolute trend) extracted from the gridded meteorological driving data set . Upper row of panels 1916-2003. Lower row of panels 1947-2003

These trends are comparable to those shown in studies of station data (e.g. Mote et al. 2005; Knowles et al. 2005) and are broadly consistent in their overall character with the analyses included in the IPCC 2001 report (IPCC 2001). As noted above, winter P

trends, although shown to be generally positive across the west from 1916-2003, are very different in the 1947-2003 period, and seem to be more strongly controlled by decadal variability in each region than by long-term changes associated with regional warming. Trends in summer P, although relatively small in absolute value over much of the domain in comparison with winter trends, are generally upwards and are more consistent for different time periods.

It is important to note that the relationships between winter temperature regimes (and elevation) and climatic trends shown in Figure 5.4 and Figure 5.5 contain relatively little *observed* information about potentially differing trends at high or low elevations. This is because the majority of stations used to construct the gridded meteorological driving data set are at moderate or low elevations. The systematic effects of topographic variations on temperature and P are taken into account by using a fixed moist-adiabatic temperature lapse rate in the gridding process and by adjusting the long-term P means at different elevations derived from PRISM means (Daly et al. 1994) as described by Maurer et al. (2002). For this reason, however, the time history of the gridded data (and therefore the temporal trend) is mostly controlled by low and moderate elevation station data. Mote et al. (2005) demonstrate, however, that (except possibly in CA) an elevation bias in the simulated VIC snow trends is not apparent, which suggests that if there are differences in high and low elevation trends in temperature and precipitation, they are generally small in comparison with the overall trends.

### ***Long-Term Water Balance Simulations***

To help illustrate some of the hydrologic characteristics of each basin that determine the results of this study, we show a simulated long-term average water balance (1916-2003) for the four large river basins that comprise our study domain (Figure 5.6). The importance of snowpack in the hydrologic cycle discussed in the introduction is readily apparent in these figures. Despite the fact that SM reservoir is a larger storage term than snowpack in the water balance for much of the West, it is only through the relatively



rapid and sustained input of snowmelt that these hydrologic systems generate significant runoff in summer.

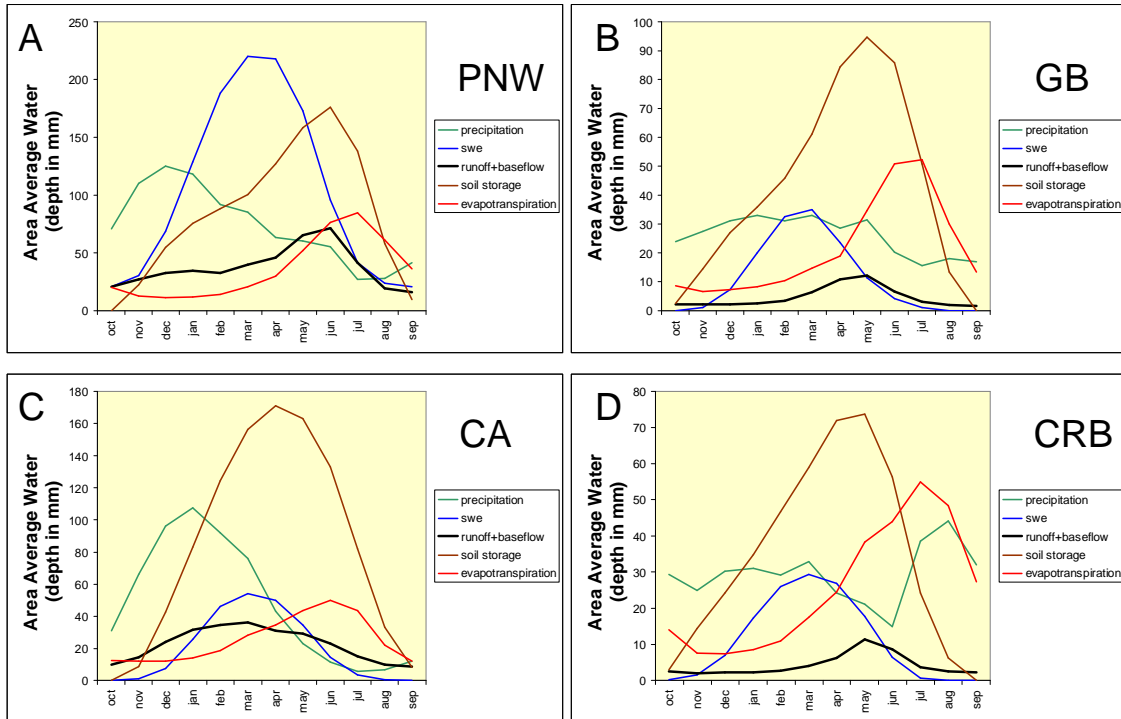


Figure 5.6: Long-term water balance for four large river basins a) Pacific Northwest, b) Great Basin, c) California, d) Colorado River basin

ET in the West is larger than precipitation from April-September (with some exceptions in the northern part of the PNW), and summer precipitation is mostly lost to ET and does not typically contribute greatly to streamflow at these spatial scales. The summer runoff contributing to streamflow is therefore approximately equal to the (negative) change in the soil and snow storage terms less the evaporation in excess of summer P. Seasonal recharge of the soil column is a complex function of the seasonality of precipitation, inputs of snowmelt in spring, and losses from ET or drainage, however soil moisture in the simulations typically peaks in May or June towards the end of the snowmelt season.

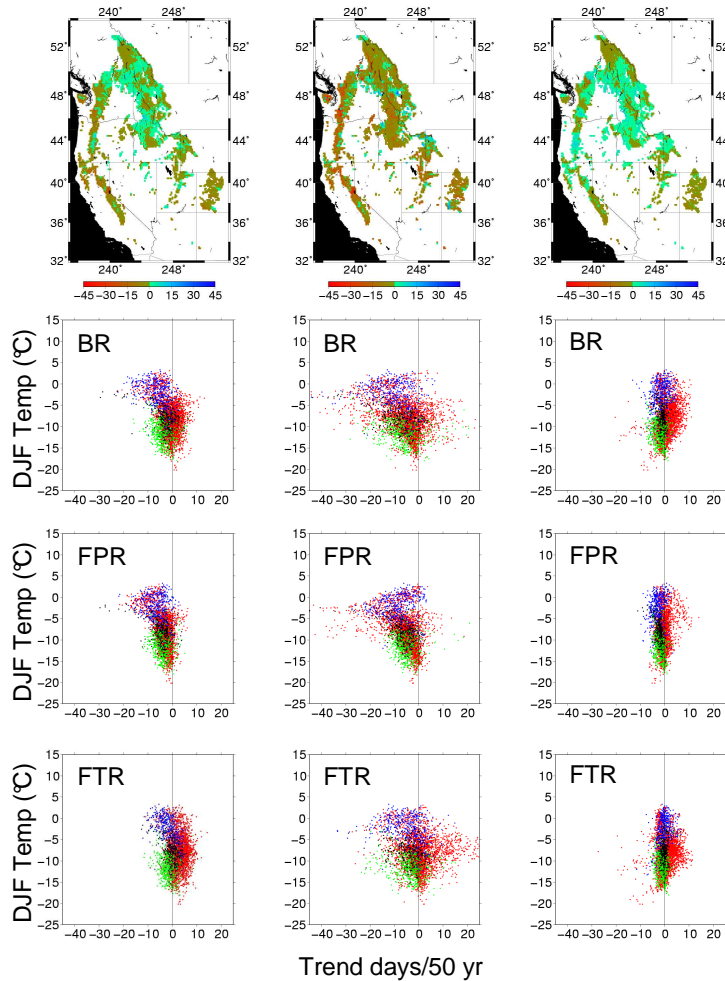


Figure 5.7: 50-year cumulative trends (absolute trend\*50) in runoff, SM, and ET from 1919-2003. First column on the left: trend in the date of 50 percent of total water year runoff. Second column: trend in the date of 80 percent of peak water year SM. Third column: trend in the date of 50 percent of total water year ET. Spatial plots show the combined effects (BR). Scatter plots show the cumulative trends as a function of DJF average temperature in each grid cell for the BRs, FPRs, and FTRs respectively.

### ***Overall Trends in the Timing of Runoff, SM, and ET***

To begin with, we show overall trends in the timing of runoff, SM recharge, and ET.

Figure 5.7 and 5.8 show 50-year cumulative trends (absolute trend times 50) in the date of occurrence of 50 percent of the total water year runoff and ET, and in the date of occurrence of 80 percent of the maximum SM. Downward trends in these values indicate more runoff, ET, or SM recharge occurring earlier in the water year. The changes in the

seasonal timing of ET are relatively small overall, and do not show great sensitivity to temperature related effects from 1916-2003.

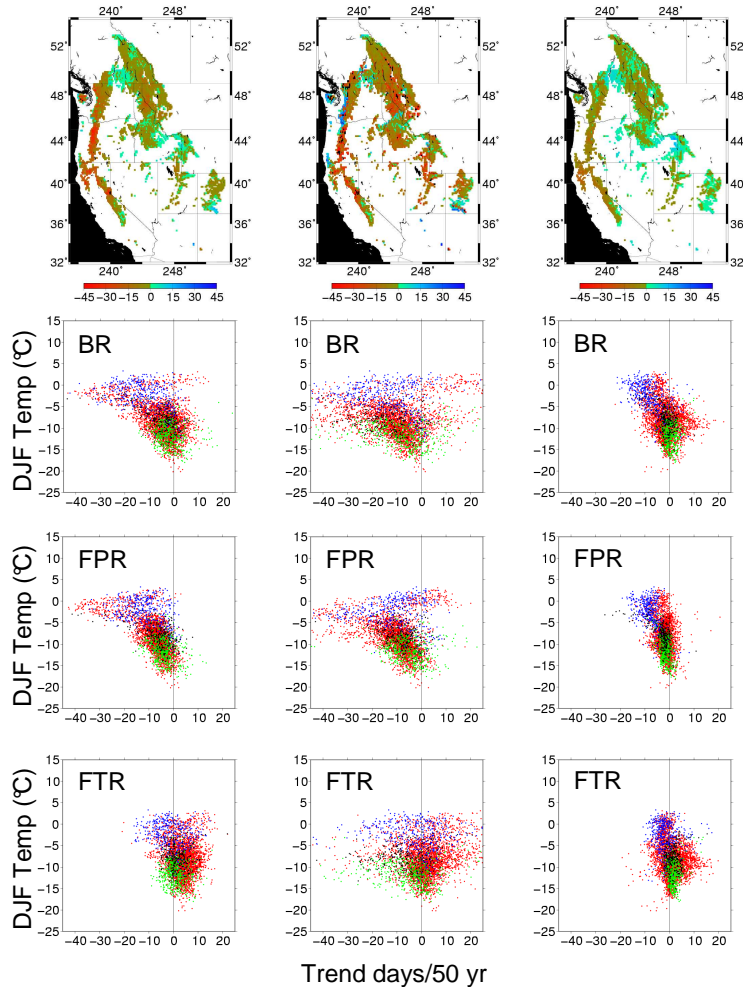


Figure 5.8: Same as figure 5.7 except for the period from 1947-2003

Some temperature sensitivity is apparent from 1947-2003 in the warm parts of the domain (particularly CA). These effects, which are discussed in more detail in the following section, are due primarily to the combined effects of greater water inputs in spring (temperature effects to snowmelt timing) and varying effects in summer associated with changes in precipitation. Changes in the timing of runoff and soil moisture recharge are substantial, and are more clearly associated with temperature-related effects that

deliver more water earlier in the water year, either directly as rain or from earlier snowmelt. There are clear trends in the simulations towards increased runoff earlier in the water year, and earlier SM recharge in spring.

The warmest parts of the domain are most sensitive to warming in this regard, which is consistent with the trends in the timing of snowmelt shown by Hamlet et al. (2005) (Chapter 4). Because the temperature trends are larger from 1947-2003, the temperature-related (and overall) trends in the timing of runoff and soil moisture recharge are much more pronounced for this time period (as are the changes in the timing of snow accumulation and melt). These effects to runoff and soil moisture recharge are discussed in more detail in subsequent sections.

#### ***Trends in Evapotranspiration and Runoff Ratio***

As noted in previous discussion, trends in ET are primarily due to changes in inferred cloud cover (net radiation), changes in T (saturated vapor pressure or dew point), or changes in water availability at different times of the year, which can be influenced both by seasonal or annual changes in P and/or snow dynamics. The model simulations demonstrate overall increasing trends in summer (April-September) ET (not shown) both from 1916-2003 and from 1947-2003 for all cells in the model domain. These overall trends in summer are associated most strongly with trends in water availability, which is related most strongly to P trends. These results are broadly consistent with the fact that ET in the West is frequently water limited in summer (particularly so in the GB and CRB), and that there are in many cases increasing trends in summer P over time in the model driving data (Figure 5.4-5.5).

A somewhat different picture emerges, however, if we examine only those cells which have a least 50 mm of SWE on April 1 and examine the seasonality of the changes. Figure 5.9 and 5.10 show the trends in ET from April-June and July-September respectively for these grid cells. From April-June, water availability in these “snow

cells” is much more strongly dependent on temperature trends which cause earlier delivery of water (and higher SM) from the melting snowpack. This can be seen most clearly in Figure 5.6 for 1947-2003 (right panels). Trends associated with P alone show no overall shift towards positive or negative trends, whereas the effects of T trends alone result in strong increasing trends in ET, and clearly dominate the combined effects due to trends in both T and P. This effect is associated with increased water delivery (via earlier snowmelt) to a primarily water limited system.

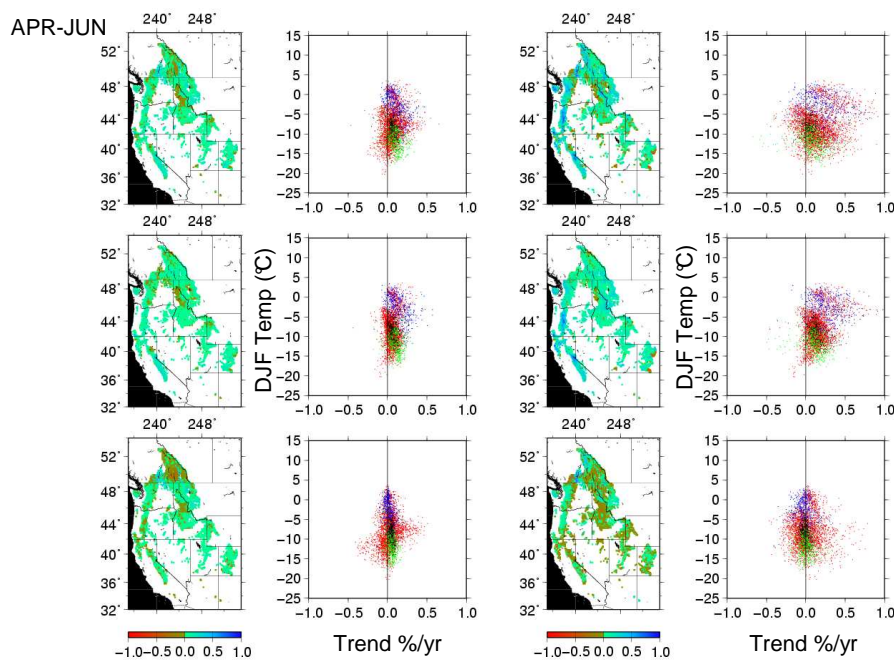


Figure 5.9: Trends in April-June ET for VIC cells with more than 50mm of average snow water equivalent on April 1. Panels to the left show trends from 1916-2003, those to the right show trends for 1947-2003. The first row shows the results for the BR simulations, the second row shows the results for the FPR, the third row shows the results for the FTR. For each time period and model run a map of trends and a scatter plot of DJF temperature vs. trend are shown. Scatter plots are color coded by region: red = PNW, blue = CA, green = CRB, black = GB.

In the later half of the summer period, the opposite is true. P effects dominate the combined results (compare scatter plots for BR to FTR) and the trends associated with T, while showing a relationship with winter temperature regimes, do not show a strong effect on overall trends (Figure 5.10). In the most arid parts of the domain (e.g. in much

of the GB and CRB), we expect trends in late summer ET to be most clearly related to summer P trends, because there is abundant energy available for evaporation and more P simply results in more ET.

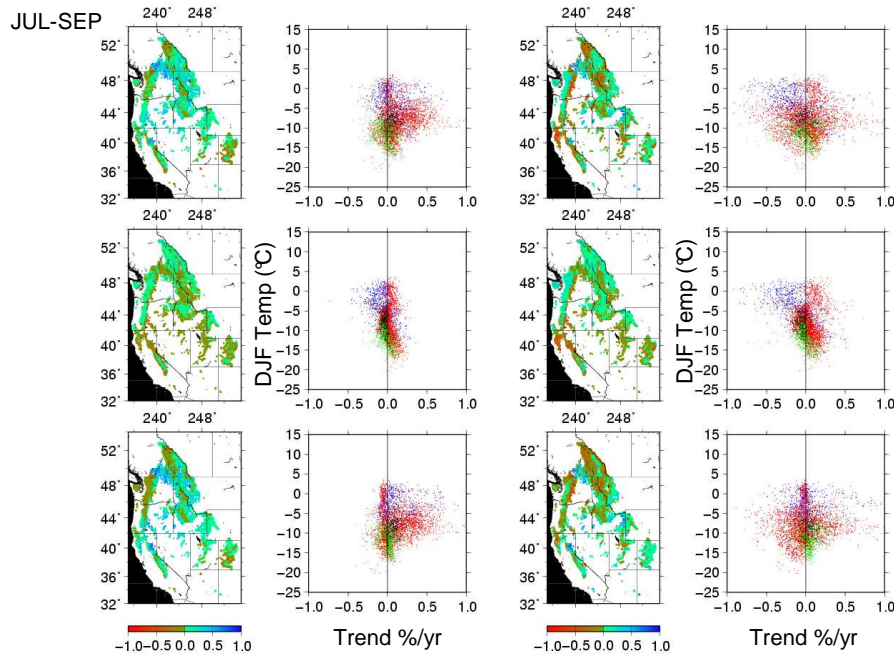


Figure 5.10: Same as for Figure 5.9 except for July-Sept ET

In some other parts of the domain, however, the effects to ET are a more complex function of trends in winter P and T. In the warmer parts of the CA domain, for example, P trends alone produce increasing trends in ET (more water availability due to greater winter P), whereas the T trends alone would decrease ET, because late summer water availability is decreased due to earlier snow melt in this sensitive area. As it turns out, the T trends dominate in this part of the domain, because CA has little summer P, and effects of temperature on the timing of snowmelt dominate (Hamlet et al. 2005 (Chapter 4)). This also explains the temperature related shifts in timing shown for this part of the domain in Figure 5.8. Trends in the annual runoff ratio  $[(\text{annual runoff})/(\text{annual P})]$  are largely related to seasonal trends in P (Figure 5.11). The effects of P trends alone show systematic increases in the runoff ratio in about half the domain, and these patterns are

clearly the primary determinant of the overall trends in the runoff ratio. In fact the T-related shifts play so small a role in the combined results that they almost cannot be seen in the plots. [This effect is somewhat counterintuitive, because in examining the FPR and FTR it would appear that the relative trends due to temperature alone are comparable in magnitude to the P-related trends. This inconsistency has to do with the fact that in the FPR the average runoff ratio used to scale the absolute trends is very small in the arid areas of the domain (GB and CRB) because of the strongly skewed P distributions. As a result the *relative* trends due to temperature appear to be comparable in the FPR and FTR. If absolute trends were plotted this would not be the case.]

The right panels in Figure 5.11 demonstrate that the effects to the runoff ratio are primarily associated with the trends in winter P (which primarily determine annual runoff in the West). Trends in summer P (which partly determine summer ET) play a smaller role. While considerable scatter is present in the relationships, in simple terms increasing trends in winter P are frequently associated with increasing trends in the annual runoff ratio. The effects for 1916-2003 (not shown) are similar.

### ***Trends in Runoff Timing***

Trends in the seasonal timing of runoff are primarily influenced by changes in snow and SM dynamics, and to a lesser extent by trends in the seasonality of P. Figure 5.12 and Figure 5.13 show trends in the fraction of annual runoff occurring in March and June respectively for all the cells with at least 50 mm of SWE on April.

The changes in runoff timing from 1947-2003 are very similar to the observed trends in streamflow timing shown by Stewart et al. (2005) for essentially the same time period. Because the snow is melting systematically earlier in the model simulations (Hamlet et al. 2005 (Chapter 4)), the simulated runoff fraction in March systematically increases, and the runoff fraction in June systematically decreases. For March the patterns are similar for 1916-2003 and 1947-2003, although the trends are stronger from 1947-2003. For

June, overall trends are generally downwards from 1947-2003, but are not as consistent for the period from 1916-2003.

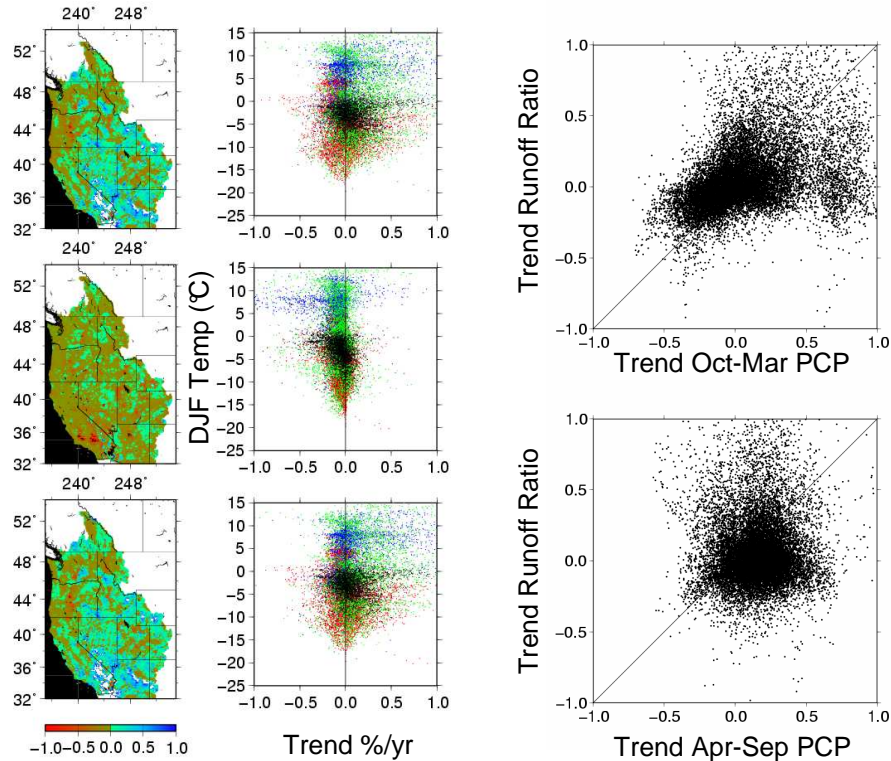


Figure 5.11: Trends in the annual runoff ratio for 1947-2003. Left panels show maps and scatter plots of the trends (see caption for Figure 5.9). Upper right panel shows a scatter plot of trend in runoff ratio vs trend in Oct-Mar precipitation. Lower right panel shows a scatter plot of trend in runoff ratio vs trend in April-Sep precipitation.

These overall trends in runoff timing in March and June can be most clearly understood by first examining the effects of T alone (center row of panels in Figure 5.12-5.13). For March the trend in the fraction of runoff in each month due to T trends alone is typically positive, and is related to a combination of trends towards earlier snowmelt and earlier soil recharge. Trends are greatest in the areas of the domain with intermediate winter temperatures, since these areas experience the start of snowmelt during this time (Figure 5.3). By June the trends in runoff fraction due to T alone are predominantly negative across the board because by June snowmelt in most of the domain has peaked and the



shifts towards earlier snowmelt tend to reduce water availability in all but the very coldest parts of the domain

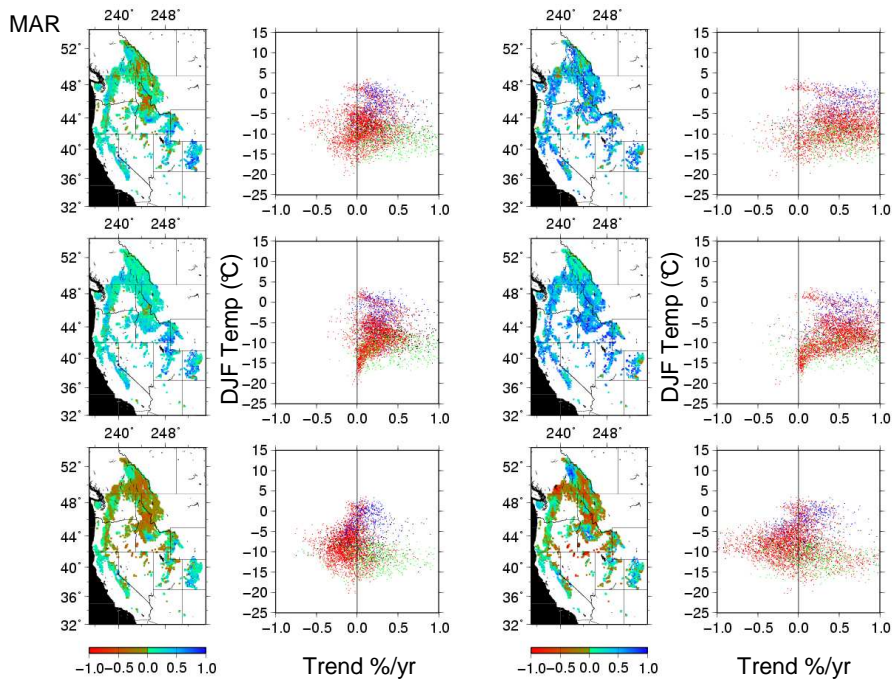


Figure 5.12: Same as Figure 5.9, except showing relative trends in the fraction of annual flow occurring in March

When P trends alone define the trends in runoff fraction (lower row of panels in Figure 5.9-5.10), the overall trends are more difficult to interpret because different areas of the domain experience different seasonal P trends in different months and different time periods. Trends associated with T alone, however, are the most important driver of the overall pattern of trends, particularly for March. Temperature related effects are also somewhat stronger in the period from 1947-2003 than for 1916-2003, but the relative roles of T and P in the two time periods are broadly similar. Results for June are similar although the role of T-related trends is somewhat weaker in this month. A similar analysis of each month and the four seasons (not shown) revealed a more gradual shift from increased runoff in the early spring to reduced runoff in mid to late summer. The monthly results also show that the shifts in runoff timing are related to winter temperature

regimes, with shifts in timing starting earlier in the year in warmer parts of the domain and later in the colder parts of the domain.

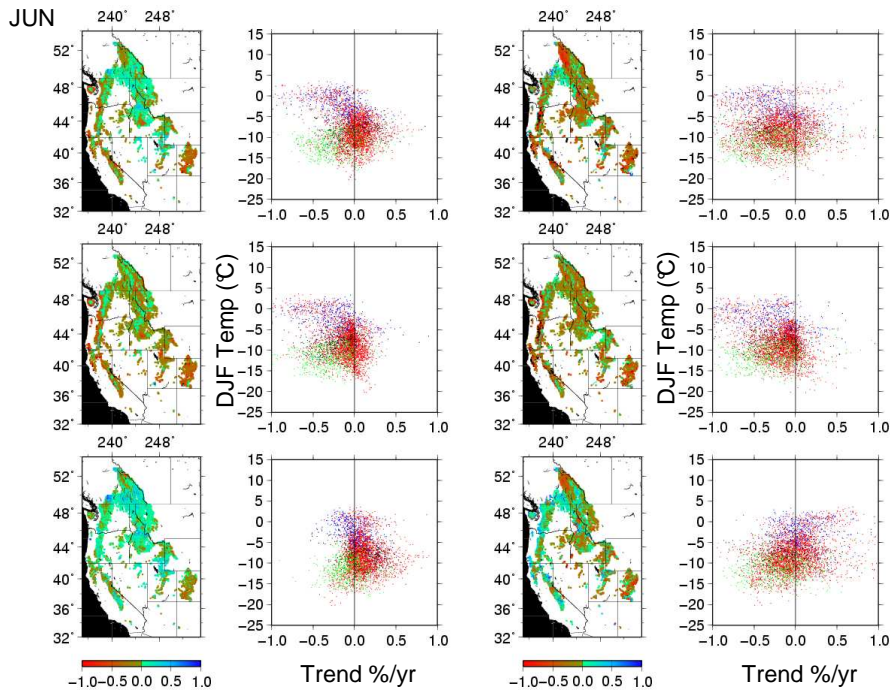


Figure 5.13: Same as Figure 5.9, except showing relative trends in the fraction of annual flow occurring in June

This is expected since the snow melt peaks earlier in the warmer parts of the domain (Figure 5.3). As a general rule, if the snowmelt is occurring earlier in time, then areas of the domain where the dates of peak snowpack occur *after* the month being examined will show upward trends in the fraction of runoff. Conversely, areas of the domain with peak snowpack occurring *before* the month being examined will show downward trends in runoff fraction for that month. Results for May, for example, (not shown) exhibit downward trends in the warmest areas of the domain (near-coastal areas in the PNW and CA) where peak snowmelt has already occurred, whereas in the coldest areas in the domain (e.g. in the PNW in British Columbia) trends in runoff fraction are still increasing in May because peak accumulation occurs later in these colder areas (Figure 5.3).

As discussed in the introduction, many hydrologic simulations in snowmelt dominant basins based on climate change scenarios show reduced runoff in late summer due in part to a longer streamflow recession period caused by earlier input of snowmelt. While downward trends are apparent in our simulations, the trends in the fraction of annual runoff occurring in late summer (not shown) are actually most sensitive to P trends. Trends in late summer low flows are therefore not very robustly linked to temperature trends alone in the late summer.

### ***Trends in Soil Moisture***

Trends in SM are somewhat more difficult to analyze than trends in runoff or ET, because SM integrates the time history of inputs from P (rain), snowmelt, and losses due to ET, runoff, and drainage (baseflow). SM is also characterized by strong autocorrelation in time, which means that lag effects in inputs or losses can be as important as those occurring at the time the impacts are actually observed. In snow melt dominant watersheds in particular, interannual SM variations observed in mid summer are most clearly associated with variability in snow accumulation that is largely determined by climatic conditions occurring as much as ten months earlier.

Trends in SM are reported as relative trends in values reported on the first of each month. We chose to show figures for April 1 and July 1 because changes in SM on these dates roughly correspond to changes in runoff for March, and June (Figure 5.12 and 5.13 respectively) I.e. if increasing trends in snowmelt and/or P falling as rain are apparent in March, then we should see increasing trends in SM on April 1.

On April 1, increasing trends in SM predominate, and are shown to be strongly temperature related, particularly for 1947-2003, during which strong temperature-related effects weaken or reverse the effects of downward trends in P in the PNW (Figure 5.14). For July 1 (Figure 5.15) the effects of P dominate the overall trends. The temperature related trends are generally consistent with the changes in runoff discussed above, i.e.

warm areas show stronger downward trends on July 1 than cold areas (as for June runoff trends in Figure 5.13) and the T-related trends are stronger from 1947-2003 than from 1916-2003.

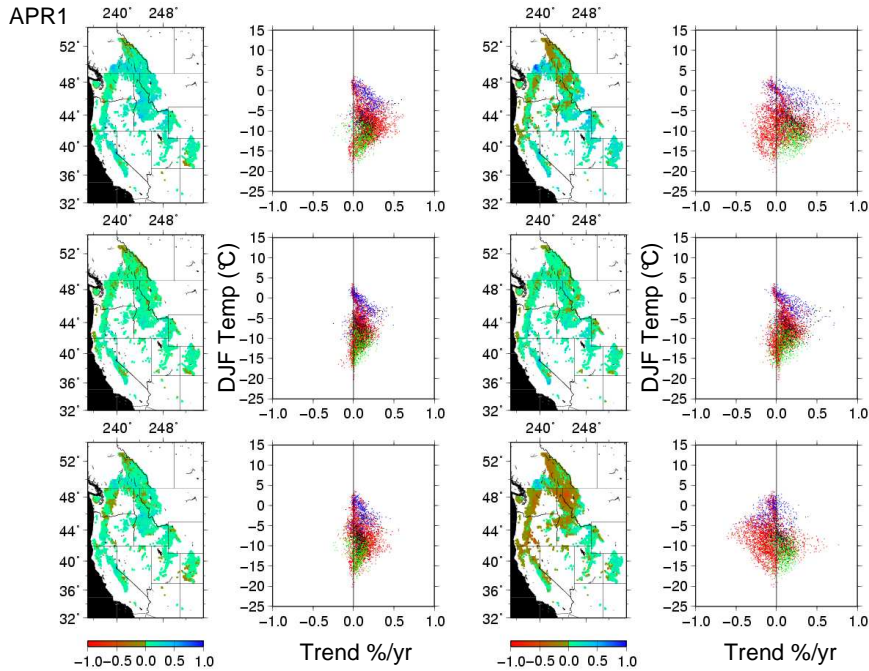


Figure 5.14: Same as Figure 5.9, except showing relative trends in April 1 soil moisture for the periods from 1920-2003 (left panels) and 1947-2003 (right panels)

Despite the fact that the T-related trends play a smaller role in determining overall trends in July 1 SM, the effects due to temperature are clearly reflected in the BR results, and systematically shift the trends associated with P alone one way or the other (Figure 5.15). In some specific cases, the effects of T are the predominant driver of SM trends. On July 1, for example, the FTR trends for the cells with warm winter temperatures are small, whereas the trends for the FPR are larger and essentially determine the BR trends for cells within this climatic regime. T trends are therefore the primary determinant in the BR run for these cells.

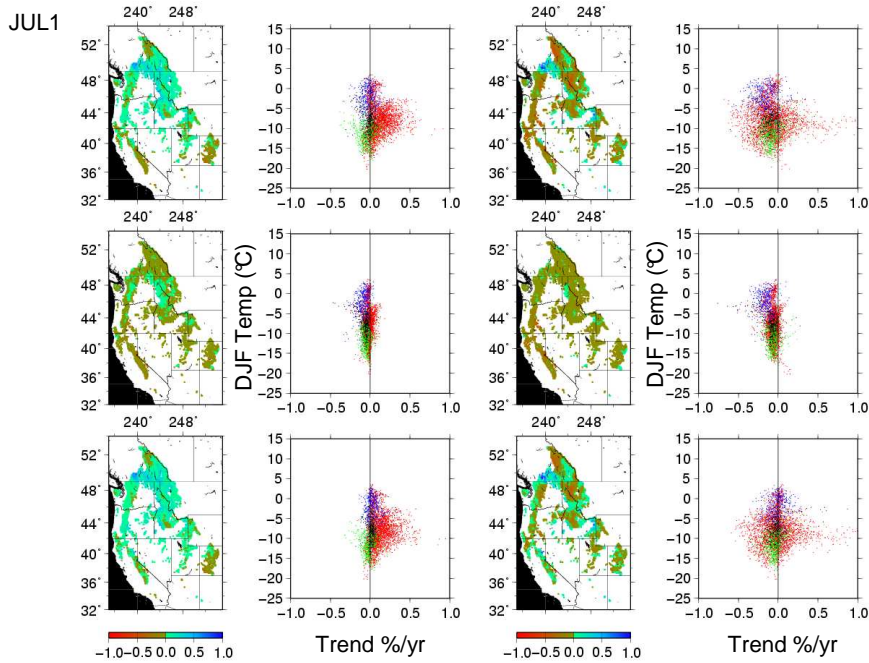


Figure 5.15: Same as Figure 5.9, except showing relative trends in July 1 soil moisture for the periods from 1920-2003 (left panels) and 1947-2003 (right panels)

This makes sense, because these parts of the domain get relatively little P in summer (Figure 5.6), and are subject to strong timing shifts in snow melt timing which are primarily T related (Hamlet et al. 2005 (Chapter 4)).

## 5.6. Summary and Conclusions

Large increasing trends in T are apparent in the gridded meteorological data sets used in this study both for the period from 1916-2003 and for the period from 1947-2003. Daily minimum temperatures are rising faster than maximum temperatures, and the T trends are much larger from 1947-2003. These trends are, by construction, consistent with observed trends in the quality controlled HCN and HCCD data sets.

P trends have been positive over much of the West from 1916-2003, but there have been large decadal excursions from these long term trends, and upward trends from 1916-2003 are most clearly associated with widespread drought in the early part of the record. The

spatial patterns of P trends from 1925-1976 and 1947-2003, for example, are very different from those in 1916-2003. In contrast to the T trends, which are quite spatially homogeneous, P trends show little evidence of spatially consistent long-term trends in the western U.S.

Simulated summer ET as a whole has followed water availability; however in cells with substantial snow accumulation in spring, some systematic changes associated with temperature are also apparent. In early spring, water availability from snowmelt has generally increased due to earlier snowmelt, and ET from April-June has followed these upward trends. Similarly in late summer, increasing T has resulted in decreasing trends in water availability from snowmelt, which has tended to reduce ET from Jul-Sept. Trends in ET in the spring are more strongly temperature controlled than they are later in the summer, because of the influence of snowmelt timing. Despite these changes there is little evidence of a systematic change in the overall seasonal timing of ET (except in CA from 1947-2003), because upward trends in early spring due to earlier snowmelt are frequently paired with upward trends later in the summer due to upward trends in precipitation.

Increasing temperatures have had an important effect on the seasonal nature of runoff in cells with substantial snow accumulation in spring. In March, trends in runoff are strongly upwards and are predominantly associated with temperature effects. In June temperature related trends are strongly downwards. Temperature plays a strong role in determining the overall trends in both months but is more important in March. These changes result in robust shifts in the timing of runoff towards earlier calendar dates that are primarily controlled by temperature trends. By September, however, the T related trends are relatively weak, and P trends begin to dominate the overall trends. These results suggest that trends in low flows in late summer are mostly controlled by P trends rather than by T trends.

Trends in April 1 SM in cells with significant snow accumulation on spring are upwards (i.e. earlier soil recharge) and are most strongly controlled by T related trends. On July 1, the T related effects are much weaker and precipitation is the major driver of the overall trends in most parts of the domain. Areas with little P in summer and large trends in snowmelt timing (e.g. coastal areas of the PNW and CA), however, show strong effects associated with temperature alone. Consistent with these effects, trends in the timing of soil moisture recharge in spring are towards earlier dates, and, as for the changes in April 1 SM, are primarily controlled by temperature trends.

Many studies evaluating global warming projections have concluded that much greater confidence should be placed in projections of increasing T than in changes in P (IPCC 2001). The results of this study are useful in this context, because we have been able to show how strongly ET, runoff, and SM are affected by T and P trends. We can conclude, for example, that future projections of changes in runoff in spring and summer are likely to be more reliable in general than projections of changes in late summer SM.

Furthermore, changes in the seasonal timing of ET in summer in coastal areas of the PNW and CA are much more clearly related to temperature changes, because there is relatively little P in summer to offset losses of water availability due to earlier snowmelt.

In this study our domain is the western U.S. as a whole, however the same analytical techniques could be applied at the river basin scale and might reveal some differing sensitivities to changing regional climate than those that have been summarized here for the larger domain. Likewise, in global warming studies the use of a discrete sensitivity analysis to separately analyze the effects of T and P changes may have value in terms of analyzing the uncertainties inherent in such projections. Forecasts of different hydrologic conditions associated with T and P changes could be weighted differently in the final analysis based on estimates of the reliability of simulated T and P trends as compared to observations, for example.

## **6. Sensitivity of Flood Risk to 20<sup>th</sup> Century Warming and Climate Variability**

This chapter excerpts and summarizes research submitted as:

Hamlet, A.F., Lettenmaier, D.P., 2006: Effects of 20th century warming and climate variability on flood risk in the western U.S., WRR (submitted)

### **6.1. Introduction**

Despite the fact that probability distributions of annual flood maxima are frequently assumed to be homogeneous in time for engineering design purposes, there is now an awareness that flood probability distributions are in fact a complex function of climatic variations over a range of time scales (Franks and Kuczera 2002; Kiem et al. 2003; Sankarasubramanian and Lall 2003). Furthermore, land use changes due to anthropogenic or natural causes such as urbanization, logging, fires, and anthropogenic or natural changes in channel structure are all known to change flood risk (e.g. Bowling et al. 2000; Jain and Lall 2001; Matheussen et al. 2000; Wissmar et al. 2004). Such changes can be important to decision processes that are affected by flood risks. One example of federal policy in the U.S. that is affected by changing flood risks is the Federal Emergency Management Administration (FEMA) flood insurance program, eligibility for which is usually based on 100-year return period flood inundation maps. These risks, and hence maps used for land use planning, are now considered static, but such assumptions may not be realistic. If they are not, important questions are raised about how such programs should be designed and managed to cope with non-stationary insurance risks.

In this paper we focus on the role of climatic variations in determining flood risks associated with natural flow in watersheds in the western U.S.. There is a steadily growing body of research that has demonstrated that climatic variations in the western



U.S. are predictable over a wide range of temporal and spatial scales (Dettinger et al. 1998; Gershunov et al. 1998; Hamlet and Lettenmaier 2000; Mote et al. 2003; Sheppard et al. 2002). Regional scale variations in winter climate associated with the El Niño Southern Oscillation (ENSO) (Battisti and Sarachik 1995) and the Pacific Decadal Oscillation (PDO) (Mantua et al. 1997; Zhang et al. 1997), for example, have been shown to be related to variations in seasonal flow in western rivers (e.g. Hamlet and Lettenmaier 1999a; Hidalgo and Dracup 2003; Redmond and Koch 1991), and these climatic variations may also create variations in flood risks for different periods in the historic record (e.g. cool vs warm PDO epochs), or in certain classes of years (e.g. warm ENSO or PDO years) on an interannual basis. Understanding the relationships between predictable climate variations (e.g. those related to ENSO) and flood risks may have important implications for water management or other decision processes where changes in flood risk can potentially be forecast with seasonal (3-12 month) lead times. Adjustments of flood control rule curves used to operate storage reservoirs, for example, could reflect different levels of flood risk in different years.

Systematic shifts in regional temperature associated with global warming (or other climatic drivers) are also a potentially important concern in the context of flooding. In the western U.S., increasing temperatures in the 20<sup>th</sup> century have already had profound effects on both the quantity and timing of melting snow in spring (Hamlet et al. 2005 (Chapter 4); Mote et al. 2005; Mote 2006). In this region, the hydrologic variability in most rivers is strongly influenced by the process of snow accumulation in fall and winter and melt in spring and summer. Regional warming over the last century has already affected the timing of runoff (Stewart et al. 2005) and (as inferred from modeling studies) soil moisture recharge (Hamlet et al. 2006 (Chapter 5)), effects which also have the potential to alter the probability distributions of floods.

In this study we seek to understand and quantify the effects of 20<sup>th</sup> century warming and interannual and interdecadal variations in winter climate on flood risks across the western

U.S., which we define as the U.S. west of the Continental Divide, and the Canadian portion of the Columbia River basin in British Columbia.

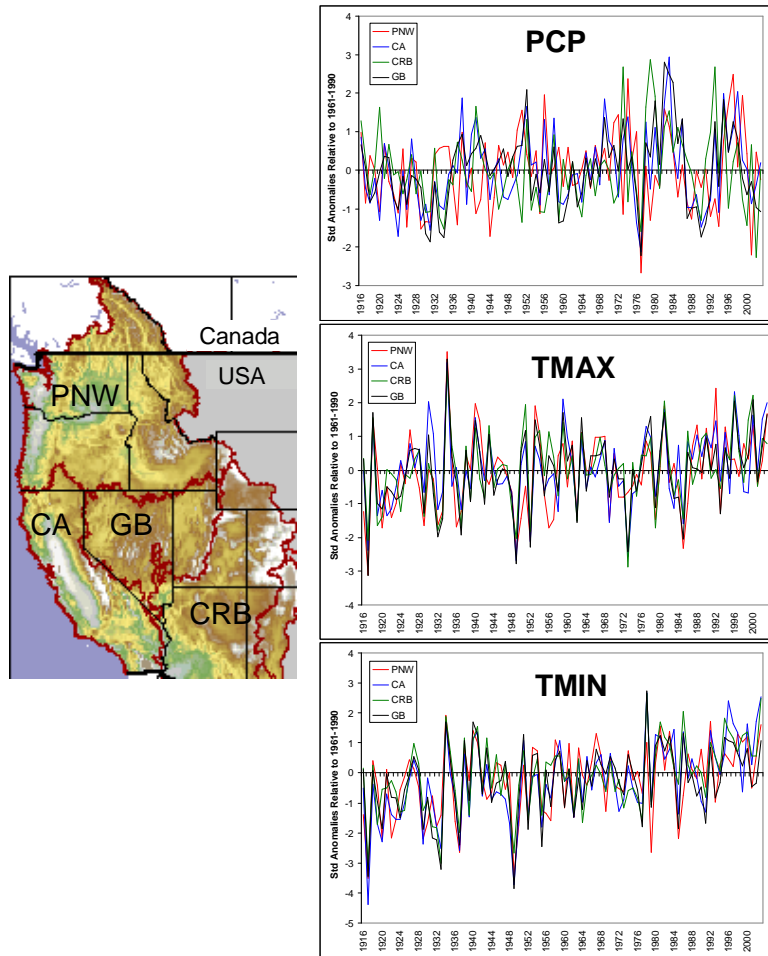


Figure 6.1 Study domain and a long-term, spatially-averaged time series of cool season (Oct-March) standardized anomalies of precipitation (PCP), maximum daily temperature (TMAX), and minimum daily temperature (TMIN) for the PNW, CA, CRB, and GB.

For purposes of discussion we have also divided this larger domain into four sub-domains: the Pacific Northwest (PNW) which comprises the Columbia River basin and coastal drainages; California (CA), which comprises rivers within the Sacramento and San Joaquin basin; the Great Basin (GB); and the Colorado River basin (CRB) (Figure 6.1). We will also demonstrate that the effects of 20<sup>th</sup> century warming and interannual

and interdecadal variations in winter climate on western U.S. flooding are in fact linked, because a general warming also affects interannual variations in river discharge. To avoid potentially confusing interactions between these two mechanisms in the observed climatic record, we develop methods to isolate the sensitivity to these two effects in the subsequent analysis.

## **6.2. 20<sup>th</sup> Century Climate Variations in the Western U.S.**

In two companion studies, Hamlet et al. (2006) (Chapter 5) and Mote et al. (2005) have examined trends in cool and warm season precipitation and temperature over the same western U.S. domain using both observations from the Historical Climatology Network (HCN) (Karl et al. 1990) and the same daily time step gridded meteorological data used here (see following sections for more details on the meteorological driving data set). We summarize below some of the key findings from the earlier papers that have a direct bearing on the hypotheses and experimental design of this study.

To begin with, there are fundamental differences between variations in precipitation and temperature over the 20<sup>th</sup> century that are important in the context of this study. From 1916-2003 essentially the entire western U.S. has experienced increases in both cool season and warm season temperatures (Mote et al. 2005; Hamlet et al. 2006 (Chapter 5)). The rate of change varies from location to location and with the time period examined, but the central tendency is on the order of one degree (C) per century from 1916-2003 (Hamlet et al. 2006 (Chapter 5)). The rate of increase from 1947-2003 is roughly double that of the longer period from 1916-2003, which is largely attributable to the fact that much of the observed warming has occurred from about 1975 to present. Although regional scale changes in temperature may or may not be directly attributable to global warming, the synchronicity and spatial extent of these changes, coupled with high correlations between the smoothed regional and global mean temperatures (Figure 6.2), provides evidence that regional temperatures are coupled to global temperatures.

The nature of precipitation variations in the western U.S. over the period 1916-2003 contrasts with the observed temperature changes. Over this period, there is little evidence of any consistent large-scale trends. Instead, precipitation variations seem to be most strongly related to natural variations at decadal time scales in particular regions (Cayan et al. 1998; Mote et al. 2005; Hamlet et al. 2006 (Chapter 5)). To illustrate this point, a comparison between the CRB and the PNW is instructive. Figure 6.2 shows that the West as a whole was relatively dry from 1925-1946 and remained dry in the CRB from 1947- 1976 after which there was an abrupt shift to wetter conditions from 1977 on (Hidalgo and Dracup 2003). In the PNW, however, the period from 1947- 1976 was anomalously wet, while the period from 1977 to at least the mid 1990s was generally dry (Figure 6.2). Thus trends in precipitation across the West have been generally upwards since the early part of the century (owing primarily to large scale drought in the early part of the record), but are opposite in sign for the PNW and the CRB in the last half century or so when global warming arguably has had its strongest influence (Mote et al. 2005; Hamlet et al. 2006 (Chapter 5)). These historic patterns support the hypothesis that long-term trends in cool season precipitation in the West are controlled primarily by natural climatic variations at the regional scale and that large scale effects associated with regional warming have (at least so far as the long-term trends are concerned) played a relatively minor role.

A lack of clear trends in cool season precipitation notwithstanding, there is an obvious change in the interannual variability across the western U.S. after about 1973 (Figure 6.1). The change in variability is characterized by increased coefficient of variation, increased period of oscillation, and increased covariation between regions (analysis not shown). This increased synchronicity and increased range of variation has also been noted in several other studies examining observed streamflow records in the western U.S. (e.g. Cayan et al. 2003; Jain et al. 2005; Pagano and Garen 2005). There is currently little conclusive evidence to tie these changes in variability to global warming per se, however

the synchronicity and spatial extent of these effects again suggests a large scale climatic influence affecting the West as a whole.

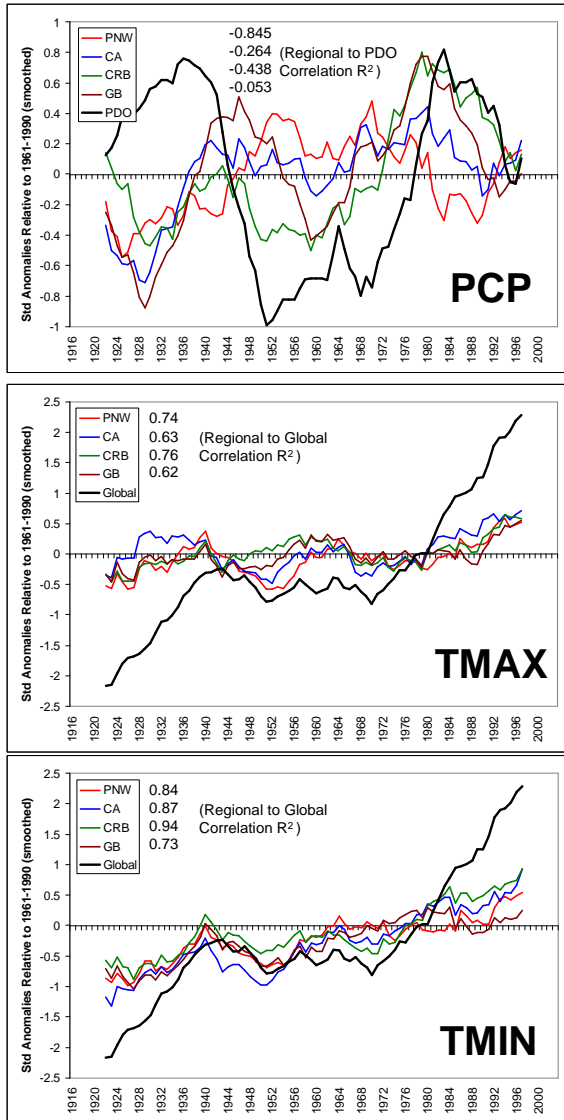


Figure 6.2 Standardized anomalies for cool season precipitation (PCP), maximum temperature (TMAX), and minimum temperature (TMIN) shown in Figure 6.1, smoothed with a 12-year running mean. Precipitation is compared to a smoothed time series of the cool season PDO index anomalies. Temperature is compared to the smoothed time series of standardized global mean temperature anomalies. Inset tables in each case show the correlation ( $R^2$ ) between the smoothed regional time series and the PDO index and global temperature time series, respectively.

These findings have important implications for investigations of evolving flood risks in the western U.S., which are potentially affected by both temperature and precipitation changes at various time scales (see discussion of mechanisms in following section). Because the West is apparently systematically warmer now than it was in the past, one objective of this study is to understand the resulting implications for flood risks. We will also examine the changes in flood risks associated with interannual climate variations associated with PDO and ENSO, as well as for the apparent changes in cool season precipitation variability that have occurred since the mid-1970s.

### **6.3. Physical Mechanisms Associated with Western U.S. Flooding**

At the most fundamental level, flooding is caused by complex interactions between storm characteristics (seasonality of storms, precipitation intensity, storm size and duration, temperature, orientation, and velocity), catchment geometry (basin area, slope, orientation), land surface characteristics (infiltration rate, depth of soils, vegetation), and the nature of antecedent hydrologic conditions (soil moisture, snowpack) (Pilgrim and Cordery 1993). For many rivers of moderate to large spatial scale in the western U.S. floods typically result from either a) large scale fall and winter storms, or b) spring snowmelt, both of which are associated with relatively large-scale climatic drivers (O'Conner and Costa 2003). In Section 6.4 below we also compare the seasonality of flooding for both model simulations and observations, which provides additional evidence that winter and spring flooding are the general rule in the western U.S. for basins larger than about 775 km<sup>2</sup> (Figure 6.3). These general characteristics are in contrast to flooding that occurs at smaller spatial scales in the arid southwestern U.S. and in other regions of the U.S., where warm-season thunderstorms affecting relatively small spatial scales are sometimes responsible for extreme flash flooding (e.g. the 1997 flood at Ft. Collins, CO, and the 1972 flood at Rapid City, Iowa).

On this basis we argue that, at least for the moderate to large river basins in the western U.S. that we will examine in this study, the causes of flooding associated with catchment geometry and storm size interactions are probably less important than in other regions, and large scale effects due to cool season climate play a more important role. This is particularly true in larger snowmelt dominant rivers where spring snowmelt flooding is often related to the spatially and temporally integrated climatic effects occurring during the entire snow accumulation season (typically Nov-March) rather than to individual winter storms (O'Conner and Costa 2003).

In the western U.S., climate variability primarily affects flood risks via storm characteristics, contributing basin area (a function of temperature and topography in mountain basins), and antecedent hydrologic conditions (particularly soil moisture and snowpack). For a given temperature regime, increases in precipitation intensity or duration at the time when floods typically occur would generally be expected to increase flood risks (Pilgrim and Cordery 1993); however, for a given regional climate, the specific physical mechanisms associated with temperature that influence flooding are potentially different for basins with different winter temperature regimes.

In rain dominant basins that are mostly above freezing in winter, floods are mostly associated with storms that produce a) extreme precipitation intensity or b) heavy precipitation over a longer duration and/or a large spatial scale. The amount of runoff produced by either kind of storm can be intensified by antecedent conditions that produce saturated soils (Pilgrim and Cordery 1993). In these basins, one might expect that systematic shifts in temperature would play a relatively minor role in changing flood risks, because floods are determined primarily by the precipitation characteristics and sequencing of observed storms.

In mountain watersheds where average mid-winter temperatures are close to freezing (sometimes referred to as “transient snow” watersheds), temperature can play an

important role in determining the amount of runoff that will occur in response to a given storm. This is particularly true in places where cool season storms are large enough in spatial extent that a large portion of the basin is affected by individual storms, with temperature controlling the contributing basin area via the form (rain or snow) of the precipitation over different parts of the basin. In near coastal mountain watersheds in WA, for example, warm winter storms (e.g. “pineapple express” storms) can produce an unusually large amount of runoff simply because the entire watershed is below the snowline (USGS FS 228-96). A similar amount of precipitation occurring in combination with colder conditions can have a much smaller contributing basin area. Antecedent snowpack can also melt during warm events, adding additional runoff to that generated by new precipitation (so-called “rain on snow” floods) (USGS FS 228-96). Thus several competing mechanisms present themselves with regard to changes in flooding in response to systematic warming in transient watersheds. Storms occurring in early winter, for example, would presumably be associated with significant antecedent snow less frequently and/or over a smaller portion of the drainage area in a warmer climate, but the effective basin area (responding to precipitation as rain) would presumably be larger. Thus, in response to warming, flood risks could potentially increase or decrease depending on the relative importance of these two factors. Seasonality of flooding may also play a role in transient watersheds. One might hypothesize, for example, that transient snow watersheds for which the largest floods typically occur in early winter would see increased flooding due to an increased effective basin area producing runoff, whereas those that typically experience flooding in the early spring might see decreases in flooding due to less antecedent snowpack.

In snowmelt dominant watersheds, for which mid-winter temperatures are frequently well below freezing, flooding typically occurs in spring when anomalously large snowpacks have accumulated and either melt rapidly due to warm temperatures or are combined with additional precipitation falling as rain. Increasing temperatures have been shown to result in decreased spring snow accumulation (Hamlet et al. 2005 (Chapter 4)), which would



suggest decreased flood risks; however earlier snowmelt and the resulting earlier soil moisture recharge (Hamlet et al. 2006 (Chapter 5)) could also potentially increase flooding during some spring storms.

#### **6.4. Methods and Experimental Design**

As in Hamlet et al. (2005) (Chapter 4) we use the Variable Infiltration Capacity (VIC) hydrologic model (Liang et al. 1994), implemented at 1/8<sup>th</sup> degree latitude/longitude resolution over the West. Additional details on the model implementation are given in Hamlet et al. 2005 (Chapter 4). In this study, we also make use of a daily time step streamflow routing model described by Lohmann et al. (1998), which is applied as a post processing step to daily time step runoff and baseflow calculated by the VIC model for each 1/8 degree grid cell. The routing model uses a unit hydrograph approach at the grid-cell scale, combined with a simple channel routing scheme that accounts for lateral movement of water between grid cells. The model does not include detailed information about spatial variations in the unit hydrographs for each cell or about the detailed hydraulic characteristics of the river channel system, but is appropriate for large-scale studies of this kind where such details are not the central concern. It is important to reiterate that we are examining hydrologic effects of climatic variability and change on natural streamflow, which is defined as the streamflow that would occur in the absence of anthropogenic effects such as water management and land use change.

At very large spatial scales (i.e. river basins with drainage areas on the order of  $10^4 - 10^5$  km<sup>2</sup>), the VIC model has been shown to reproduce naturalized monthly streamflows for a number of basins across the western U.S. with good fidelity (Maurer et al. 2002). At smaller spatial scales the model typically displays more bias, although monthly streamflow anomalies associated with climatic variability are often well simulated when the model bias is removed via statistical procedures (Voisin et al. 2006).

Previous studies have also shown that the macro-scale changes in snowpack and runoff timing associated with warming and changing precipitation regimes in the western U.S. are faithfully reproduced by the model, despite bias at smaller spatial scales (Hamlet et al. 2005, 2006 (Chapter 4 and 5); Mote et al. 2005). The model is evaluated in the context of climatic effects on flooding below.

### *Climatic Data*

We take as our starting place the gridded 1/8<sup>th</sup> spatial resolution meteorological data set for the western U.S. described by Hamlet and Lettenmaier (2005) (Chapter 3) and used in previous studies to investigate hydrologic trends in the region (Hamlet et al. 2005, 2006 (Chapter 4 and 5); Mote et al. 2005). To investigate the effects of 20<sup>th</sup> century warming on floods, two variations of this daily temperature and precipitation data set were constructed, each representing an identical precipitation time series for a specific temperature regime associated with early and late 20<sup>th</sup> century conditions. To construct these detrended data sets, for each grid cell and each calendar month, linear trends in the monthly average of daily maximum temperature (Tmax) and daily minimum temperatures (Tmin) were removed from the time series relative to a specific “pivot year” as follows:

$$T_{\text{adj}}[\text{month}][\text{year}] = T_{\text{orig}}[\text{month}][\text{year}] + \text{Trend}[\text{month}] * (\text{Pivot\_Year} - \text{year})$$

Thus for a positive trend in temperature, temperatures in years before the pivot year were increased, while temperatures in years after the pivot year were decreased. After the monthly trend was removed, the original daily data were scaled to recreate the adjusted monthly value, while retaining the time series elements of the daily variations within the month. Thus the long-term trends in maximum and minimum temperature were removed but the daily covariability of temperature and precipitation was maintained as in the historic record, and most of the statistics of the spatial, seasonal, and interannual

variability of temperature and precipitation are preserved in the adjusted data sets. Note, however, that the trends in Tmax and Tmin were adjusted separately for each month.

This procedure was carried out for a pivot year of 1915 (i.e. to create a data set consistent with early 20<sup>th</sup> century temperatures), and for a pivot year of 2003 (i.e. to create a data set consistent with late 20<sup>th</sup> century temperatures). The advantage of using this approach is that a long time series of precipitation and temperature variability, reflecting a wide range of natural variability over the 20<sup>th</sup> century, can be examined in the context of a consistent overall temperature regime. Thus we can examine the effects of natural variability that occurred early in the century for a temperature regime consistent with the late 20<sup>th</sup> century, and vice versa. This also provides a large sample for evaluating in quantitative terms the effects on flood statistics.

Climate categories (warm, neutral, cool) for interannual ENSO and PDO variations were based on the NINO3.4 index of Trenberth (1997), the PDO index of Mantua et al. (1997) and the definitions shown in Table 1.

Table 6.1 Retrospective definitions of warm, neutral, and cool ENSO and PDO years

Climate Category	Index Used	Definition
warm ENSO	NINO3.4	> 0.5 std deviations above the mean for DJF mean
ENSO neutral	NINO3.4	neither warm nor cool
cool ENSO	NINO3.4	< -0.5 std deviations for DJF mean
warm PDO	PDO	> 0.5 std deviations above the mean for ONDJFM mean
PDO neutral	PDO	neither warm nor cool
cool PDO	PDO	< -0.5 std deviations for ONDJFM mean

Note that we will examine the implications of interannual variations in the PDO index (rather than an epochal formulation) based on the analysis of Newman et al. (2003) (Also see discussion in Chapter 2).

### ***Flood Frequency Estimation***

For each river basin, and each of several daily streamflow simulation time series (representing different temperature regimes and/or composites based on climatic categories), the annual maximum series (AMS) (i.e. a time series of the maximum daily flow in each water year) was extracted. The Generalized Extreme Value (GEV) probability distribution was fitted to each AMS using L-moment parameter estimation techniques (Hosking and Wallis 1993; Stedinger et al.1993). Other parameter fitting techniques for the GEV distribution were also tried using LH2 and LH4 moments (Wang 1997) and log normal (LN) and Extreme Value Type I (EV I) distributions were also fitted to the data (Stedinger et al.1993). The conclusions for this large scale study were not found to be very sensitive to the choice of distribution or fitting technique, and the GEV distribution using L-moment parameter estimators was used throughout given that the true probability distributions (and the nature of the changes in these distributions) in each case are not known (Potter and Lettenmaier 1990). Although a regional fitting procedure could also potentially be used, we intentionally use at-site fits of the GEV, because we are interested in quantifying the effects of warming on basins with different mid-winter temperature regimes, and in identifying the spatial signature of PDO and ENSO effects, effects that would potentially be masked by regional estimators.

When fitting the probability distributions for flooding associated with ENSO and PDO climate categories, and data from 1973-2003, the AMS from each basin was first composited according to the climate category (i.e. flows for years that do not match the climate category were excluded), and the data were then processed exactly as for the entire data set.

Using the GEV parameters estimated in each case, the 5, 10, 20, 50, 100, 200, and 500-year return period floods were calculated for each model forcing data set and climate category. While the absolute value for each recurrence interval is estimated, we are

primarily interested in changes in these quantities, and will present the results as changes relative to a base condition.

### ***Model Evaluation***

As noted above, the VIC model has previously been used and evaluated mostly for relatively large river basins at the monthly time scale (e.g. Maurer et al. 2002). In this study, we are fitting distributions to AMS for smaller spatial scales (down to about 1700 km<sup>2</sup>). In this section we evaluate the ability of the model to capture the broad behavior of flood regimes across the region using daily streamflow data from the USGS Hydro-Climatic Data Network (HCDN) (Slack et al. 1993) – a set of stations with long records that are nominally unaffected by diversions or reservoir regulation. The test stations were selected based on basin size (drainage area > 775 km<sup>2</sup> (300 mi<sup>2</sup>)), the availability of serially complete daily data for at least 50 years, and coincidence with the pre-existing VIC stream routing network. 80 stations satisfying these criteria were identified with records from water year (WY) 1953-2003 [Note that we extended the HCDN records (which originally ended in 1988) through 2003, using current USGS station records]. These gaging stations were then registered with the VIC stream routing network, and VIC simulations were made for a coincident time period using observed temperature and precipitation data (without temperature detrending). GEV probability distributions were fit to the observed and simulated AMS as described above. The mean annual flood (computed from the AMS, rather than the fitted distribution) and the average date of the annual maximum (daily) flow were also calculated for both observed and simulated data.

To begin with, the model displayed considerable bias in attempting to reproduce the mean annual flood in each test basin. Many of the HCDN basins are fairly small in size, which exacerbates errors in the spatial distribution of precipitation in the gridded driving data sets, and even in larger basins up to about 26,000 km<sup>2</sup> (the largest in the test data set) errors in the simulated mean annual flood (not shown) were frequently on the order of 50%. From this analysis it was clear that for accurately estimating the absolute value of

annual daily peak flows in each individual basin, the model and driving data sets were not suitable for the intended analysis.

Several aspects of the flood response in each basin that are important to this study, however, were reasonably well simulated. Firstly, the model captured the seasonality of flooding in each basin with reasonable fidelity in most of the test basins (Figure 6.3 upper left). This is important in the context of evaluating temperature related impacts on flooding regimes, because the seasonal timing of flooding is strongly related to temperature effects associated with snow accumulation and contributing basin area in the western U.S.. Secondly the model was able to produce plausible simulations of the ratio of the 100-year flood to the mean annual flood (Figure 6.2 upper right and lower panels). This analysis demonstrated that once the bias in the simulated mean annual flood was removed, the estimates of flood quantiles from the fitted GEV distributions were reasonable in most cases. To exploit the strengths of the model and to avoid the issue of bias in the simulation of the mean annual flood, we will report only the relative changes in flood quantiles associated various climatic drivers.

The climate sensitivity of the model and probability distribution fitting procedure was also examined by compositing the data from 1953-2003 in two ways. In the first case (Figure 6.4 left panel) we composite the data for the period from 1973-2003 (31 of 51 years) for both observed and simulated data, fit GEV parameters, and estimate the 100 year event for each sample. The 100 year event for the composited data was then compared to the 100-year event for the unconditional sample (all data from 1953-2003) for both VIC and HCDN observations. In the second case (Figure 6.4 right panel) the same procedure is followed except data are composited for all warm ENSO years from 1953-2003 (17 years of 51).

The period from 1973-2003 is characterized both by warmer temperatures and increased cool season precipitation variability in comparison with the entire 1953-2003 period (Figure 6.1).

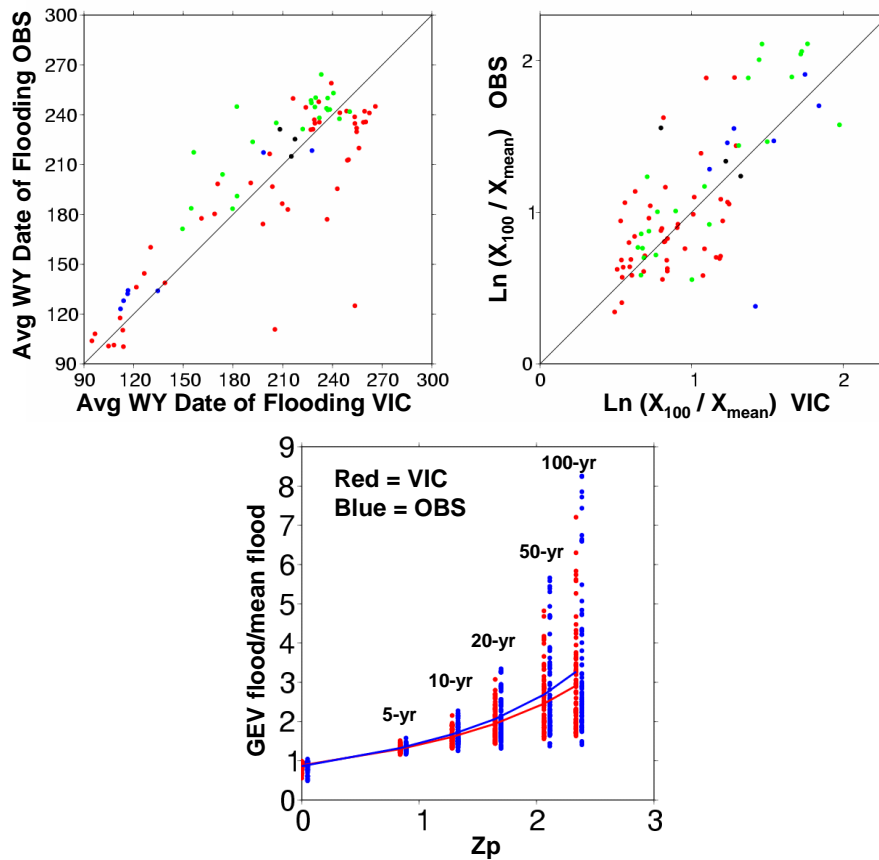


Figure 6.3. Flood statistics from the VIC simulations compared with observations from the HCDN network from 1953-2003: upper left: scatter plot of simulated vs observed average WY date of flooding (day 1 = Oct 1), upper right: scatter plot of the natural log of the ratio of the 100 year flood to the mean annual flood; lower: summary of GEV fits for all stations for 5, 10, 20 50, and 100 yr return intervals, dots show individual stations, line plots show the central tendency for all stations. Stations are color coded by region in upper two panels: Red = PNW, Blue = CA, Green = CRB, Black = GB

The model suggests that increases in flood risks have occurred overall, and this is corroborated by the observations, although the model signals are stronger than observed in some cases, particularly in the PNW. Some bias towards predictions of “false

increases” (the lower right quadrant of the figure) are also apparent. Regional scale changes are simulated more accurately, however (colored lines in Figure 6.4).

In the case of the warm ENSO composite, the smaller sample size results in a large increase in the absolute errors, which makes interpretation more difficult. This sample size is not representative of that available in the sensitivity analysis shown in following sections (where both PDO and ENSO composites have sample sizes of about 30) so the absolute errors shown are not the primary concern.

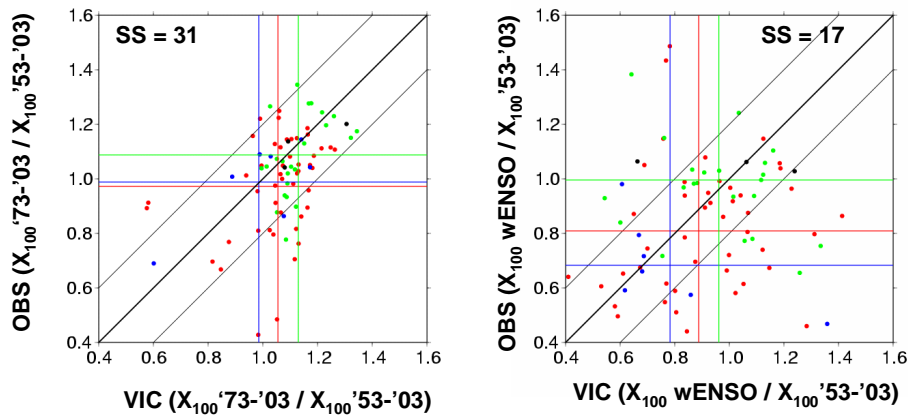


Figure 6.4 Evaluation of model climate sensitivity; left panel: comparison of VIC and HCDN changes in the 100-year flood expressed as ratio between the 100-year event for the 1973-2003 composite (sample size = 31) and the 1953-2003 100 year event; right panel: comparison of VIC and HCDN changes in the 100-year flood expressed as ratio between the 100-year event for a warm ENSO composite (sample size = 17) and the 1953-2003 100-year event. Stations are color coded: Red = PNW, Blue = CA, Green = CRB, Black = GB. Color coded lines in both panels show regional average changes along the x axis (VIC changes, shown as vertical lines), and along the y axis (OBS changes, shown as horizontal lines). Light lines parallel to the one-to-one line show approximate 20% error bounds.

Climatic signals associated with ENSO are broadly characterized by regional scale redistributions of winter precipitation combined with moderate temperature anomalies.

On a station by station basis, the model is not a very reliable predictor of changes in flood risk associated with ENSO, especially for this relatively small temporal sample.

However, on a regional scale the model does better. For the PNW (red dots and lines in Figure 6.4) a moderate shift towards lower flood risks is apparent in both the observations and simulations. For CA (blue dots and lines in Figure 6.4), flood risks are



strongly lower in warm ENSO years in both the observations and simulations. In the CRB (green dots and lines in Figure 6.4) the observations and simulations show little overall shift in flood risks. Each of these effects is also broadly consistent with the regional scale precipitation and streamflow signals associated with warm ENSO discussed in the introduction.

From the analysis described above we conclude that while the model has significant limitations for estimating changes in flood risks in any particular basin, it is well suited to identifying large-scale changes in flood risks associated with climate variability, which is our primary objective here. We should state clearly that large-scale hydrologic experiments of the kind we undertake here, while providing potentially useful information about the changing nature of flood risks on a regional basis, cannot be considered a replacement for more detailed studies at the basin scale.

### *Test Basins*

Having evaluated the model using a limited observed data set, we then constructed a larger set of test basins to evaluate the sensitivity of flood risks to climate across the region. Rather than select test basins according to specific river locations (e.g. U.S. Geological Survey (USGS) gaging sites) we instead designed a large-scale sensitivity study in which we used model simulations of AMS for all drainage basins within the region with drainage areas lying within specified size ranges. In this way we can examine the scale dependence of the results, while retaining a relatively large sample size. This approach also has some advantages when interpreting the effects of changing flood risks as a function of mid-winter basin temperature regimes and other climatic effects, because we can show the effects over a wider range of conditions in a consistent manner. The basin size ranges were selected according to ranges of  $1/8^{\text{th}}$  degree cells shown in Table 6.2.

The basins in each category were selected so that they a) fall within the range of cells and b) are unique (in the sense that the selected basins do not “nest” within any others in the same size range). Because each basin is selected by following the routing path downstream until the first basin within the size range is found, in general the location closest to the lower bound of the category is selected first (and basins whose downstream most points are cells somewhat further downstream are not duplicated in the list). For each basin, the unadjusted daily average temperature from the VIC driving data set was summarized for DJF for the period 1915-2003, and retained for use in subsequent categorization of results.

Table 6.2 Size definitions for simulated test basins used in the west-wide sensitivity study

Basin Size Range (number of 1/8 <sup>th</sup> degree cells)	Approximate Basin Size (km <sup>2</sup> )
12-25	1728
25-50	3600
50-100	7200
100-200	14400
200-400	28800
400-800	57600
800-1600	115200
1600-3200	230400
> 3200	> 460800
> 4000	> 576000
> 5000	> 720000

In a few isolated cases the “flow” from a simulated drainage network in the model does not represent a point in a river channel. The largest drainage network in the GB, for example, represents the combined drainages that feed the Great Salt Lake, which is a closed basin. One could argue that daily flood frequencies in these specific cases are probably not the most appropriate metric for high flow events, but for completeness we nonetheless include these combined drainages in the analysis.

## 6.5. Results and Discussion

In the following sections we present results from the three model sensitivity studies showing the effects of century scale warming, retrospective PDO ENSO variability, and

changes in cool season precipitation variability since the mid-1970s on flood risks across the western U.S..

### *Effects of Century-Scale Warming*

In this section we compare calculated flood risks associated with the 2003 temperature regime with those associated with the 1915 temperature regime and diagnose the dominant mechanisms that are responsible for the changes in the different test basins. Figure 6.5 shows the changes in the 20-year flood for the smallest basins ( $\sim 1700 \text{ km}^2$ ) expressed as a ratio of the 2003 20-year flood divided by the 1915 20-year flood.

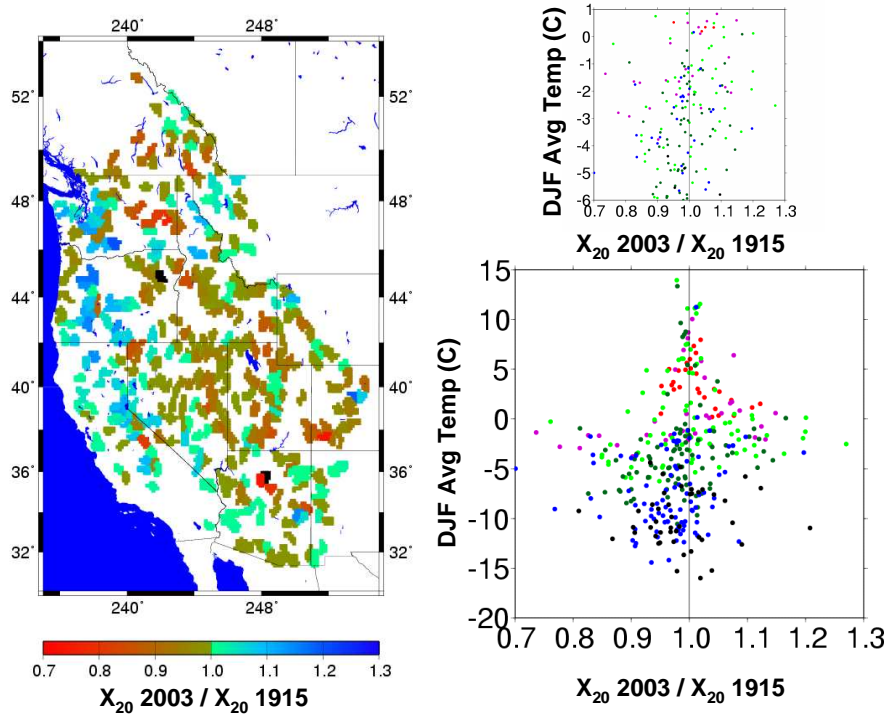


Figure 6.5. Ratio of estimated 20-year flood quantiles (2003 temperature regime/ 1915 temperature regime) for the smallest basin size (12-25 cells) shown as a spatial plot (left panel) and a scatter plot (lower right) showing the ratio as a function of DJF average temperatures in each basin. Inset figure (upper right) shows a scatter plot of basins with DJF temperatures between  $-6^{\circ}$  and  $1^{\circ}$  C. Color coding in the scatter plots identifies the month when flooding typically occurs in the simulations: red = Jan, purple = Feb, light green = Mar, dark green = April, blue = May, black = June

Figure 6.6 shows the same results for three different basin sizes. Relationships for flood changes at longer return intervals (e.g. the 100-year flood) are similar (Figure 6.7). In the scatter plots the relationship between basin average DJF temperatures (and the month when flooding typically occurs) and the ratio of flood quantiles are shown. Basin DJF temperatures broadly categorize the response to warming for different basins. For basins with mid-winter temperatures above  $5^{\circ}\text{C}$  (i.e. rain dominant), systematic changes in floods are relatively small, and are probably due to modest changes in antecedent soil moisture conditions associated with changes in evaporation. For DJF temperatures below about  $-6^{\circ}\text{C}$ , flood risks are mostly reduced by the observed warming. Most of these basins are strongly snowmelt dominant, and experience annual peak flows in spring (usually in May or June).

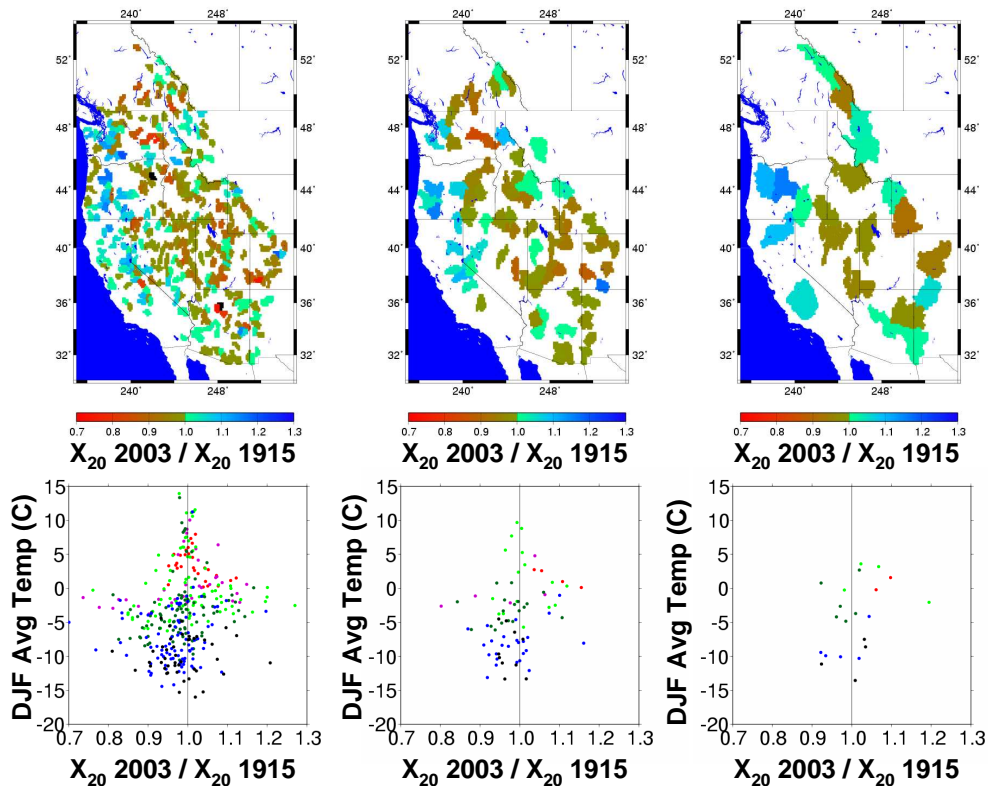


Figure 6.6 . Same as Figure 6.5, but showing results for three different basin sizes: 12-25 cells (left), 50-100 cells (center), and 200-400 cells (right).

Flood risks tend to decline in these basins because of systematic reductions in spring snowpack. In some basins, however, the largest precipitation events occur in late spring, at a time when most of the snowpack has already melted. For these basins, the annual floods can increase in magnitude due to a combination of elevated soil moisture in the spring (Hamlet et al. 2006 (Chapter 5)) or enlarged contributing basin area due to warmer temperatures.

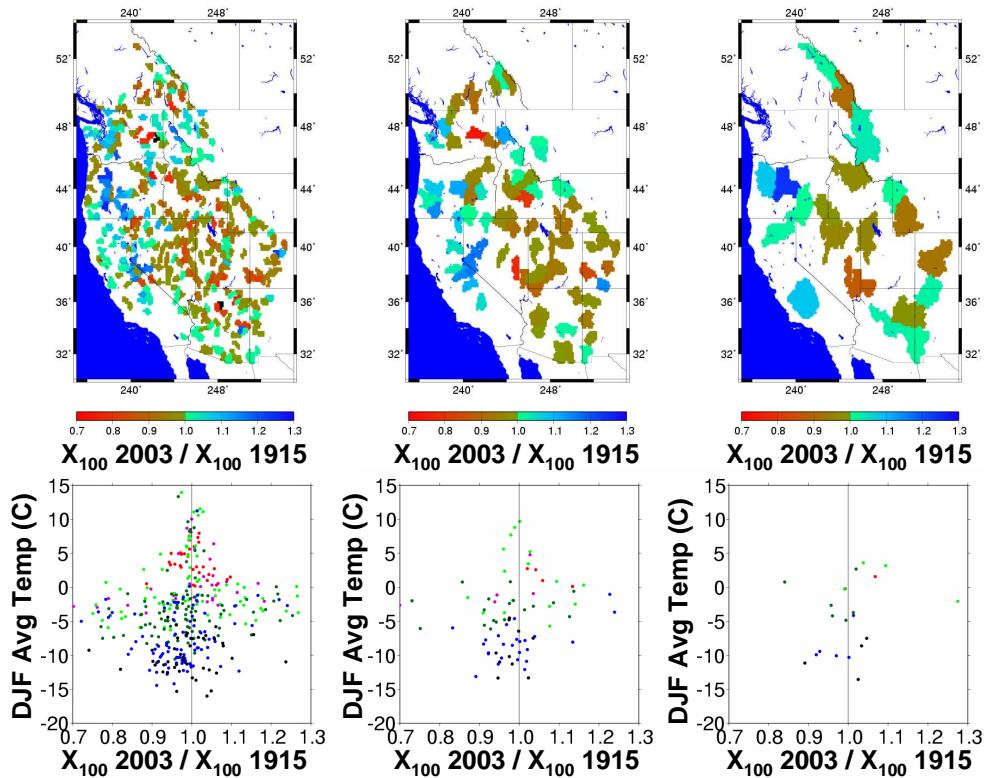


Figure 6.7. Same as Figure 6.6, but showing the estimated 100-year quantiles.

For basins with moderate mid-winter temperatures between about  $-6^{\circ}\text{C}$  and  $1^{\circ}\text{C}$ , a wide range of effects is apparent. The inset scatter plot for this DJF temperature range (Figure 6.5) shows that there is a relationship between mid-winter temperatures and the change in the 20-year flood (i.e. warmer basins are less likely to show a decrease, and cooler basins are more likely to show a decrease in the 100-year flood). In this kind of basin, the effects on flood risks are ultimately determined by complex tradeoffs between antecedent

snow conditions and the effective basin area contributing to runoff from rainfall. Consider a transient snow basin with mid-winter temperatures close to freezing that typically experiences flooding in February or March. In the 2003 climate the basin will typically have accumulated less snow in December and January than in the 1915 climate, which would tend to reduce flood risk, whereas in the 2003 climate the contributing basin area will tend to be larger than in the 1915 climate. Depending on the relative size of these two effects, the flood risk will either increase or decrease. These mechanisms are broadly consistent with the dependence of changes in the 20-year flood on mid-winter temperatures, because the warmer basins tend to have less antecedent snowpack than cooler basins –i.e. in warmer basins the effect of basin enlargement dominates, whereas in cooler basins the reduction in antecedent snow dominates.

Transient snow basins are also sensitive to the seasonality of trends in temperature in each particular basin. For example, in a hypothetical basin that typically floods in February or March, if the warming trends are relatively large in December and January, but are relatively small in February and March, then the effects due to decreased antecedent snow will tend to dominate and the 20-year flood would tend to decrease. If the situation is reversed and the warming trends are small in December and January and large in February and March, then the effects associated with enlarged contributing basin area would tend to dominate. These tradeoffs are probably also present in the case of snowmelt dominant basins (as discussed above), but transient basins are more sensitive because the two effects are similar in magnitude.

Figures 6.6-6.7 show the results for three different basin sizes for 20 and 100-year recurrence intervals respectively (note that the left most panels in Figure 6.6 shows the same results as Figure 6.5). The character of the results is similar, however the uncertainties in the 100-year flood estimates (and their changes with warming) are inherently larger than those shown for the shorter return interval. This increased uncertainty in the 100-year flood changes is characteristic of flood estimates based on

fitted probability distributions, a process which tends to amplify the noise present in the changes in more frequent flood events when extrapolating to flood quantiles with longer return intervals. [Note that such uncertainties would tend to be filtered out if a regional scale analysis were used to obtain the fitted probability distributions, but for the reasons discussed above we want to retain the spatially explicit information.]

Figure 6.6 and Figure 6.7 also compare the effects discussed above for several basin sizes. Changes for larger spatial scales tend to be smaller, presumably due to cancellation of effects from different changes in different sub basins. While there are some differences between these results in terms of the absolute value of the changes (decreasing as basin area increases), there is nothing here to suggest that the fundamental mechanisms associated with warming that influence flooding at daily time scales vary strongly with basin scale.

### *Effects of Climate Variability on Flooding Risks*

In this section we show the effects to flood risks due to a) temperature and precipitation variability as related to PDO and ENSO categories, and b) increased cool season precipitation variability since 1973. In each case the unconditional (not composited) AMS used as a standard of comparison is based on the 88-year time series for the detrended 2003 temperature regime. After compositing this time series by climate category (e.g. extracting all warm ENSO years), the 100-year flood based on the composited data (see methods section) is compared to the 100-year flood from the unconditional 2003 distribution. Thus we examine PDO and ENSO variability in the context of a systematically warmer climate associated with the end of the 20<sup>th</sup> century. This approach avoids problems with earlier years in the data set having a significantly cooler temperature regime than latter years, a potentially confounding element.

Figure 6.8 and Figure 6.9 show the changes in the 100-year flood at the smallest spatial scale simulated. The clustering of flood changes in particular geographic areas of the

domain (e.g. effects of ENSO in near coastal areas of WA, OR and Northern CA) and the lack of a coherent response associated with basin temperature regimes (scatter plots in Figure 6.8 and Figure 6.9) suggests that the primary mechanism that determines flood risks in certain climate categories is the spatial distribution of winter storms. This is not to say that cool season temperatures do not vary with ENSO and PDO, or that these variations do not play some role in determining flood risks, but such effects are apparently secondary to storm track behavior.

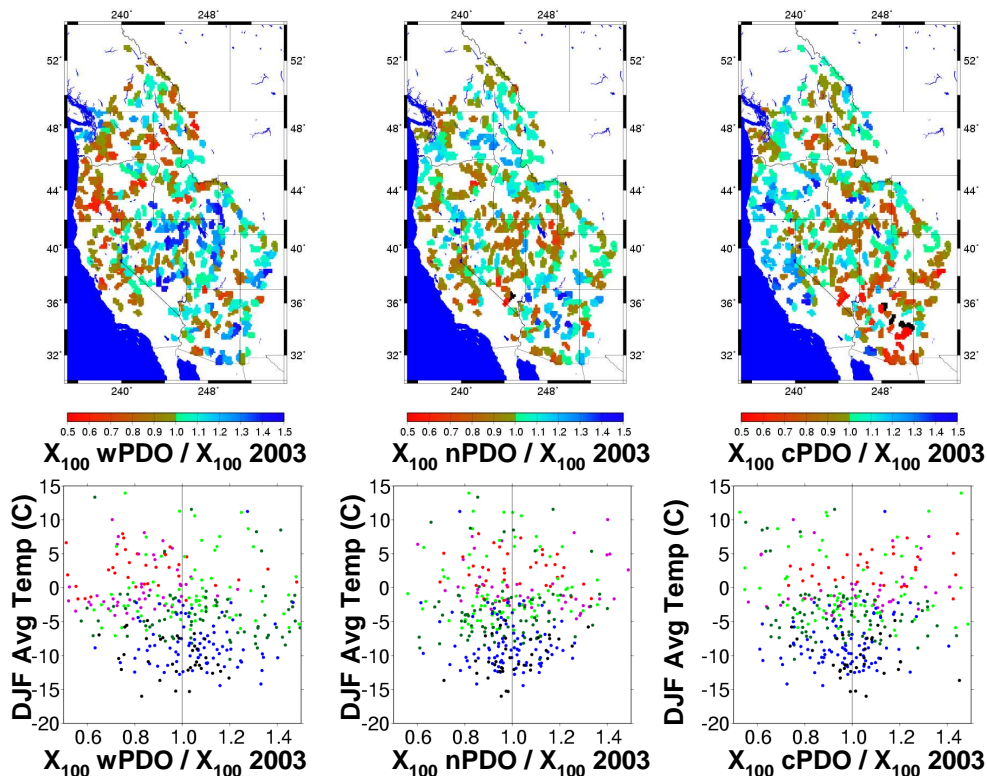


Figure 6.8 Spatial and scatter plots for the smallest basin size (as in Figure 6.5) showing the ratio of the estimated 100-year flood for warm PDO (left panels), neutral PDO (center panels), and cool PDO (right panels) composites to the estimated 100-year flood for the unconditional probability distribution. Both composite and unconditional probability distributions are extracted from the 2003 temperature regime streamflow simulations. Color coding in the scatter plots identifies the seasonality of flooding as in Figure 6.5.

During warm PDO and ENSO years, flood risks are generally lower in the PNW and northern CA, and higher in southern CA, the GB, and the CRB. For cool PDO and ENSO categories this pattern is reversed. These bimodal spatial patterns are consistent



with earlier studies examining cool season precipitation anomalies associated with PDO and ENSO (e.g. Dettinger et al. 1998; Gurshenov and Barnett 1998).

The seasonality of flooding can also play a considerable role in the changes in flood risk associated with ENSO and PDO variations, which have their greatest effect on climate in mid-winter. In areas that typically flood in January or February in the simulations (i.e. relatively warm coastal areas) when precipitation signals are most pronounced, changes in floods associated with ENSO and PDO may be unusually large. This can be seen in the effects of ENSO on flood risks in basins in western Washington and Oregon, for example (Figure 6.9).

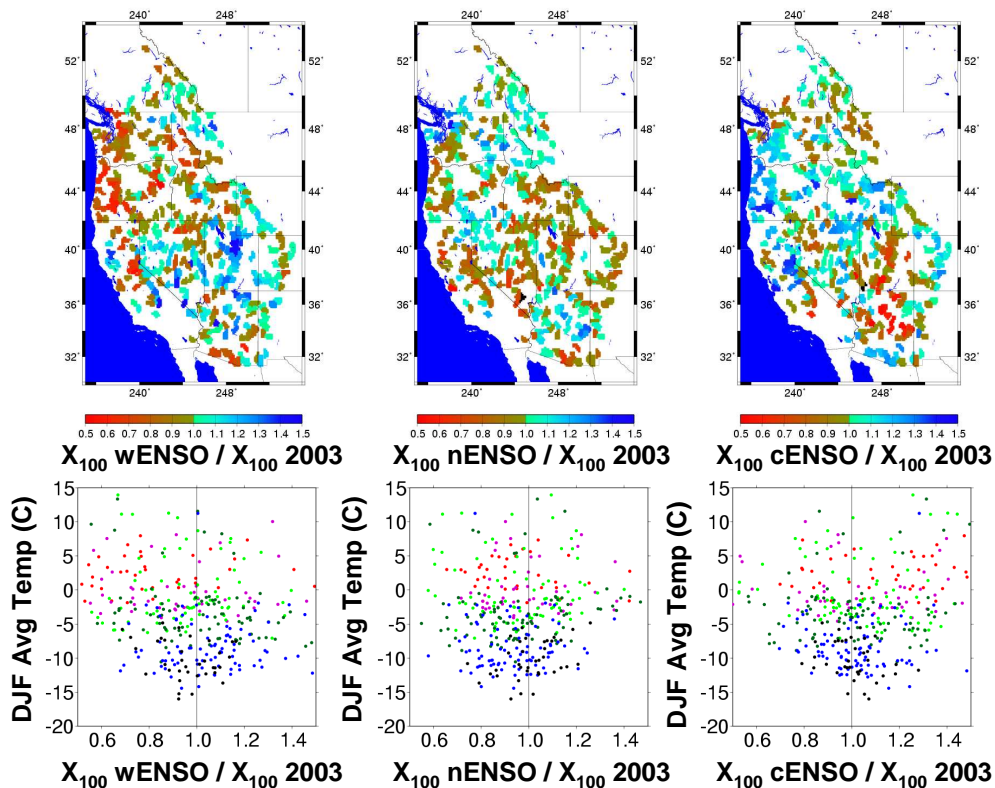


Figure 6.9. Same as Figure 6.8 but showing warm ENSO (left panels), neutral ENSO (center panels), and cool ENSO (right panels) composites.

Previous studies have shown positive reinforcement between PDO and ENSO effects (Gershunov and Barnett 1998; Hamlet and Lettenmaier 1999a; Mote et al. 2003), and

Figure 6.10 shows “in phase” (i.e. warm PDO/warm ENSO and cool PDO/cool ENSO) effects from the simulations. Although the sample sizes are quite small in this instance (about 12 in each case), and the sensitivity of individual basins may not be robust, there does appear to be some positive reinforcement between PDO and ENSO effects in the context of flood risks at the regional scale, particularly in the southwest.

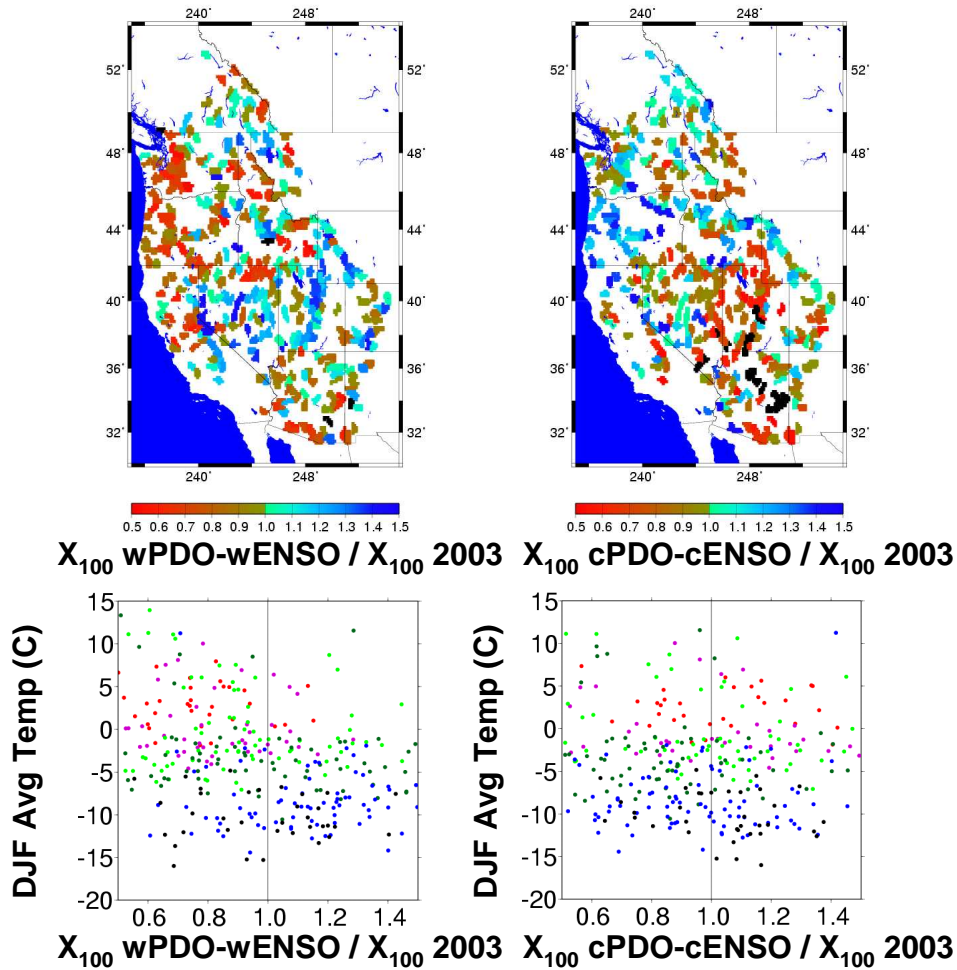


Figure 6.10. Same as Figure 6.8 except showing only warm-PDO/warm-ENSO (left column) and cool-PDO/cool-ENSO (right column) composites. [Black areas in the spatial plots are off scale on the low side]

While the spatial distribution of effects is shown to be influenced by ENSO and PDO, there is a random component to the simulated effects that is evident at the spatial scales shown in Figures 6.8, 6.9, 6.10. The performance of the model in identifying changes in

individual basins of this size does not encourage assigning great confidence to these basin specific effects, and these patterns may in fact simply be an expression of modeling or GEV parameter fitting uncertainties. At larger spatial scales, however, there are sometimes spatially cohesive precipitation signals associated with PDO and ENSO that create large changes in flood risks.

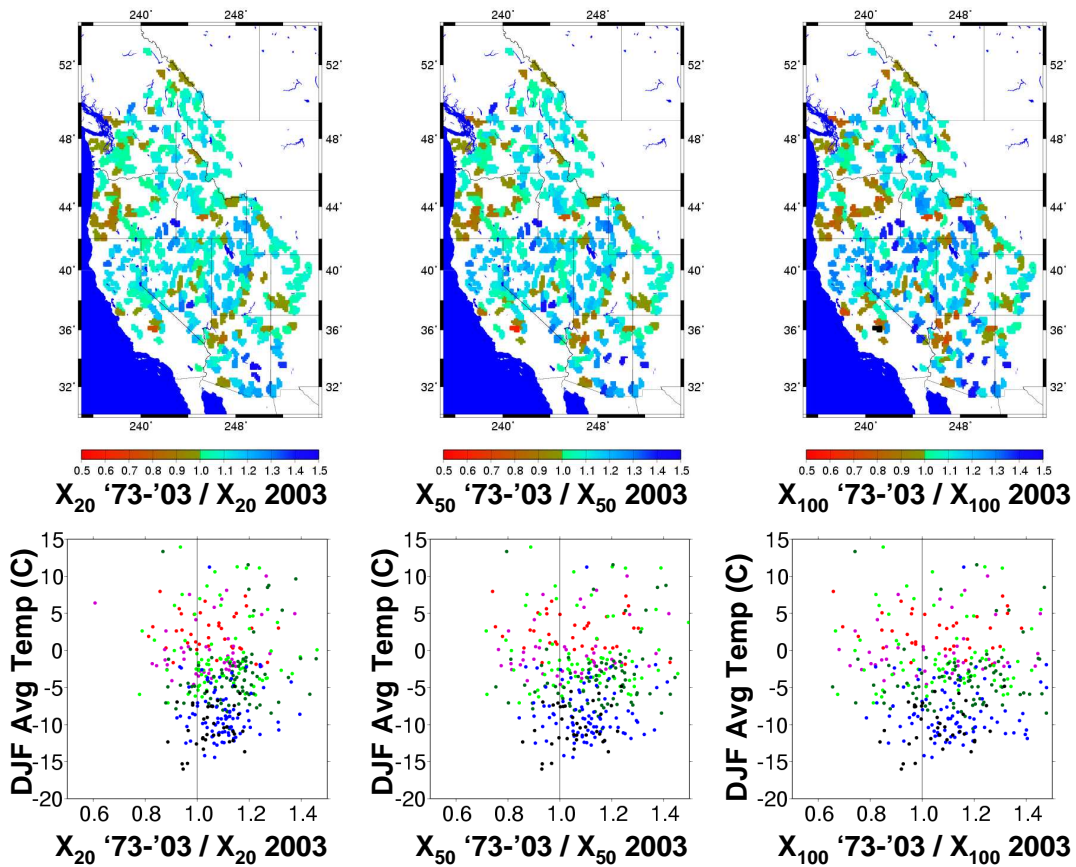


Figure 6.11. Same as for Figure 6.8 except showing composites based on all years from 1973-2003 for the 20-year (left panels), 50-year (center panels), 100-year (right panels) return intervals compared to the same values for the unconditional probability distributions (all years from pivot 2003 simulations).

For the entire Sacramento San Joaquin basin (120,000 km<sup>2</sup>), for example, the simulated 100-year flood (not shown) is about 35% higher during cool ENSO years in comparison with an unconditional sample, and at this spatial scale the model’s performance is reasonably robust (see previous sections, Figure 6.4). The effects of increased cool

season precipitation variability on flood risks for a consistent late 20<sup>th</sup> century temperature regime is shown in Figure 6.11. These simulations suggest that increases in flood risk have occurred over most of the region as a result of the observed increases in precipitation variability, despite the lack of any clear trends in precipitation. Because these effects are similar over large areas of the domain, they are also largely scale independent, with large and small basins showing similar changes.

## 6.6. Summary and Conclusions

Our simulations suggest that large scale warming over the western U.S. in the 20<sup>th</sup> century (on the order of 1° C) has resulted in changes in flood risks in many parts of the region. These changes, rather than being organized geographically or regionally, are instead characterized by mid-winter temperature regimes in each river basin. Relatively warm rain dominant basins ( $> 5^{\circ}$  C in mid winter) show little systematic change. Relatively cold snowmelt basins ( $< -6^{\circ}$  C in mid winter) typically show reductions in flood risks due to reductions in spring snowpack. Moderately cold transient snow basins show a very wide range of effects depending on competing factors associated with the relative role of antecedent snow and contributing basin area during storms that cause flooding. While the absolute value of changing flood risks is affected somewhat by basin scale, the fundamental relationship to basin temperatures in mid-winter is largely scale independent in the simulations.

Climate variability associated with PDO and ENSO also affect flood risk in the simulations. In contrast to the effects associated with 20<sup>th</sup> century warming, these effects are characterized by regional scale patterns that are consistent with the geographic distribution of cool season precipitation that has been identified in many previous studies. These effects are, in general, not scale independent in the simulations, although in some areas where climatic signals are cohesive over fairly large spatial scales, very large changes in flood risks can occur in response to precipitation patterns associated with

PDO and ENSO. As for seasonal variations in cool season precipitation, the largest changes in flood risks are associated with years when PDO and ENSO are in phase.

The gridded precipitation data sets used in this study show clear increases in the variability of cool season precipitation over essentially the entire region after about 1973. When examined in the context of a consistent late 20<sup>th</sup> century temperature regime, these changes in variability are shown in the simulations to increase flood risks over most of the region. In contrast to the effects related to temperature and PDO ENSO variability discussed above, there is no evidence in the simulations that these changes in precipitation are affecting the flood risks in different regions or basin types in a unique manner. More work is needed to determine if these kinds of changes in variability can be rigorously attributed to global warming processes.

The simulated effects of century-scale warming, climatic variations associated with the PDO and ENSO, and late 20<sup>th</sup> century changes in precipitation variability on flood risks across the region provide evidence that flood risks are not constant in each year and are slowly evolving as the region warms. The systematic nature of some of these changes (particularly the effects of warming) raises interesting and important research questions regarding how to best account for these gradually evolving flood risks in determining design standards, updating flood inundation maps, or creating scenarios for long-term water planning studies. The evidence of interannual effects on flood risks associated with ENSO and PDO variations raises similar questions with regard to water management applications at seasonal to interannual time scales. It is not immediately clear, for example, whether the advantages associated with identifying a potentially altered flood probability distribution outweigh the disadvantages associated with a smaller sample size and increased uncertainty. The effects of increased cool season precipitation variability since the mid-1970s (whose root causes are not presently well understood) also presents a number of interesting questions about how to apply this information to planning and management applications. In particular it is not clear whether the changes in precipitation

variability over the region in the late 20<sup>th</sup> century are systematic in nature (like temperature changes), or whether this is just one of a number of normal modes of natural variability that has been coincident with large scale warming. If these changes prove to be related to systematic large-scale precipitation changes associated with global warming, then the potential to provide updated information on flood risks exists (as for temperature effects). If these changes can not be shown to be systematic in nature, then it is probably inappropriate to isolate this time period in estimating flood risks.

## 7. Final Overview and Conclusions

A summary and conclusions section is included in each of the preceding chapters, and the reader is directed to these sections for a more detailed overview and discussion of each component of the research. This section will present some overall conclusions at a somewhat broader level of detail.

The results presented in the preceding chapters demonstrate that hydrologic variability in the West has been evolving as the West has warmed in the 20th century, and provides evidence that temperature and precipitation trends are fundamentally different in character and have played contrasting roles in this evolution. The hydrologic effects of precipitation variability and trends are difficult to interpret for several reasons. First, in contrast to cool season temperatures, there are no consistent large scale trends in cool season precipitation that have accompanied the warming from 1916-2003. For the period from 1947-2003, for example, a period when regional temperatures strongly increased in the West, precipitation trends varied widely in different parts of the West and were not consistent overall with trends from 1916-2003 (Chapter 4,5,6). Second, a lack of consistent large-scale cool season trends notwithstanding, there have been dramatic changes in cool season precipitation variability over the West as a whole since the mid-1970s (Chapter 6). Third, while cool season precipitation appears not to be changing in magnitude in a systematic manner as the West warms, warm season precipitation has increased steadily in many areas of the West, and these observed trends are relatively robust to the time period examined (Chapter 5). The changes in observed precipitation raise important questions about whether they are related in some way to regional warming, why these effects vary seasonally, and how they can best be projected forward in the context of predicting regional-scale precipitation changes. The hydrologic impacts of cool season precipitation changes are sometimes profoundly influenced by temperature (e.g. in the effects to snowpack and runoff timing discussed in Chapter 4 and 5), however

there are also instances when precipitation related effects are largely independent of temperature. This is the case for trends in high elevation snowpack (Chapter 4), and for changes in flood risk associated with ENSO, PDO, and increased precipitation variability from 1973-2003 (Chapter 6).

Although many important questions remain unanswered about evolving precipitation variability in the West, the effects of regional warming itself are relatively unambiguous. Chapters 4-6 present evidence from model simulations (corroborated by observations) that increased temperatures have resulted in important hydrologic changes in areas of the West with substantial snow accumulation in winter. These impacts include reduced snowpack, earlier snowmelt timing, earlier peak runoff, increased runoff in spring and less in mid summer, earlier soil moisture recharge, increased ET in spring, and systematic changes in flood risks. The hydrologic impacts of warming are organized spatially according to mid-winter temperature regimes. Coastal mountain ranges, where temperatures are near the freezing level in mid winter, are clearly identified as the most sensitive areas to warming. Both warmer and cooler locations are, in general, less sensitive to warming alone, and instead respond more directly to changes in precipitation variability.

Observed warming in the western U.S. since the early part of the 20<sup>th</sup> century has been on the order of one degree C. Future projections based on global climate model simulations suggest that an additional rise in temperature of roughly two degrees C by the second half of the 21<sup>st</sup> century is probable (IPCC 2001). The evidence of hydrologic changes in the 20th century in response to an evolving climate system call attention to important flaws in the central assumptions of many planning and management decision processes that are dependent on quantitative analyses of the hydrologic record, or on the nature of hydrologic variability. In particular, the assumption that the hydrologic variability of the past is both homogeneous in time and representative of the future variability is a pervasive one in many water resources planning and management decisions. This



dissertation presents evidence that such assumptions are already questionable in sensitive areas, and are likely to become inappropriate on much larger scales as warming progresses. In particular, changes in runoff timing (Chapter 5) and flood risks (Chapter 6), suggest that ongoing changes in water management policies may be needed both to respond to the warming that has taken place so far, and to cope effectively with the continued warming expected for the 21<sup>st</sup> century. In complex multi-objective reservoir systems (e.g. the Columbia River basin, Colorado River basin, and Sacramento/San Joaquin basins), adaptation to changes in hydrologic variability will present challenging legal, economic, socio-political, and engineering problems.

Although a detailed discussion of these planning and management problems and specific approaches to their solution is beyond the scope of this work, hydrologic modeling provides an important input to studies designed to address these issues. With regard to the impacts directly related to warming, water resources planners and managers in the West are presented with the extraordinary, and perhaps even unprecedented, situation in which forecasts of gradually evolving and apparently largely monotonic increases in temperature projected into the 21<sup>st</sup> century facilitate the prediction of systematic changes in hydrologic variability that have direct bearing on long-term planning. This research, in addition to quantifying the changes that have taken place so far, also outlines analytical approaches that are potentially useful in evaluating future impacts. In particular the mechanistic relationship between DJF temperatures and the severity of temperature-related impacts is a useful one with broad application to many global warming investigations. The differences between precipitation and temperature related effects in the historic record discussed above also suggest that changes in future hydrologic variability will be defined by systematic increases in temperature in conjunction with (possibly altered) decadal scale precipitation variability. This implies that both “warm and wet” and “warm and dry” periods are likely to occur at different times in the future, with uncertain sequencing. Long-term planning for water resources systems, which are

by their nature long-lived systems, should probably consider both scenarios in the context of adaptation.

## References

- Andreadis, K.M., Clark, E.A., Wood, A.W., Hamlet, A.F., and Lettenmaier, D.P., 2005: 20th century drought in the conterminous United States, *J. Climate*, 6 (6): 985-1001
- Barnston, A.G., Van den Dool, H.M., Zebiak, S.E., Barnett, T.P., Ji, M., Rodenhuis, D.R., Cane, M.A., Leetmaa, A. Graham, N.E., Ropelewski, C.R., Kousky, V. E., O'Lenic, E.A., and Livezey, R.E., 1994: Long-lead seasonal forecasts---where do we stand?, *Bull. Am. Met. Soc.*, 75 (11): 2097-2114
- Battisti, D.S. and Sarachik, E., 1995: Understanding and Predicting ENSO. *Review of Geophysics*, 33: 1367-76
- Bowling, L.C., Storck, P. and Lettenmaier, D.P., 2000: Hydrologic effects of logging in Western Washington, United States, *Water Resources Research*, 36 (11): 3223-3240
- Cayan D.R., 1996: Interannual climate variability and snowpack in the western United States, *J. of Climate*, 9 (5): 928-948
- Cayan, D. R., M. D. Dettinger, H. F. Diaz, and N. Graham, 1998: Decadal variability of precipitation over western North America. *J. Climate*, 11 (12): 3148-3166
- Cherkauer K.A., Lettenmaier D.P., 2003: Simulation of spatial variability in snow and frozen soil, *J. of Geophysical Research*, 108 (D22): 8858
- Christensen N.S., Wood A.W., Voisin N., Lettenmaier D.P. and Palmer R.N., 2004: Effects of Climate Change on the Hydrology and Water Resources of the Colorado River Basin, *Climatic Change*, 62 (1-3): 337-363
- Cosgrove B.A., Lohmann D., Mitchell K.E., Houser P.R., Wood E.F., Schaake J.C., Robock A., Marshall C., Sheffield J., Duan Q.Y., Luo L.F., Higgins R.W., Pinker R.T., Tarpley J.D., Meng J., 2003: Real-time and retrospective forcing in the North American Land Data Assimilation System (NLDAS) project, *J. of Geophysical Research*, 108 (D22): Art. No. 8842
- Clark M.P., Gangopadhyay S., Brandon D., Werner K., Hay L., Rajagopalan B., Yates D., 2004: A resampling procedure for generating conditioned daily weather sequences, *Water Resources Research*, 40 (4)
- Clark MP, Hay LE, 2004: Use of medium-range numerical weather prediction model output to produce forecasts of streamflow, *J. of Hydrometeorology*, 5 (1): 15-32

Daly C., Neilson R. and Phillips D., 1994: A Statistical-Topographic Model for Mapping Climatological Precipitation Over Mountainous Terrain, *Journal of Applied meteorology*, 33: 140-158

Dettinger M.D., Cayan D.R., 1995: Large-scale atmospheric forcing of recent trends toward early snowmelt runoff in California, *J. of Climate*, 8 (3): 606-623

Dettinger, M.D., Cayan D.R., Diaz, H.F., Meko, D.M., 1998: North-south Precipitation Patterns in Western North America on Interannual-to-Decadal Timescales, *J. of Climate*, Dec, 11 (12) : 3095-3111

Dettinger MD, Cayan DR, Meyer M, Jeton AE, 2004: Simulated hydrologic responses to climate variations and change in the Merced, Carson, and American River basins, Sierra Nevada, California, 1900-2099, *Climatic Change*, 62(1-3): 283-317

Franks, S.W., Kuczera, G., 2002: Flood frequency analysis: Evidence and implications of secular climate variability, New South Wales, *Water Resources Research*, 38 (5): Art. No. 1062

Gamble, J.L., Furlow J., Snover, A.K., Hamlet, A.F., Morehouse, B.J., Hartmann, H., and Pagano T., 2004: Assessing the Impact of Climate Variability and Change on Regional Water Resources: The Implications for Stakeholders, in *Water: Science, Policy, and Management*, R. Lawford et al., editors, AGU Press Monograph

Gershunov A., Barnett T.P., 1998: Interdecadal modulation of ENSO teleconnections, *Bullentin of the American Meteorological Society*, 79: (12): 2715-2725

Gleick P.H., Chalecki E.L., 1999: The impacts of climatic changes for water resources of the Colorado and Sacramento-San Joaquin River Basins, *J. of the American Water Res. Assoc.*, 35 (6): 1429-1441

Gleick P.H., 2000: *Water: The Potential Consequences of Climate Variability and Change for the Water Resources of the United States*, Report of the Water Sector Assessment Team of the National Assessment of the Potential Consequences of Climate Variability and Change, Pacific Institute for Studies in Development, Environment, and Security, Oakland, CA ISBN #1-893790-04-5

Hamlet, A.F., Lettenmaier, D.P., 1999a: Columbia River Streamflow Forecasting Based on ENSO and PDO Climate Signals, *ASCE Jour. of Water Res. Plan. and Mgmt.*, 125 (6): 333-341

- Hamlet, A.F., Lettenmaier, D.P., 1999b: Effects of Climate Change on Hydrology and Water Resources in the Columbia River Basin, *Am. Water Res. Assoc.*, 35 (6): 1597-1623
- Hamlet, A.F., Lettenmaier, D.P., 2000: Long-Range Climate Forecasting and its Use for Water Management in the Pacific Northwest Region of North America, *J. of Hydroinformatics*, Volume 02.3: 163-182
- Hamlet, A.F., Huppert, D., Lettenmaier, D.P., 2002: Economic Value of Long-Lead Streamflow Forecasts for Columbia River Hydropower, *ASCE J. of Water Res. Planning and Mgmt*, 128 (2): 91-101
- Hamlet A.F., Lettenmaier D.P., 2005: Production of temporally consistent gridded precipitation and temperature fields for the continental U.S., *J. of Hydrometeorology*, 6 (3): 330-336
- Hamlet A.F., Mote P.W, Clark M.P., Lettenmaier D.P., 2005: Effects of temperature and precipitation variability on snowpack trends in the western U.S., *J. of Climate*, 18 (21): 4545-4561
- Hamlet A.F., Mote P.W, Clark M.P., Lettenmaier D.P., 2006: 20th Century Trends in Runoff, Evapotranspiration, and Soil Moisture in the Western U.S. , *J. of Climate* (in review)
- Hamlet, A.F., Lettenmaier, D.P., 2006: Effects of 20th century warming and climate variability on flood risk in the western U.S., *Water Res. Research* (submitted)
- Hamming, R.W., 1989, *Digital Filters*, Prentice Hall, 284pp.
- Hidalgo H.G., Dracup J.A., 2003: ENSO and PDO effects on hydroclimatic variations of the Upper Colorado River basin, *Journal of Hydrometeorology*, 4 (1): 5-23
- Hosking, J.R.M., Wallis, J.R., 1993: Some statistics useful in regional frequency analysis, *Water Res. Research*, 29 (2): 271-281
- IPCC, 2001: *Climate Change 2001: The Scientific Basis. Contribution of Working Group I to the Third Assessment Report of the Intergovernmental Panel on Climate Change* [Houghton, J.T., Y. Ding, D.J. Griggs, M. Noguer, P.J. van der Linden, X. Dai, K. Maskell, and C.A. Johnson (eds.)], Cambridge University Press, Cambridge, UK and New York, NY, USA, 881pp
- Jain S., Lall, U., 2001: Floods in a changing climate: Does the past represent the future? *Water Resources Research*, 37 (12): 3193-3205

- Jain, S., Hoerling, M., and Eischeid, J., 2005: Decreasing reliability and increasing synchronicity of Western North American streamflow. *J. Climate*, 18 (5): 613-618
- Kalnay E., Kanamitsu M., Kistler R., Collins W., Deaven D., Gandin L., Iredell M., Saha S., White G., Woollen J., Zhu Y., Chelliah M., Ebisuzaki W., Higgins W., Janowiak J., Mo K.C., Ropelewski C., Wang J., Leetmaa A., Reynolds R., Jenne R., Joseph D., 1996: The NCEP/NCAR 40-year reanalysis project, *Bulletin of the American Meteorological Society*, 77 (3): 437-471
- Karl, T.R., Williams, C.N. Jr., Quinlan F.T., and Boden T.A., 1990: United States Historical Climatology Network (HCN) Serial Temperature and Precipitation Data, Environmental Science Division, Publication No. 3404, Carbon Dioxide Information and Analysis Center, Oak Ridge National Laboratory, Oak Ridge, TN, 389 pp
- Kiem, A.S., Franks, S.W., Kuczera, G., 2003: Multi-decadal variability of flood risk *Geophysical Research Letters*, 30 (2): Art. No. 1035
- Knowles N., Cayan D.R., 2002: Potential effects of global warming on the Sacramento/San Joaquin watershed and the San Francisco estuary, *Geophysical Research Letters*, 29 (18): 1891
- Knowles N., Cayan D.R., 2004: Elevational dependence of projected hydrologic changes in the San Francisco Estuary and watershed, *Climatic Change*, 62 (1-3), 319-336
- Knowles N., Dettinger M.D., Cayan D.R., 2005: Trends in snowfall vs rainfall for the western United States, 1949-2004, *J. of Climate* (in review)
- Körner, C., 1998: A re-assessment of high elevation treeline positions and their explanation, *Oecologia*, 115: 445-459
- Latif M., Barnett T.P., 1994: Causes of decadal climate variability over the North Pacific and North America, *Science*, 266 (5185): 634-637
- Latif M., Anderson D., Barnett T., Cane M., Kleeman R., Leetmaa A., O'Brien J., Rosati A., Schneider E., 1998: A review of the predictability and prediction of ENSO, *J. of Geophysical Research*, 103 (C7): 14375-14393
- Leung LR, Qian Y, Bian XD, Washington WM, Han JG, Roads JO, 2004: Mid-century ensemble regional climate change scenarios for the western United States, *Climatic Change*, 62 (1-3):75-113

Lettenmaier, D.P., and Gan T., 1990: An exploratory analysis of the hydrologic effects of global warming on the Sacramento-San Joaquin River Basin, California Water Resources Research, 26 (1): 69-86.

Lettenmaier D.P., Wood A.W., Palmer R.N., Wood E.F., Stakhiv E.Z., 1999: Water resources implications of global warming: A US regional perspective, Climatic Change, 43 (3): 537-579

Liang X., Lettenmaier D.P., Wood E.F. and Burges S.J., 1994: A Simple Hydrologically Based Model of Land Surface Water and Energy Fluxes for General Circulation Models, J. Geophys. Res., 99 (D7): 14,415-14,428

Lohmann, D., Raschke, E., Nijssen, B., and Lettenmaier, D. P., 1998: Regional scale hydrology: I. Formulation of the VIC-2L model coupled to a routing model. Hydrological Sciences Journal, 43: 131-141

Mantua, N., Hare, S., Zhang, Y., Wallace, J.M., Francis, R., 1997: A Pacific Interdecadal Climate Oscillation with Impacts on Salmon Production, Bulletin of the American Meteorological Society, 78 (6): 1069-1079

Matheussen B., Kirschbaum, R.L., Goodman, I.A., O'Donnell, G.M., and Lettenmaier, D.P., 2000: Effects of land cover change on streamflow in the interior Columbia basin, Hydrological Processes, 14 (5): 867-885

Maurer, E.P., G.M. O'Donnell, D.P. Lettenmaier, and J.O. Roads, 2001: Evaluation of the land surface water budget in NCEP/NCAR and NCEP/DOE reanalyses using an off-line hydrologic model, J. Geophys. Res. 106 (D16): 17,841-17,862

Maurer E.P., Wood A.W., Adam J.C., Lettenmaier D.P., and Nijssen B, 2002: A long-term hydrologically-based data set of land surface fluxes and states for the conterminous United States, J. Climate, 15 (22): 3237-3251

McCabe G.J., Wolock D.M., 1999: General-Circulation-Model Simulations of Future Snowpack in the Western United States, Journal of the Amer. Water Res. Assoc., 35 (6): 1473-1484

McCabe G.J., Wolock D.M., 2002: Trends and temperature sensitivity of moisture conditions in the conterminous United States, Climate Research, 20 (1): 19-29

Mekis, É. and Hogg W.D., 1999: Rehabilitation and Analysis of Canadian Daily Precipitation Time Series. Atmosphere-Ocean, 37 (1) 1999: 53-85

- Miles, E.L., Snover A.K., Hamlet A.F., Callahan B., and Fluharty D., 2000: Pacific Northwest regional assessment: The impacts of climate variability and climate change on the water resources of the Columbia River Basin. *Journal of the American Water Resources Association*, 36 (2): 399-420
- Miller NL, Bashford KE, Strem E, 2003: Potential impacts of climate change on California hydrology, *J. of the Amer. Water Res. Assoc.*, 39 (4): 771-784
- Mote P.W., 2003a: Trends in temperature and precipitation in the Pacific Northwest during the twentieth century, *Northwest Science*, 77 (4): 271-282
- Mote P.W., 2003b: Trends in snow water equivalent in the Pacific Northwest and their climatic causes, *Geophysical Research Letters*, 30 (12): 1601
- Mote, P.W., E.A. Parson, A.F. Hamlet, K.G. Ideker, W.S. Keeton, D. P., Lettenmaier, N.J. Mantua, E.L. Miles, D.W. Peterson, D.L. Peterson, R., Slaughter, and A.K. Snover, 2003: Preparing for climatic change: the water, salmon, and forests of the Pacific Northwest, *Climatic Change*, 61 (1-2): 45-88
- Mote P.W., Hamlet A.F., Clark M.P., Lettenmaier D.P., 2005: Declining mountain snowpack in western North America, *BAMS*, 86 (1): 39-49
- Mote P.W., 2006: Climate driven variability and trends in mountain snowpack in western North America, *J. Climate* (in press)
- Newman, M., Compo G. P., and Alexander M. A., 2003: ENSO-forced variability of the Pacific decadal oscillation. *J. Climate*, 16 (23): 3853–3857
- Nijssen, B., R. Schnur, and D.P. Lettenmaier, 2001: Global Retrospective Estimation of Soil Moisture Using the Variable Infiltration Capacity Land Surface Model, 1980-93. *J. Climate*, 14: 1790-1808.
- Nijssen B, O'Donnell GM, Hamlet AF, Lettenmaier DP, 2001: Hydrologic vulnerability of global rivers to climate change, *Climatic Change*, 50 (1-2): 143-175
- O'Conner, J.E., Costa, J.E., 2003: Large Floods in the U.S.: Where They Happen and Why, U.S. Geological Survey Circular 1245, (<http://pubs.usgs.gov/circ/2003/circ1245/>)
- Pagano, T., Garen, D., 2005: A recent increase in western US streamflow variability and persistence, *J. of Hydrometeorology*, 6 (2): 173-179



- Payne J.T., Wood A.W., Hamlet A.F., Palmer R.N., and Lettenmaier D.P., 2004: Mitigating the effects of climate change on the water resources of the Columbia River basin, *Climatic Change*, 62 (1-3): 233-256
- Piechota T.C., Dracup J.A., Fovell R.G., 1997: Western US streamflow and atmospheric circulation patterns during El Nino Southern Oscillation, *J. of Hydrology*, 201 (1-4): 249-271
- Pilgrim, D.H., Cordery, I., 1993: Flood Runoff, *Handbook of Hydrology*, D. R. Maidment, ed., McGraw-Hill, Inc, New York.
- Potter, K.W., Lettenmaier, D.P., 1990: A Comparison of regional flood frequency estimation methods using a resampling method, *Water Resources Research*, 26 (3): 415-424
- Redmond, K. T., and R. W. Koch, 1991: Surface climate and streamflow variability in the western United States and their relationship to large-scale circulation indices. *Water Resour. Res.*, 27 (9): 2381–2399
- Regonda S., Rajagopalan B., Clark M., and Pitlick J., 2004: Seasonal cycle shifts in hydroclimatology over the Western US, *J. of Climate*, 18 (2): 372-384
- Roads J., Bainto E., Kanamitsu M., Reichler T., Lawford R., Lettenmaier D., Maurer E., Miller D., Gallo K., Robock A., Srinivasan G., Vinnikov K., Robinson D., Lakshmi V., Berbery H., Pinker R., Li Q., Smith J., von der Haar T., Higgins W., Yarosh E., Janowiak J., Mitchell K., Fekete B., Vorosmarty C., Meyers T., Salstein D., Williams S., 2003: GCIP Water and Energy Budget Synthesis, *J. Geophys. Res.*, 108, (D16): 8609
- Robock, A., et al., 2003: Evaluation of the North American Land Data Assimilation System Over the Southern Great Plains During the Warm Season. *J. Geophys. Res.*, 108 (D22): 8846
- Sankarasubramanian, A., Lall, U., 2003: Flood quantiles in a changing climate: Seasonal forecasts and causal relations, *Water Resources Research*, 39 (5): Art. No. 1134
- Service R.F., 2004: As the west goes dry, *Nature*, 303: 1124-1127
- Serreze M.C., Clark M.P., Armstrong R.L., McGinnis D.A., Pulwarty R.S., 1999: Characteristics of the western United States snowpack from snowpack telemetry (SNOTEL) data, *Water Resources Research*, 35 (7): 2145-2160
- Shepard D.S., 1984: Computer mapping: The SYMAP interpolation algorithm, *Spatial Statistics and Models*: 133-145, Reidel Publishing Company

- Sheppard P.R., Comrie A.C., Packin G.D., Angersbach K., Hughes M.K., 2002: The climate of the US Southwest, *Climate Research*, 21 (3): 219-238
- Shuttleworth, W.J., 2003: *Handbook of Hydrology* (Maidment, D.R., ed), McGraw-Hill, Inc, New York, San Francisco, Chapter 4, pp 4.13
- Slack, J.R., Lumb, A.M., and Landwehr, J.M., 1993: Hydro-Climatic Data Network (HCDN): Streamflow Data Set, 1874 – 1988, US Geological Survey Water-Resources Investigations Report 93-4076
- Snover AK, Hamlet AF, Lettenmaier DP, 2003: Climate-change scenarios for water planning studies, *Bulletin of the American Meteorological Society*, 84 (11): 1513-1518
- Stedinger, J. R., Vogel, R. M., and Foufoula-Georgiou, E., 1993: Frequency analysis of extreme events. *Handbook of Hydrology*, D. R. Maidment, ed., McGraw-Hill, Inc, New York
- Stewart I.T., Cayan D.R., Dettinger M.D., 2004: Changes in snowmelt runoff timing in western North America under a 'business as usual' climate change scenario, *Climatic Change*, 62 (1-3): 217-232
- Stewart I.T., Cayan D.R., Dettinger M.D., 2005: Changes toward earlier streamflow timing across western North America, *J. Climate*, 18 (8): 1136-1155
- Storck P., 2000: Trees, Snow and Flooding: An Investigation of Forest Canopy Effects on Snow Accumulation and Melt at the Plot and Watershed Scales in the Pacific Northwest, Water Resources Series Technical Report No. 161, Dept of Civil and Env. Eng., University of Washington
- Storck P., Lettenmaier D.P., and Bolton S, 2002: Measurement of snow interception and canopy effects on snow accumulation and melt in mountainous maritime climate, Oregon, USA, *Water Resources Res.*, 38 (11): 1223-1238
- Thornton P.E., Running S.W., 1999: An improved algorithm for estimating incident daily solar radiation from measurements of temperature, humidity, and precipitation, *Agricultural and Forest Meteorology*, 93 (4): 211-228
- Trenberth, K. E., 1997: The definition of El Niño. *Bull. Amer. Meteor. Soc.* 78 (12): 2771-2777

Trenberth, K.E., and co-authors, 1998: Progress During TOGA in Understanding and Modeling Global Teleconnections Associated with Tropical Sea Surface Temperatures, *Journal of Geophysical Research*, 103, (C7): 14,291-14,324

USGS, FS 228-96, What Causes Floods in Washington State, U.S. Geological Survey Fact Sheet # FS 228-96,  
([http://wa.water.usgs.gov/projects/pugethazards/urbanhaz/PDF/FS\\_228-96.pdf](http://wa.water.usgs.gov/projects/pugethazards/urbanhaz/PDF/FS_228-96.pdf))

VanRheenen N.T., Wood A.W., Palmer R.N., and Lettenmaier D.P., 2004: Potential implications of PCM climate change scenarios for Sacramento - San Joaquin River Basin hydrology and water resources, *Climatic Change*, 62 (1-3): 257-281

Vincent L.A., and Gullett D.W., 1999: Canadian historical and homogeneous temperature datasets for climate change analyses, *International Journal of Climatology*, 19: 1375-1388

Voisin, N., Hamlet, A.F., Graham, L. P., Pierce, D. W., Barnett, T. P., and Lettenmaier D. P., 2006: The role of climate forecasts in western U.S. power planning, *Journal of Applied Meteorology* (in press).

Wang, Q.J., 1997: LH moments for statistical analysis of extreme events, *Water Res. Research*, 33 (12): 2841-2848

Wissmar, R.C., Timm, R.K., Logsdon, M.G., 2004: Effects of changing forest and impervious land covers on discharge characteristics of watersheds *Environmental Management*, 34 (1): 91-98

Wood A.W., Maurer E.P., Kumar A. and Lettenmaier D.P., 2002: Long range experimental hydrologic forecasting for the eastern U.S. *J. Geophys. Res.*, 107 (D20): 4429

Wood, A.W., Kumar A., Lettenmaier D.P., 2005: A retrospective assessment of NCEP climate model-based ensemble hydrologic forecasting in the western U.S., *J. Geophys. Res.* 110 (D4): Art. No. D04105

Zhang Y., Wallace, J.M., Battisti, D.S., 1997: ENSO-like interdecadal variability: 1900-93, *J. of Climate*, 10 (5): 1004-1020

## Vita

### Education:

BA in Mathematics, University of Rochester, 1981  
 BS in Mechanical Engineering, University of Washington, 1992  
 MSE in Civil and Environmental Engineering, University of Washington, 1996  
 Ph.D. in Civil and Environmental Engineering, University of Washington, 2006

### Positions Held:

Research Scientist  
 CSES Climate Impacts Group, University of Washington, 1996-present

Water Resources Engineering Consultant  
 Malcolm Pirnie (1996, 1997); NW Florida Water Management District (1996-2000);  
 Northwest Hydraulic Consultants (1999).

### Research Interests:

Hydrologic modeling  
 Water resources simulation and optimization modeling  
 Water resources management  
 Long range water planning  
 Impacts of climate variability and climate change on US water resources systems  
 Long-lead climate and streamflow forecasts  
 Water resources applications of long-lead climate forecasts

### Honors and Awards:

**2001 AWRA Boggess Award, Best Paper in 2000.** Journal of the American Water Resources Association.

(Miles, E.L., A.K. Snover, A. Hamlet, B. Callahan, and D. Fluharty, 2000, Pacific Northwest regional assessment: The impacts of climate variability and climate change on the water resources of the Columbia River Basin. Journal of the American Water Resources Association, 36(2), pp 399-420, Apr)

**Best Practice Oriented Paper in 2002.** Am. Society of Civil Engineers Journal of Water Resources Planning and Management.

(Hamlet, A.F., Huppert, D., Lettenmaier, D.P., 2002, Economic Value of Long-Lead Streamflow Forecasts for Columbia River Hydropower, ASCE J. of Water Res. Planning and Mgmt, 128 (2), pp 91-101, mar/apr)

**Outstanding Student Paper Award, 2006,** Hydrology Section of the American Geophysical Union.

(Wetter or drier? Estimating regional precipitation uncertainties in the IPCC Fourth Assessment global warming scenarios using a GCM super ensemble approach)

### **Biography:**

After receiving his bachelor's degree in mathematics at the University of Rochester (NY) in 1981, Mr. Hamlet went on to study acting at conservatory, and moved to Seattle, where he pursued an acting career for about 10 years, enjoying considerable success (albeit very little of it financial in nature) in more than 35 student, semi-professional, and professional productions. During this time he also held a number of interesting "day jobs" to support himself, including working for a singing telegram company doing strip-o-grams (not as racy as it sounds), and eventually working full time as a Volvo mechanic in the day, while continuing to act at night. In 1988 he was married to Carys Kresny, a theater director whom he met in the Seattle theater community, and in 1989 he returned to school to pursue a second bachelor's degree in Mechanical Engineering (1992) at the University of Washington, followed by a master's degree in Civil and Environmental Engineering (1996) also at the UW. He remains happily married after 18 years and has two children, Rhys (age 8), and Anya (age 6) at the time of this writing.

Since 1996, Mr. Hamlet has been a core member of the CSES Climate Impacts Group at the University of Washington with joint affiliation with the Department of Civil and Environmental Engineering under Prof. Dennis Lettenmaier. He has conducted extensive hydrologic research on the effects of climate variability and climate change on the Columbia River basin. Other areas of interest include the development of long-lead streamflow forecasting systems and related water resources applications. He was a lead participant in the Pacific Northwest component of the U.S. National Assessment of Climate Variability and Change (Hamlet and Lettenmaier 1999b; Mote et al. 2003). In addition to his own research he has collaborated with Pacific Northwest water resources researchers, planners, and managers at the Northwest Power and Conservation Council (Appendix N of the NWPCC 5<sup>th</sup> Power Plan), the US Bureau of Reclamation, and the US Army Corps of Engineers on several recent climate change projects. He is currently completing a five-year study on the effects of observed climate change in the western U.S. over the 20<sup>th</sup> century, much of which comprises this dissertation.

### **Selected Publications:**

Cohen, S.J., Miller, K., Hamlet, A., Avis, W., 2000: Climate change and resource management in the Columbia River basin, *Water International*, 25 (2): 253-272

Hamlet, A.F., Lettenmaier, D.P., 1999a: Columbia River streamflow forecasting based on ENSO and PDO climate signals, *ASCE J. of Water Res. Planning and Mgmt.*, 125 (6): 333-341

- Hamlet, A.F., Lettenmaier, D.P., 1999b: Effects of climate change on hydrology and water resources in the Columbia River basin, *J. of the American Water Resources Association*, 35 (6): 1597-1623
- Hamlet, A.F., Lettenmaier, D.P., 2000: Long-range climate forecasting and its use for water management in the Pacific Northwest region of North America, *J. Hydroinformatics*, Volume 02.3: 163-182
- Hamlet, A.F., Huppert, D., Lettenmaier, D.P., 2002: Economic value of long-lead streamflow forecasts for Columbia River hydropower, *ASCE J. of Water Res. Planning and Mgmt*, 128 (2): 91-101
- Hamlet A.F., Lettenmaier D.P., 2005: Producing temporally consistent daily precipitation and temperature fields for the continental U.S., *J. of Hydrometeorology*, 6(3): 330-336
- Hamlet A.F., Mote P.W, Clark M.P., Lettenmaier D.P., 2005: Effects of temperature and precipitation variability on snowpack trends in the western U.S., *J. of Climate*, 18 (21): 4545-4561
- Leung, L.R., Hamlet, A.F., Lettenmaier, D.P., Kumar, A., 1999: Simulations of the ENSO hydroclimate signals in the Pacific Northwest Columbia River basin, *BAMS*, 80 (11): 2313-2329
- Miles, E.L., Snover, A.K., Hamlet, A.F., Callahan, B., and Fluharty, D., 2000: Pacific Northwest regional assessment: The impacts of climate variability and climate change on the water resources of the Columbia River Basin. *J. of the American Water Resources Association*, 36 (2): 399-420
- Mote, P., D. Canning, D. Fluharty, R. Francis, J. Franklin, A. Hamlet, M. Hershman, M. Holmberg, K. Gray-Ideker, W.S. Keeton, D. Lettenmaier, R. Leung, N Mantua, E. Miles, B. Noble, H. Parandvash, D.W. Peterson, A. Snover, and S. Willard, 1999: *Impacts of Climate Variability and Change, Pacific Northwest*, National Atmospheric and Oceanic Administration, Office of Global Programs, and JISAO/SMA Climate Impacts Group, Seattle, WA. 110 pp.
- Mote, P.W., E.A. Parson, A.F. Hamlet, K.G. Ideker, W.S. Keeton, D. P., Lettenmaier, N.J. Mantua, E.L. Miles, D.W. Peterson, D.L. Peterson, R., Slaughter, and A.K. Snover, 2003: Preparing for climatic change: the water, salmon, and forests of the Pacific Northwest, *Climatic Change*, 61: 45-88
- Mote P.W., Hamlet A.F., Clark M.P., Lettenmaier D.P., 2005: Declining mountain snowpack in western North America, *BAMS*, 86 (1): 39-49

Nijssen, B., O'Donnell G.M, Hamlet, A.F., Lettenmaier, D.P., 2001: Hydrologic sensitivity of global rivers to climate change, *Climatic Change*, 50: 143-145

Payne, J.T., A.W. Wood, A.F. Hamlet, R.N. Palmer, and D.P. Lettenmaier, 2004: Mitigating the effects of climate change on the water resources of the Columbia River basin, *Climatic Change*, 62 (1-3): 233-256

Snover, A.K., Hamlet, A.F., Lettenmaier, D.P., 2003: Climate change scenarios for water planning studies, *BAMS*, 84 (11): 1513-151

### **Books:**

Gamble, J.L., John Furlow, Amy K. Snover, Alan F. Hamlet, Barbara J. Morehouse, Holly Hartmann, and Thomas Pagano, 2002: Assessing the Impact of Climate Variability and Change on Regional Water Resources: The Implications for Stakeholders, in *Water: Science, Policy, and Management*, R. Lawford et al., editors, AGU Press Monograph

Hamlet, A.F., 2003: The Role of Transboundary Agreements in the Columbia River Basin: An Integrated Assessment in the Context of Historic Development, Climate, and Evolving Water Policy, *Climate and Water: Transboundary Challenges in the Americas*, Eds. H. Diaz and B. Morehouse, Kluwer Press, Dordrecht/Boston/London

Lettenmaier, D.P, Hamlet, A.F., 2003: Chapter 7, Improving Water Resources System Performance Through Long-Range Climate Forecasts: the Pacific Northwest Experience, *Water and Climate in the Western United States*, William M. Lewis Jr., editor, University Press of Colorado, Boulder

### **Other Publications:**

Cohen S., R. de Loe, A. F. Hamlet, R. Herrington, L. Mortsch, D. Shrubsole, 2003, Chapter 15 -Integrated and Cumulative Threats to Water Availability, in *Threats to Fresh Water Availability in Canada*, Environment Canada, [http://www.nwri.ca/threats2full/intro-e.html]

Hamlet, A.F., 2001, Effects of climate change on water resources in the Pacific Northwest: Impacts and policy implications. Preparatory White Paper for Climate and Water Policy Meeting, Skamania, Washington, July 16-17, 2001.

(Available at:

ftp://ftp.hydro.washington.edu/pub/hamleaf/climate\_change\_white\_papers/Pub145.pdf)